YOLLA GAS FIELD - UPPER EVCM REVIEW

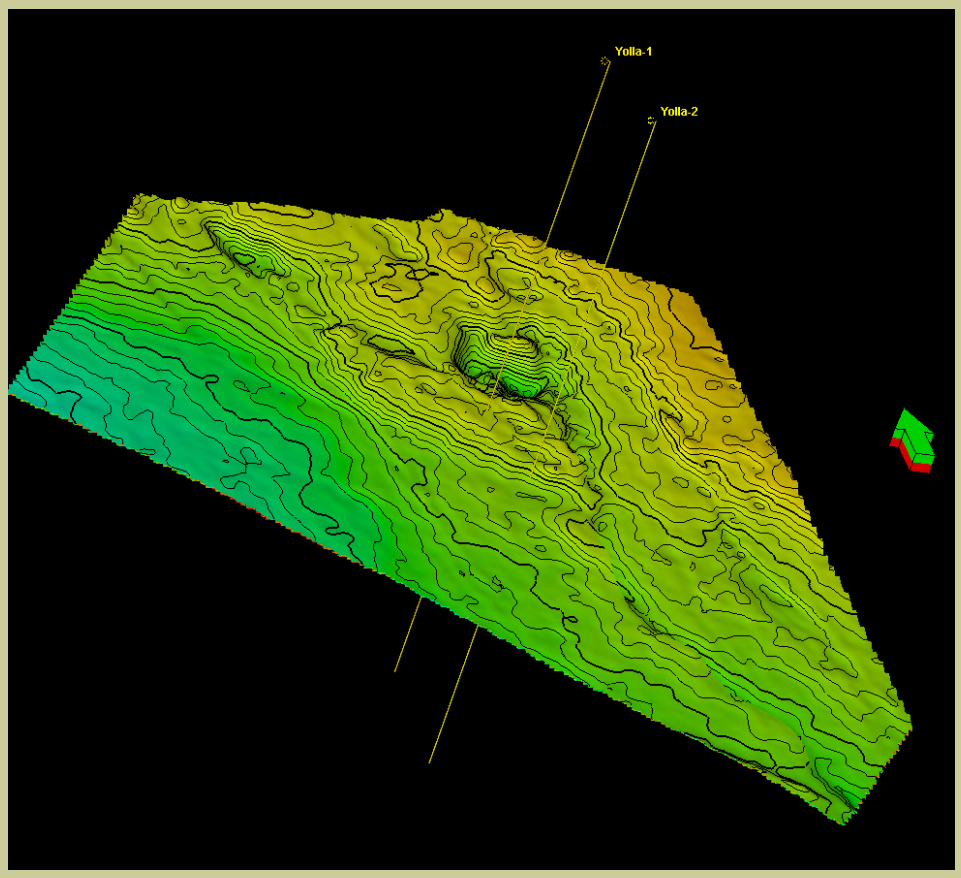

2002

Stuart Tye
Chung Chen
Chris Shield
Randall Taylor

Origin energy
delivering the goods

EXECUTIVE SUMMARY

The purpose of this report is to review the available data from the Upper Eastern View Coal Measures (EVCM) reservoir in the Yolla field, and to assess any potential feasilbility for joint development with the Intra-EVCM reservoirs or the requirement for appraisal.

The Upper EVCM was remapped following the reprocessing of the 3D seismic survey in early 2000. These depth maps form the basis for the 3D geological model that was constructed for volumetric analysis.

A petrophysical review study showed that the TEV4 (1830 - 1838m KB) stratigraphic zone in Yolla-1 contains 8m of net pay with an average porosity of 25% and water saturation of 48.9%. Yolla-2 was interpreted to be water-saturated throughout the Upper EVCM.

The quality of data concerning fluid contacts is not conclusive in Yolla-1. The Oil-water contact is inferred at 1842.3m KB (1831.2m SS) based on log analysis. The RFT data is inconclusive and cannot accurately determine contact levels. PLT data tends to confirm the log interpreted OWC and indicates a possible GOC above 1833.2m KB (1822.1m SS). This inference is also supported by DST 2A in Yolla-1 which produced both oil followed by gas (suggesting gas coning) from 1833.2 – 1833.8m KB.

Based on these fluid contacts HIP volumes were calculated deterministically for varying sensitivities of reservoir continuity, and are presented below:

Case	HIP	
	Oil (mil bbls)	Gas (bcf)
3000m range	12.2	10.1
2000m range	13.0	10.5
1000m range	14.6	11.3
500m range	15.5	13.0
100m range	15.8	12.7

A two dimensional, three phase conceptual single well radial model was used to attempt to match DST data in the field, and to provide a notional production and recovery forecast. Three THPs were investigated (1200, 725 and 430 psi) and a 2 3/8" tubing size was selected in order to maintain stable vertical lift performance over the 5 to 10 year production life. Field life progressively extended with lower THP but gas recoveries were extremely low. The best recovery under the 430-psi THP is only 1.6% of oil and 5.9% of gas.

The key finding from the simulation study is that low hydrocarbon recovery with sharp production decline can be expected from the 1830m Sand. Small tubing such as 2 3/8" is required to provide long-term wellbore production stability.

Detailed economic analysis has not been performed, but these low recoveries do not appear to justify consideration of development at this time.

It is recommended that the Upper EVCM be further evaluated in proposed gas development wells prior to any decision being taken to develop the zone for production. The main priorities for appraisal of the zone are:

- Coring of the Upper EVCM interval
- Confirmation of fluid contacts by high resolution logging and by taking further pressure data
- Confirmation of productivity through some form of production test conducted over a period of no less than several days

Such an appraisal programme has been included in the design and costing for the proposed Yolla-3 Intra-EVCM development well.

Table of Contents

List of Figures

1 INTRODUCTION

The Yolla Gas Field is located in T/RL1 in the Bass Basin, 120km offshore from Tasmania and 220km SSE of Melbourne in a water depth of 80m. The field is a large northwest-southeast trending anticlinal feature which has been compartmentalized by major faults.

Two wells have been drilled in the Yolla Field. Yolla 1 was drilled in June 1985 and encountered gas in both the top of the Eastern View Coal Measures (EVCM) and also in the Intra-EVCM. Gas Pay was encountered in five separate zones within the latter interval and this has been the principal focus for potential appraisal and development.

The focus of the development plan for the Yolla Field is the intra-EVCM (OERL 2001). A hydrocarbon-bearing zone, however, was also intersected in the upper part of the EVCM in Yolla 1. Three DSTs were conducted, and the final DST-3 over the interval 1813-1833.8m KB flowed 11.8 MMscfd gas and 892 stbd oil/condensate.

A 3D seismic survey was shot over the Yolla Field in mid 1994 with the aim of enabling more accurate depth mapping for the purpose of reserves estimation and appraisal/development planning. These data were subsequently reprocessed in early 2000. Updated depth maps of the Upper Eastern View Coal Measures (EVCM) were produced in December 2000 and January 2001 and form the basis for the latest field review contained herein.

The purpose of this report is review the current data on the upper EVCM, provide an updated HIP estimate and a forward plan for further appraisal/development of this interval in future wells.

The previous reserves audit of the upper EVCM was undertaken by Boral Energy Resources Ltd following the drilling of Yolla-2 in 1998. This review predicted total HIP volumes of approximately 33 to 35 bcf gas and 40 to 44 MMstb oil. A more realistic volume of 4 to 8 bcf gas and 19 MMstb oil was predicted for hydrocarbons in high porosity sands.

In this latest review, a geological model for the upper EVCM was constructed within Petrel software from which a deterministic estimate of HIP was calculated. This model was subsequently upscaled for input into Eclipse reservoir simulation software.

2 YOLLA 3D INTERPRETATION AND DEPTH MAPPING

2.1 Time Structure Mapping

The reprocessed Yolla 3D Seismic Survey was loaded into Schlumberger's Geoframe software and interpreted using the IESX and Geoviz modules. Eight horizons were interpreted as shown in Figure 2.1 and Table 2.1. The upper horizons were used for the interval velocity depth conversion.

Horizon Interpreted	Seismic Character	Purpose
Water Bottom (WB)	Strong Peak	Interval velocity depth conversion
Lower Mid Miocene (LMM)	Strong Peak	Interval velocity depth conversion
Top Volcano (V)	Strong Peak	Interval velocity depth conversion
Base Volcano (BV)	Strong Peak	Interval velocity depth conversion
Near top EVCM	Strong Trough	Secondary target
Middle M.Diversus (MDIV)	Strong Peak	Used to constrain picks on deeper horizons
Top 2718 Sand	Weak Peak	Uppermost sand of the main reservoir section
Top 2809 Sand	Weak Peak	Most prominent event within main reservoir section

Table 2.1: Horizons interpreted as a part of the remapping of the Yolla Field.

2.2 Well Ties

Synthetic seismograms were generated with the "Geoframe Synthetic" software and used to tie the well data into the 3D grid. A composite traverse between the wells shows the final tie of the Gamma ray logs to the seismic data (Fig. 2.2).

Time Interpretation

Time structure maps were produced for all horizons shown in Table 2.1. Picks were interpreted on every 5th inline and cross-lines were interpreted as required. Auto-tracking was used to fill in the remaining lines in the 3D grid. Time picks for the 2809 sand to the north of the field could not be made due to a deterioration in data quality, however this region is outside the area of the gas accumulation. Time maps for the main three target horizons are shown in Figures 2.3 to 2.5.

2.3 Dykes and Sills

The Yolla 3D region is intersected by a number of prominent dykes and several smaller ones that disrupt the stratigraphy. These features are prominent on the variance-cube time-slices, on which they can be seen to strike approximately N-S, (Fig. 2.6). The dykes are interpreted to be the primary source of the mid-Tertiary volcanism and also to be the source of a number of sills that have intruded the Eastern View Coal Measure

sequence, (Fig. 2.1). Several smaller dykes are interpreted to intersect the fault block containing the gas reservoirs. These may be partial barriers to the transmissibility of gas and have therefore been included in the interpretation and subsequent reservoir modelling.

Sub-Seismic Sills

While no major sills are currently recognized from the seismic to significantly effect the main reservoir section, the wells do contain a number of thin sills within the reservoir section, that are either below or close to the limits of seismic resolution. These thin sills have the potential to locally adversely modify the reservoir through the effects of heating. Further analyses such as Acoustic Impedance (AI) inversion of the seismic data is recommended to help avoid some of these features prior to the final well design. One such feature that needs further investigation may occur in the vicinity of the proposed Yolla 3 (section 5.1.1).

2.4 Depth Conversion Methodology

As shown in Figure 2.1 and 2.5, a volcano lies immediately adjacent to the Yolla Gas field. This feature, together with a number of dykes and sills has a major influence on seismic velocities over the structure. The time depth curves from the check-shot surveys of Yolla 1 and 2 show a strong divergence, indicating that the interval velocities are highly laterally-variant, (Fig. 2.7). It is for this reason, together with the sparse well control, that a horizon-based velocity analysis approach was taken to the depth conversion.

CMP gathers from 33 2D lines were extracted from the 3D survey and used for horizon based stacking and interval velocity analysis. Twenty in-lines and 13 cross-lines were extracted. The gathers had all pre-processing steps applied, up to but excluding DMO. They were loaded into Paradigm Geophysical's "Power2D" module to perform the analyses. Full details of the depth conversion methodology may be found in the Yolla 3D 2000 reprocessing interpretation report (Taylor, in prep). A brief explanation of the method used is included below.

Horizon based velocity analysis

Both Horizon Stacking Velocity Analysis (HSVA) and Interval Velocity Analysis (IVA) were used to derive velocity information for depth conversion. The HSVA velocities were used for an average velocity depth conversion and the IVA velocities were used for an interval velocity depth conversion.

HSVA is simply regular stacking velocity applied along an interpreted time horizon. It can be scaled to approximate average velocity. HSVA analysis was done for the EVCM and 2718 horizons.

IVA is akin to HSVA but computes the semblance for a range of velocities in a target layer defined by 2 interpreted horizons. It is a layer stripping process that builds up a velocity model for successive layers from the top down. Ray-tracing is used to account for non-hyperbolic move-out. Its ability to derive the velocity field for a given layer relies on the accuracy of the velocity field derived in the overlying section. The

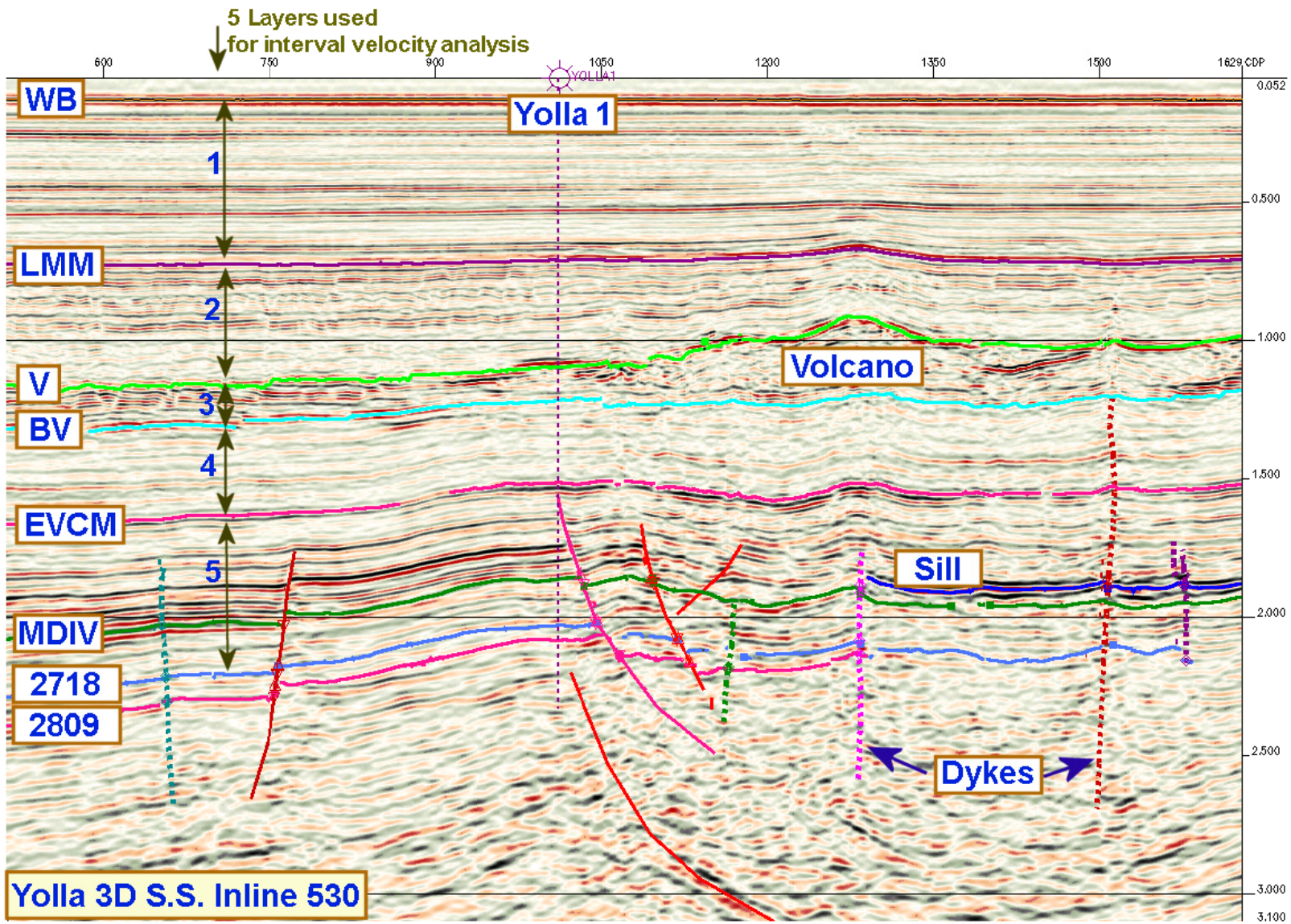
5 Layers used
for interval velocity analysis
600
750
900
1050
1200
1350
1500
1629 CDP
YOLLA1
Yolla 1
WB
LMM
V
BV
EVCM
MDIV
2718
2809
1
2
3
4
5
Volcano
Sill
Dykes
Yolla 3D S.S. Inline 530
0.052
0.500
1.000
1.500
2.000
2.500
3.000
3.100

Figure 2.1

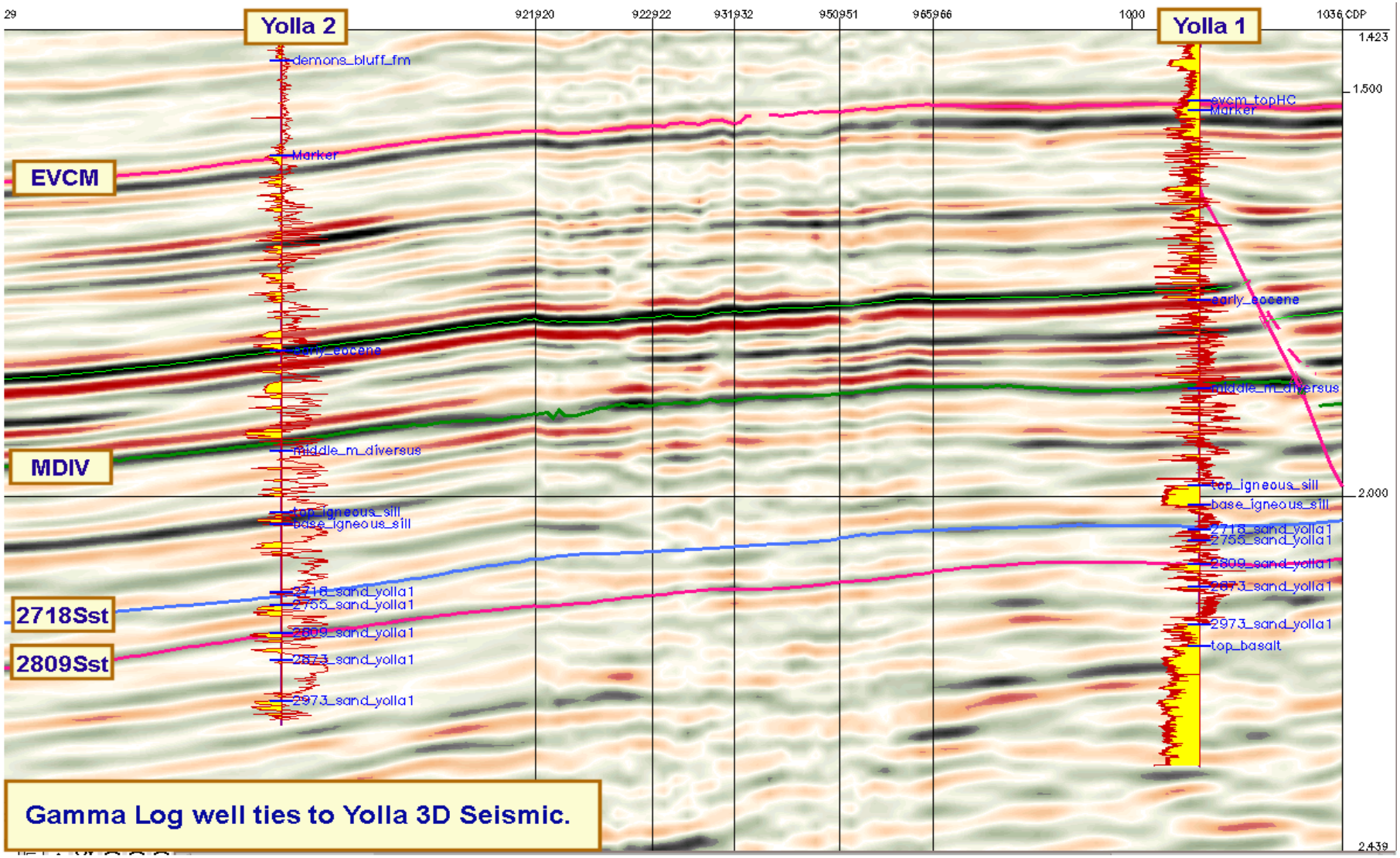

Figure 2.2

Gamma Log well ties to Yolla 3D Seismic.

Yolla Gas Field T/RL1

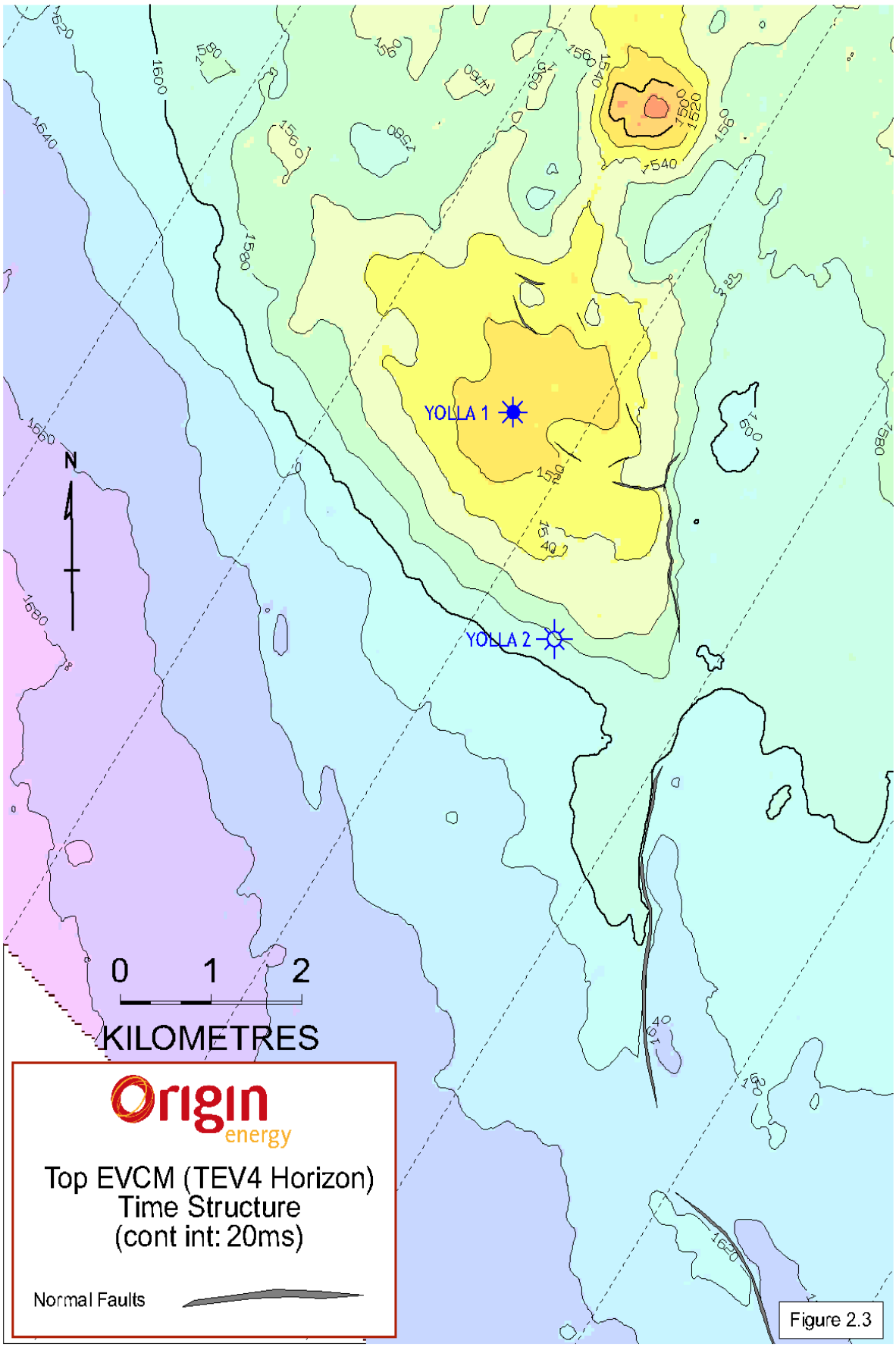

Figure 2.3

Yolla Gas Field T/RL1

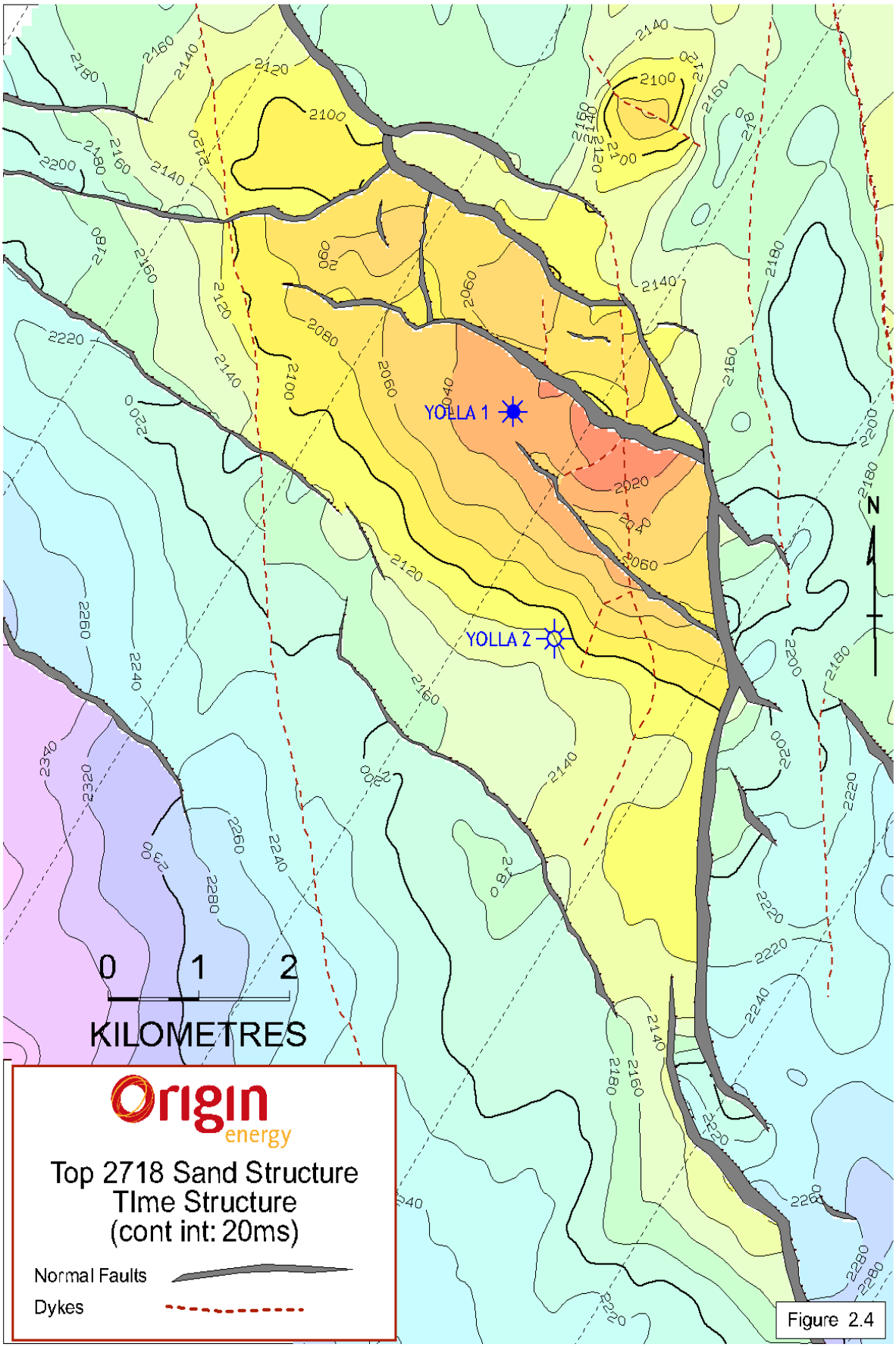

Figure 2.4

Yolla Gas Field T/RL1

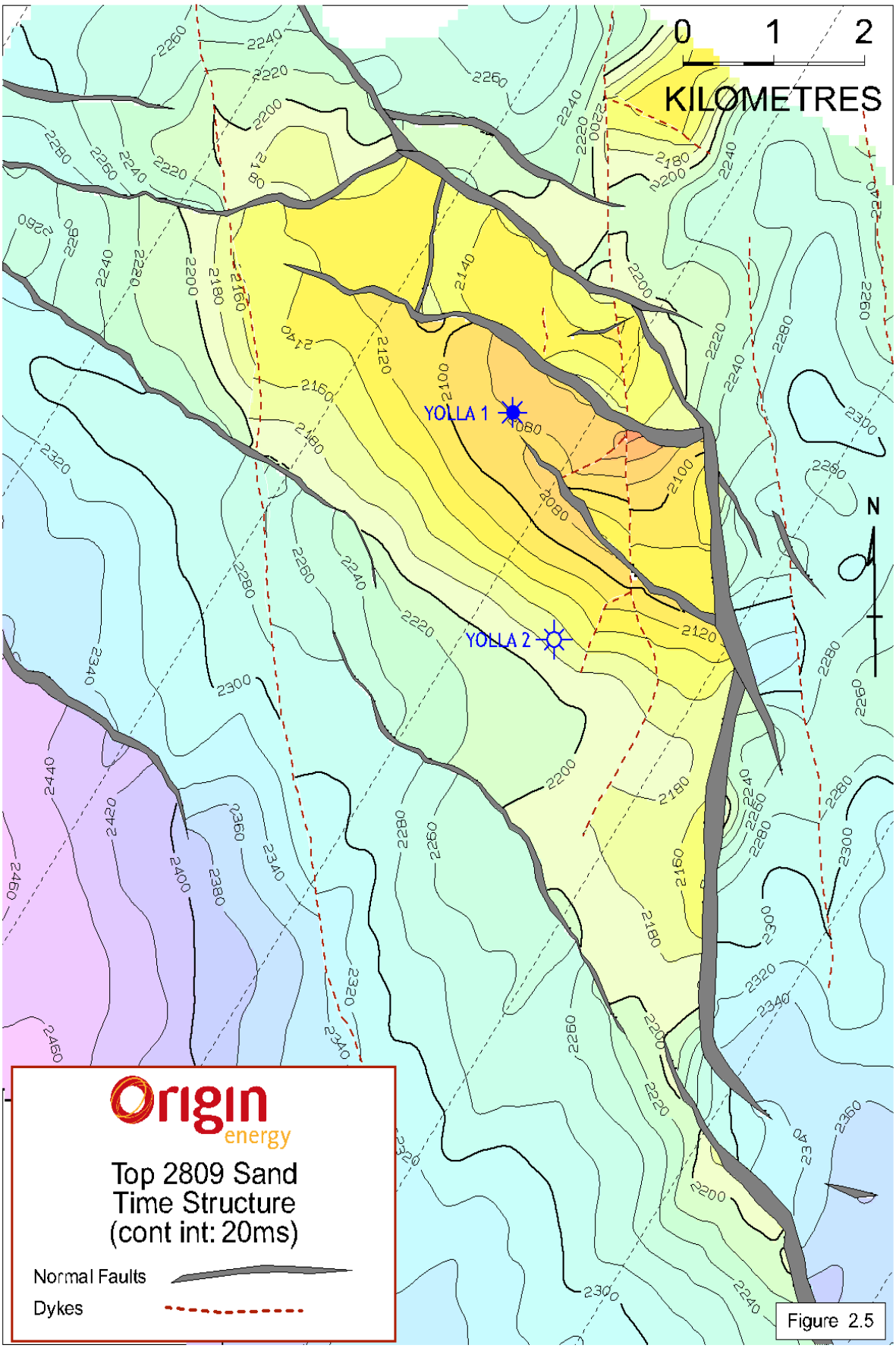

Figure 2.5

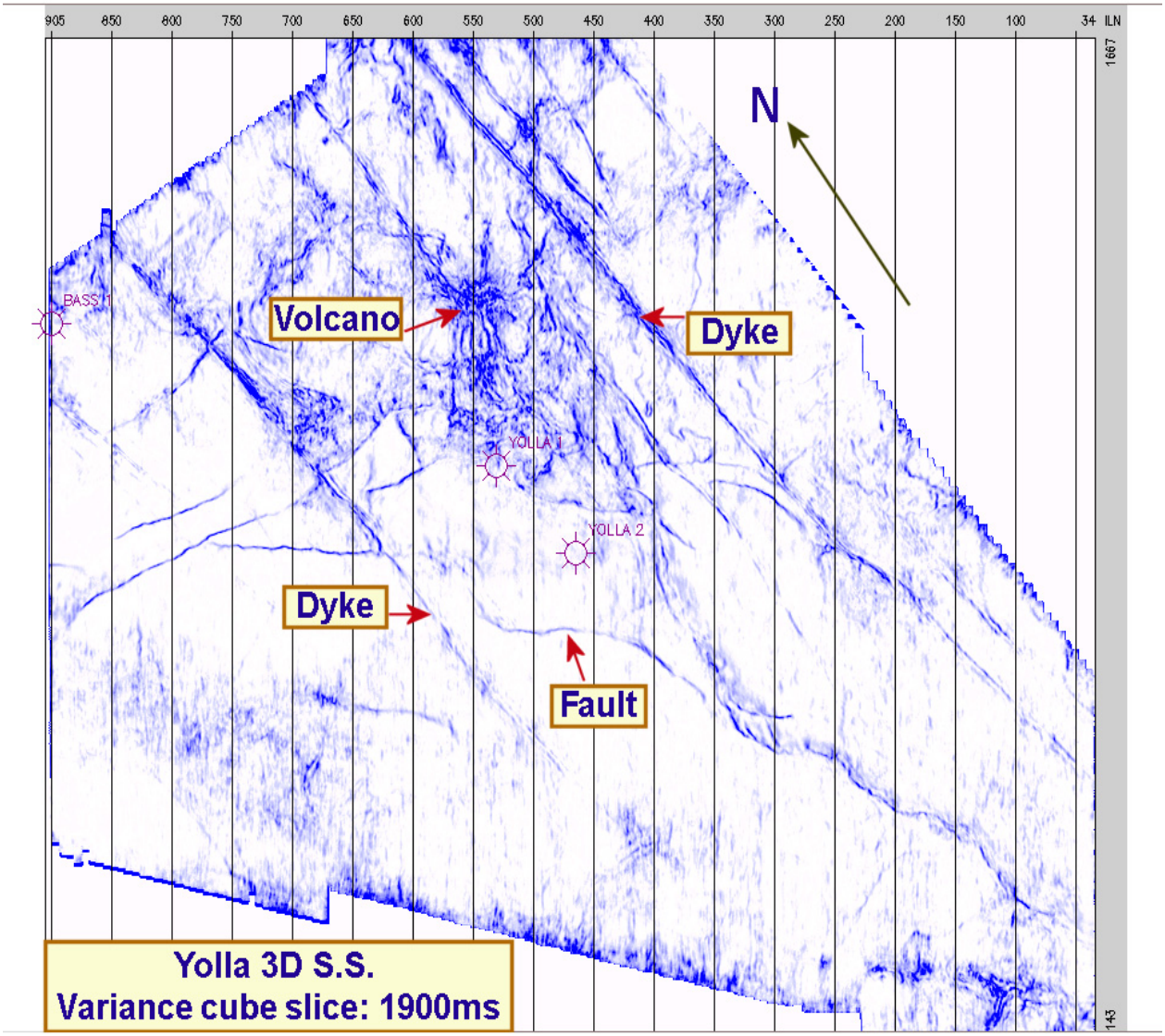
905
850
800
750
700
650
600
550
500
450
400
350
300
250
200
150
100
34
ILN
1667
143
N
BASS 1
Volcano
Dyke
YOLLA 1
YOLLA 2
Dyke
Fault
Yolla 3D S.S.
Variance cube slice: 1900ms

Figure 2.6

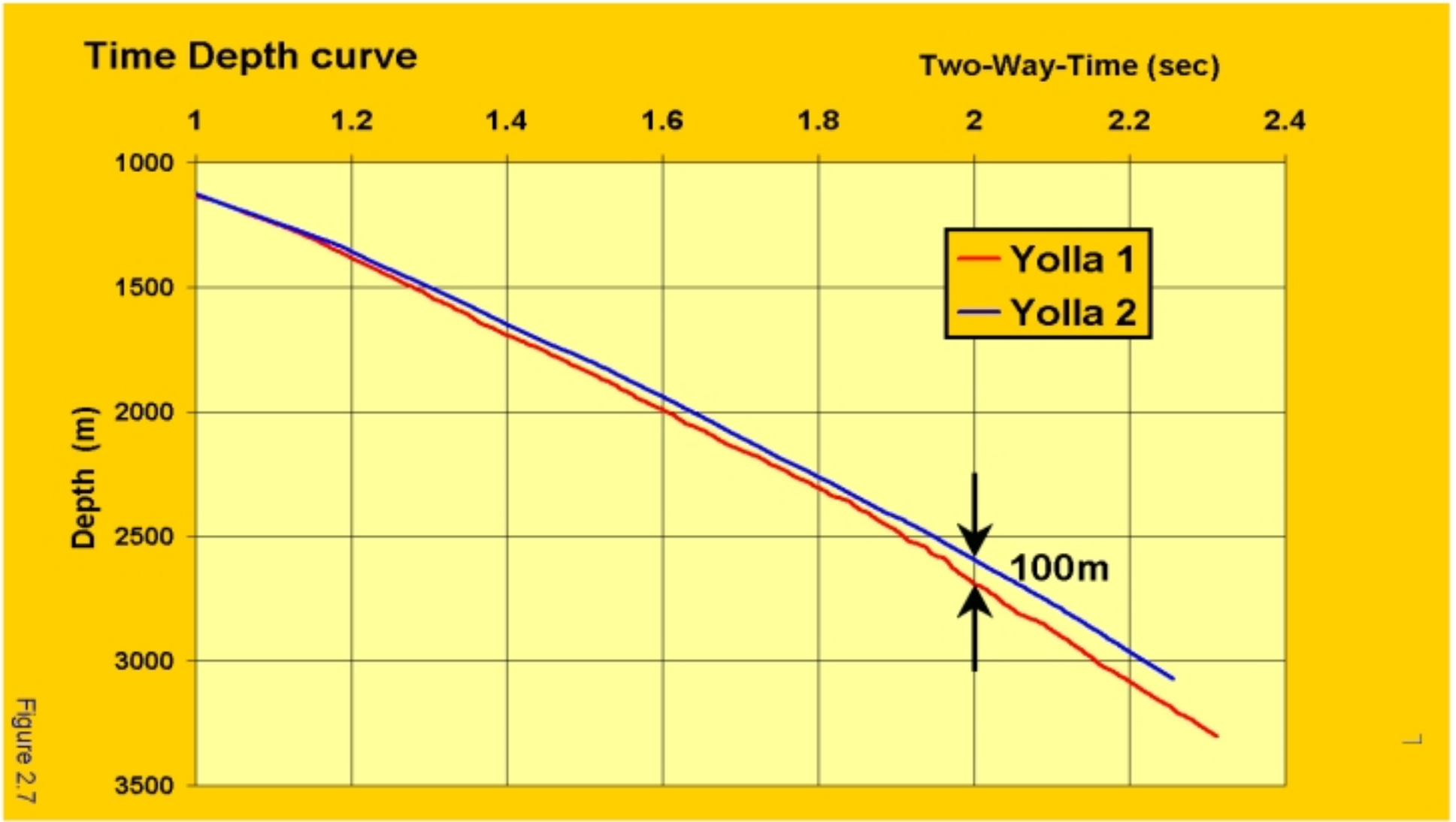
Time Depth curve
Two-Way-Time (sec)
1
1.2
1.4
1.6
1.8
2
2.2
2.4
1000
1500
2000
2500
3000
3500
Depth (m)
Yolla 1
Yolla 2
100m

Figure 2.7

method employed was the coherency inversion technique, as implemented in Paradigm Geophysical's "Power2D" module.

IVA was applied to the 5 layers bounded by the horizons shown in Figure 2.1. This was done for each of the 33 2D lines extracted from the 3D survey. For each successive layer, the interval velocity semblances on all lines were interpreted simultaneously, to produce a consistent grid of velocity picks, before proceeding to analyse the next layer. This was an important step as it minimised any systematic line to line errors.

2.5 Depth Conversion

The main method of depth conversion was an interval velocity approach using map-migration to convert successive layers to depth. The maps produced using this technique were the P50 case for volumetric estimates (Fig 2.8).

All velocity maps were calibrated to check-shot velocities in the wells. For the upper horizons the well Bass 1 was included together with Yolla 1 and 2. For each layer, the seismically derived velocities were scaled by a constant factor to approximately tie the check-shot velocities, then map-migrated to depth. A hand contoured mistie map was then used to flex the grids to exactly tie the wells.

The overall effect of the volcano on the velocity field can be seen by examining the final average velocity map produced by dividing the final depth conversion of the 2809 sand by the two-way-time map (Fig. 2.9). It shows that the volcano has a large bearing on the velocities with the average velocity decreasing in a concentric manner away from the centre of the volcano. This is a reasonably plausible given the expected effect of volcanic activity and is therefore taken as support for the veracity of the depth conversion.

Yolla Gas Field T/RL1

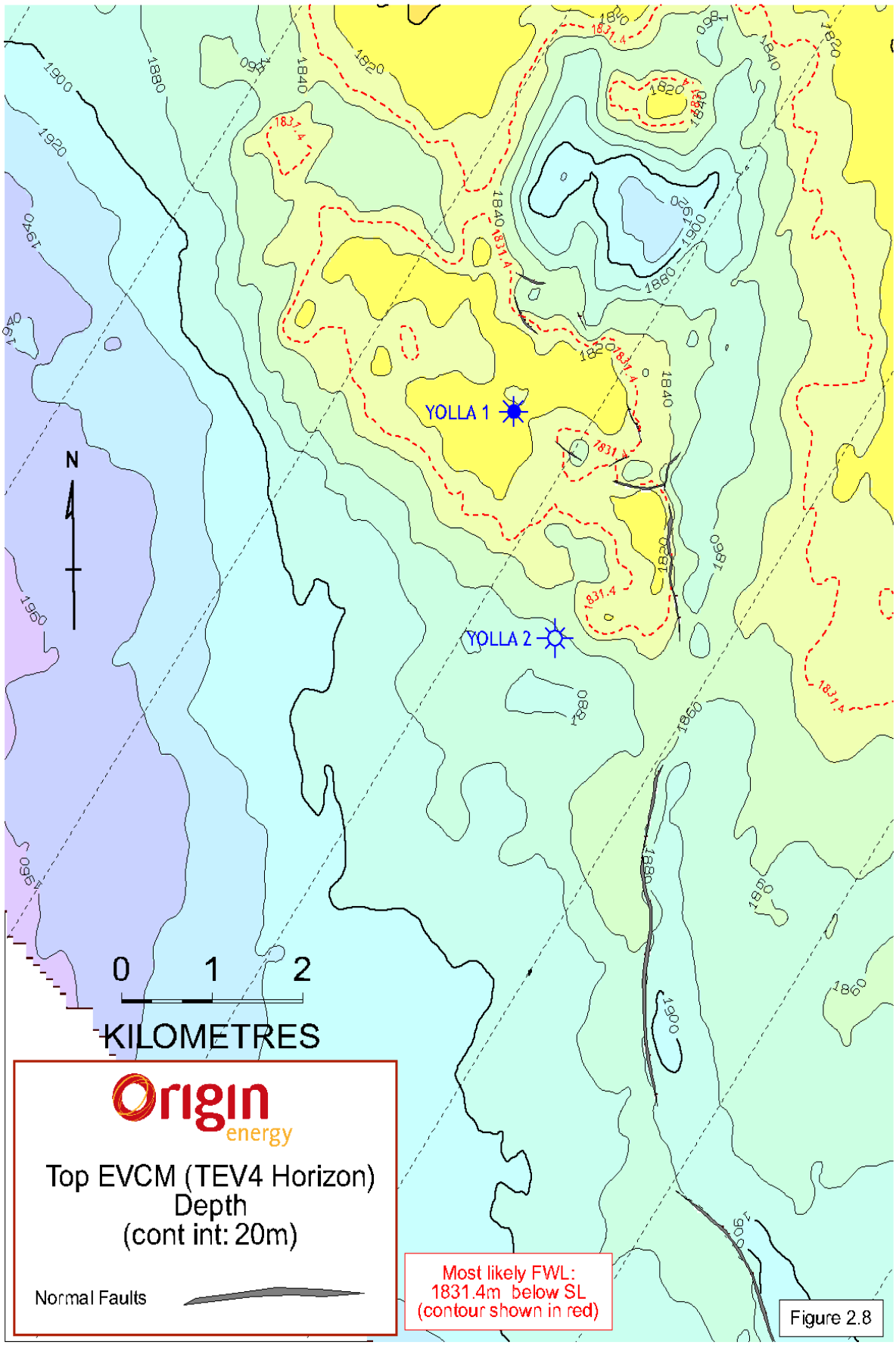

Figure 2.8

Yolla Gas Field T/RL1

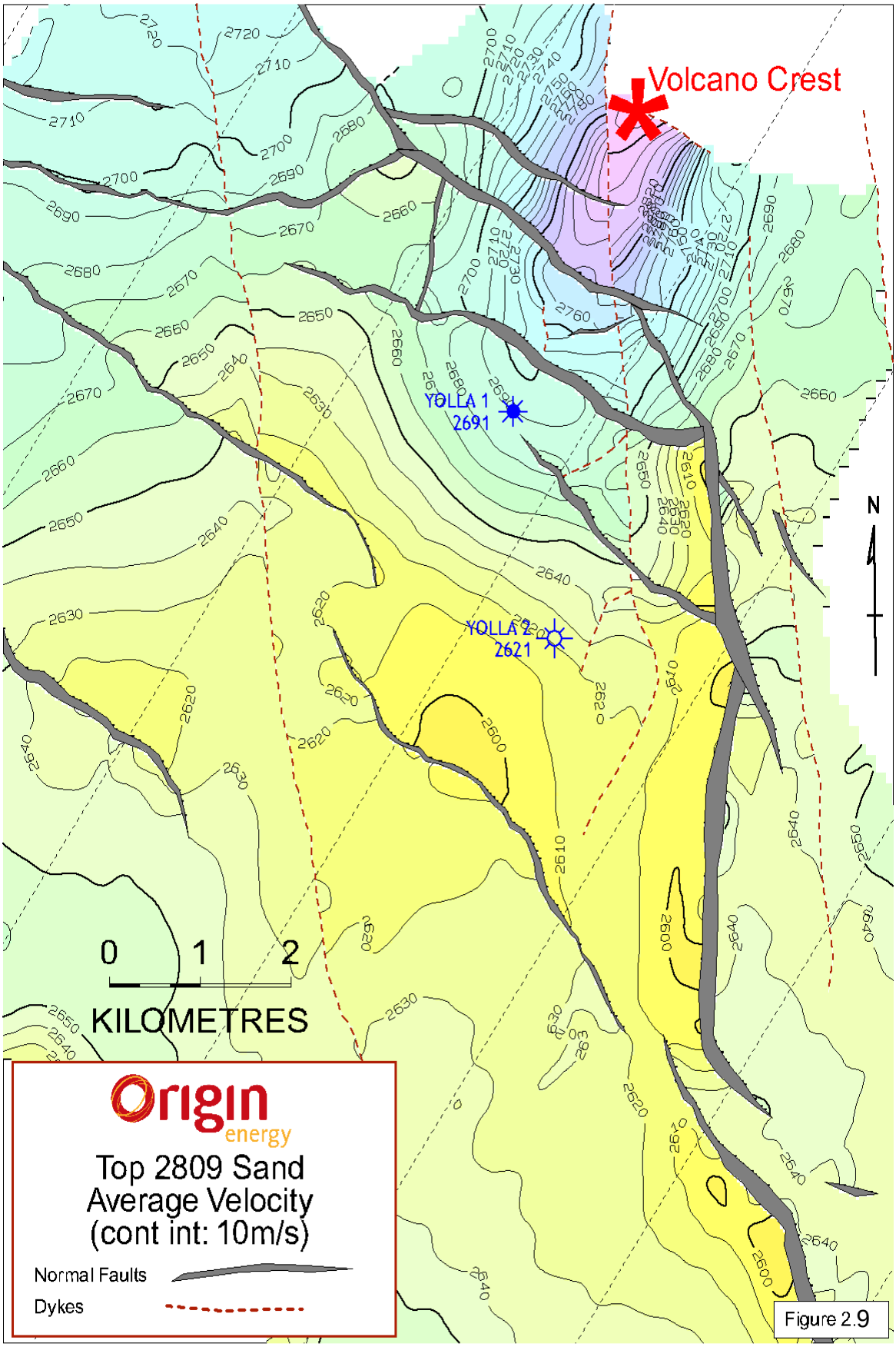

Figure 2.9

3 GEOLOGICAL MODEL

3.1 Exploration history

Yolla-1 was drilled in May 1985. It intersected an interval with gas shows and fluorescence at approximately 1805m KB. Significant gas shows were also intersected at 1830 – 1834m KB. Three DSTs were conducted over the unit. The results are as follows:

1. DST 2: 1830 – 1835.2m KB. Flowed GTS at 2.2 MMcfd, RTSTM condensate/oil and 1675 bpd water. The water was interpreted to be channeling behind casing due to poor cementation.
2. DST 2A: 1833.2 – 1833.8m KB. (After several cement squeezes). Flowed GTS at 1.0 MMcfd, 302 stbpd oil/condensate and no water. Oil:gas ratio fell throughout the test, possibly due to the onset of gas coning.
3. DST 3: 1820.5 – 1840.5m KB. Flowed GTS at 11.8 MMcfd and OTS at 892 stbpd and no water. (Note: Perforations are now interpreted to be off depth relative to those reported at the time - see section 4.3).

A single core was cut over the interval from 1838 to 1847.8m KB with only 29% recovery. RFT and wireline log data were obtained over the interval.

Yolla-2 was drilled in April 1998. It intersected the top EVCM at 1844.0m KB. Log analysis (section 3.4) indicates that the unit is water-bearing. No DSTs or RFT data were collected over this interval.

3.2 Stratigraphy

Based on the stratigraphic section intersected in Yolla 1 and Yolla 2 the upper EVCM has been subdivided into seven zones which can be correlated on wireline logs between the wells. These zones are shown in Figure 3.1 and are summarized in Table 3.1.

Zone	Yolla-1		Yolla-2	
	mKB	mSS	mKB	MSS
TEV1	1800	1788.9	1845	1832.5
TEV1A	1807	1795.9	1854.2	1841.7
TEV2	1817.5	1806.4	1863	1850.5
TEV3	1823	1811.9	1869	1855
TEV4	1830	1819.2	1875	1863.1
TEV5	1838	1826.9	1882	1869
TEV6	1843	1832.7	1889	1876.5
TEV7	1858	1846.9	1903	1890.5
TEV7 Base	1880	1869.6	1925	1913.2

Table 3.1: Stratigraphic zones used in geological modeling and petrophysical interpretation.

3.3 Reservoir facies and quality

Data is sparse concerning the facies of the Upper EVCM at Yolla 1. Core 1 from Yolla 1 had poor recovery and was significantly fractured. The whole core that is recovered shows the sandstone to be fine-grained and strongly bioturbated suggesting a significant marine influence in deposition. The log character in Yolla 1 suggests an interbedded sequence of dominantly argillaceous sandstone and minor siltstone (TEV4 – TEV6; 1829 – 1856.6m KB; Fig. 3.1) overlain by a siltstone and claystone interval. In Yolla 2 a clear upward-coarsening trend is discernable over the correlative interval (TEV4 - TEV6; 1875.7 – 1891.7m KB; Fig 3.1). The lithology is again interpreted to be interbedded argillaceous sandstone and siltstone. The available evidence for the upper EVCM in the Yolla Field indicates a progradational shallow marine sequence in the TEV4-6. The depositional environment is probably lower to middle shoreface or delta mouthbar. The overlying shale-dominated section (TEV1 – TEV3) was probably deposited at the onset of the transgression that culminated in the deposition of the Demons Bluff Formation. The most likely environment of deposition for this interval is offshore marine.

Reservoir quality data is available for the cored interval in Yolla 1 and is presented in Table 3.2.

Depth	Ambient Porosity (%)	Ambient horizontal permeability (mD)
1845.40	29.6	75.00
1845.70	25.2	17.00
1846.00	25.8	11.00
1846.40	30.4	65.00
1846.70	30.0	51.00
1847.00	29.2	37.00
1847.30	30.0	42.00

Table 3.2: Upper EVCM core data – Yolla 1.

The most striking characteristic of this data is the relatively low permeability associated with the high porosity of the samples. When a trendline is placed through this data (Fig. 3.2) the following equation can be derived linking porosity and permeability:

$$\text{Permeability (md)} = 0.0100e^{(0.28696 \times \text{Porosity (\%)})}$$

A petrology study (Baker 2001; Appendix 1) was conducted on 4 samples from the upper EVCM in September 2001. Much of the porosity of the samples is interpreted to be microporosity associated with pore-filling detrital and

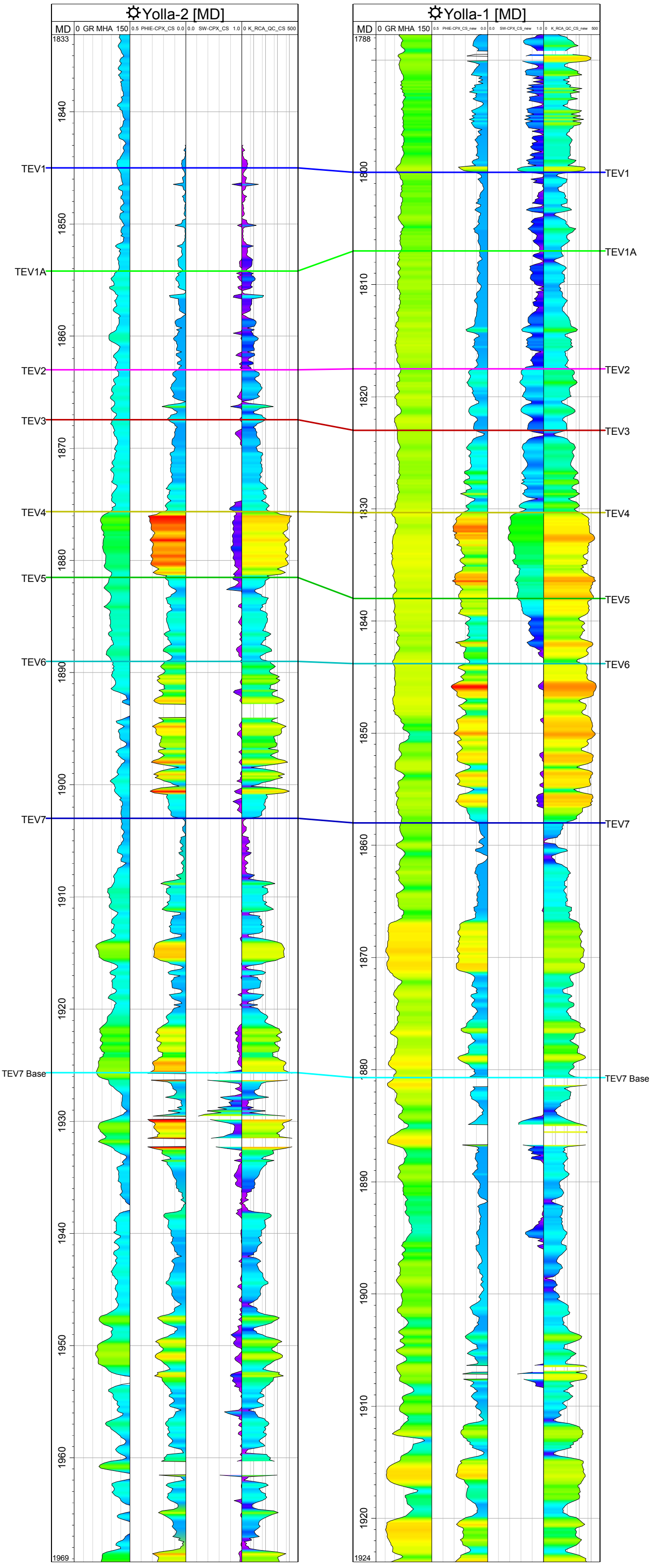

Figure 3.1: Cross-section through Upper EVCM in Yolla 1 and Yolla 2 showing stratigraphic zones, porosity, Sw and permeability curves

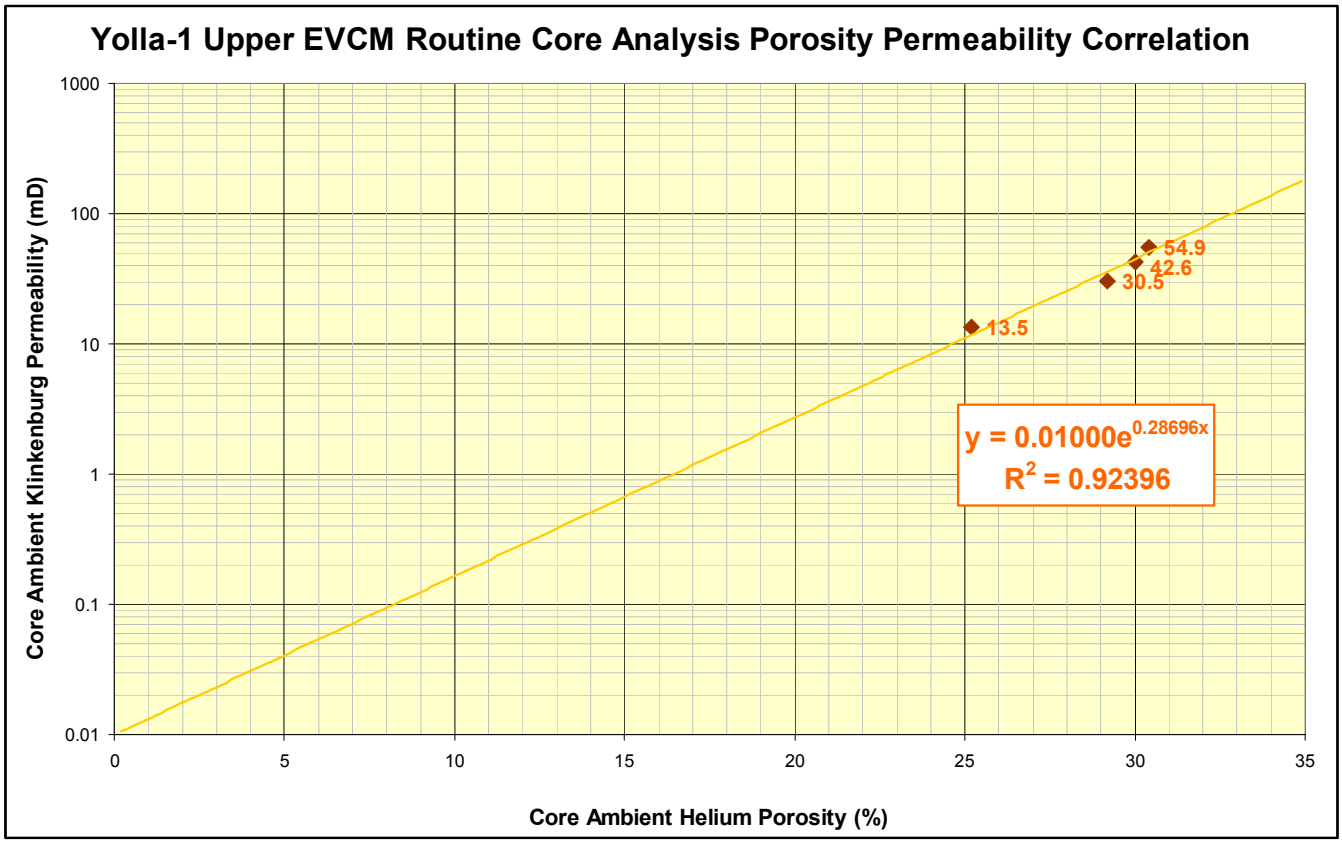

Figure 3.2: Porosity-Permeability data for the Upper EVCM in Yolla 1. Trendline and corresponding equation is also shown.

authigenic clay and siderite. The relative low permeability is also due to the clay and sideritic pore-fill. XRD and SEM analyses show this clay to be dominated by fine-grained authigenic kaolinite.

3.4 Petrophysics

A petrophysical review was conducted of the reservoir quality and hydrocarbon charge potential of the upper EVCM Formation sediments intersected whilst drilling the exploration well, Yolla-1 in TR/L1 in the Bass Basin, Tasmania (Appendix 1). The study entails an analysis of all available lithological data, an evaluation of the quality of the hydrocarbon shows, and a complete petrophysical analysis (Table 3.3).

Zonation					Gross Rock	Net Reservoir						Net Pay		
Name	Top		Base		Thickness	Thickness	Av. Clay Volume	Av. Eff. Porosity	Av. Permeability	Ave. kH	Net Res/Gross	Thickness	Av. Water Sat.	Net Pay/Gross
	mKB	mSS	mKB	mSS	metres	metres	%	%	mD	mD.ft	%	metres	%	%
TEV0	1765	1753.9	1800	1788.9	35.0	1.2	30.2	21.4	29.66	118.7	3.5	0		0.0
TEV1	1800.0	1788.9	1807.0	1795.9	7.0	0.0	----	----	----	----	0.0	0.0		0.0
TEV1A	1807.0	1795.9	1817.5	1806.4	10.5	2.7	33.2	11.7	0.81	7.3	26.1	0.0		0.0
TEV2	1817.5	1806.4	1823.1	1812.0	5.6	5.3	28.6	14.0	1.71	29.9	95.2	0.0		0.0
TEV3	1823.1	1812.0	1829.5	1818.4	6.4	5.8	23.2	16.8	3.46	65.7	90.5	0.0		0.0
TEV4	1829.5	1818.4	1839.6	1828.5	10.1	10.1	17.7	25.0	53.59	1775.8	100.0	6.7	46.6	66.4
TEV5	1839.6	1828.5	1843.0	1831.9	3.4	2.4	33.2	20.4	38.50	308.2	71.8	0.0		0.0
TEV6	1843.0	1831.9	1857.8	1846.7	14.8	13.9	21.6	24.2	57.84	2632.0	93.7	0.0		0.0
TEV7	1857.8	1846.7	1866.5	1855.4	8.7	0.2	36.8	14.1	0.61	0.3	1.7	0.0		0.0
TEV8	1866.5	1855.4	1871.4	1860.3	4.9	5.0	5.1	25.0	13.47	222.3	102.7	0.0		0.0
TEV9	1871.4	1860.3	1911.4	1900.3	40.0	9.5	26.9	17.2	2.73	84.6	23.6	0.0		0.0
TEV10	1911.4	1900.3	1929.0	1917.9	17.6	15.5	13.9	21.6	9.53	485.9	88.3	0.0		0.0
Total	1800.0	1788.9	1880.0	1869.6	164.0	71.7	19.6	21.6			43.7	6.7	46.6	4.1
DST-2A	1833.2	1822.1	1833.8	1822.7	0.6	0.6	20.9	24.4	112.26	221.0	100.0	0.6	47.2	100.0
DST-3	1822.0	1810.9	1842.0	1830.9	20.0	17.1	20.4	22.1	17.12	958.6	85.4	6.7	46.6	33.6
Best Sand	1830.3	1819.2	1833.3	1822.2	3.0	3.0	9.6	27.7	74.26	730.9	100.0	3.0	41.4	100.0

Table 3.3: Petrophysical Reservoir Summary

Very-fine grained, quartzose sandstones with a high (20-40%) volume of clay, interbedded with, claystones, and coals were intersected within the upper EVCM Formation (Fig. 3.3). Porosity, measured from core analysis and derived from log analysis, is higher than expected for sandstones with such a large volume of clay. Petrology indicates that the kaolinitic clay present contributes a significant amount of secondary micro-porosity, which would not contribute to recovery. Calculated permeabilities are moderate (3-53mD) in the sandstones that are hydrocarbon-bearing (TEV3 and 4). The reservoir would be expected to flow hydrocarbons at moderate rates.

Lower reservoirs (TEV5,6, and 8) have less clay, and would be expected to have better deliverability. These reservoirs are below the hydrocarbon-water contact at Yolla-1.

TEV4 Depth structure

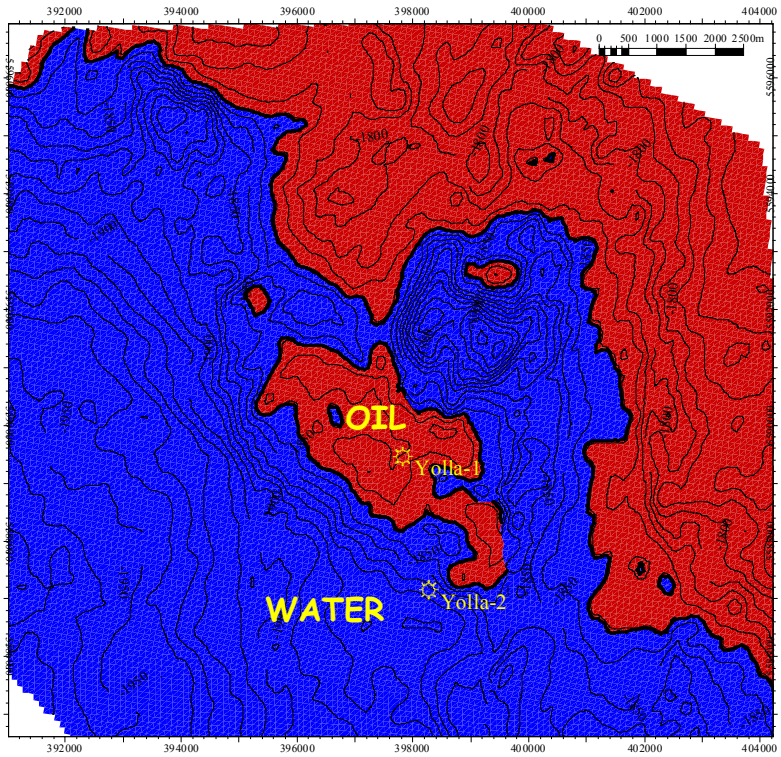

FLUID CONTACT: 1831.1m SS

TEV3 Depth structure

No closure

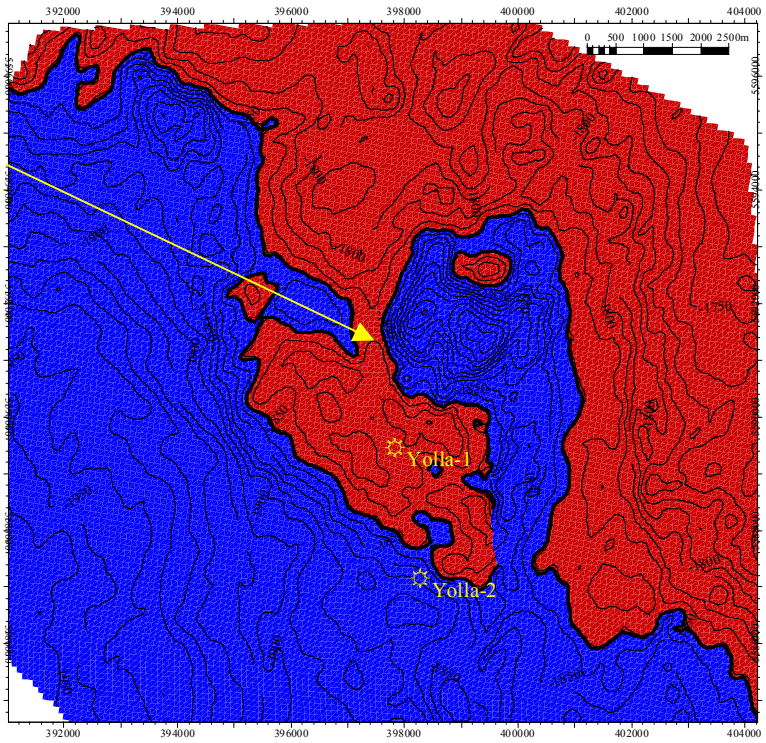

Figure 3.4: Comparison of top TEV3 and top TEV4 depth maps. The contact between red and blue represents OWC/GWC contact at 1831.1m SS. This diagram clearly shows that there is no closure above the TEV4 stratigraphic interval

A gas-oil contact is postulated at 1832.1 mMDRT, but its exact location may be questioned due to the high clay content within the reservoirs masking any potential density-neutron effect. An oil-water contact is apparent from the logs at 1842.3 mMDRT, and occurs at the base of a claystone bed. The top of the transition zone is interpreted at 1840.7 mMDRT.

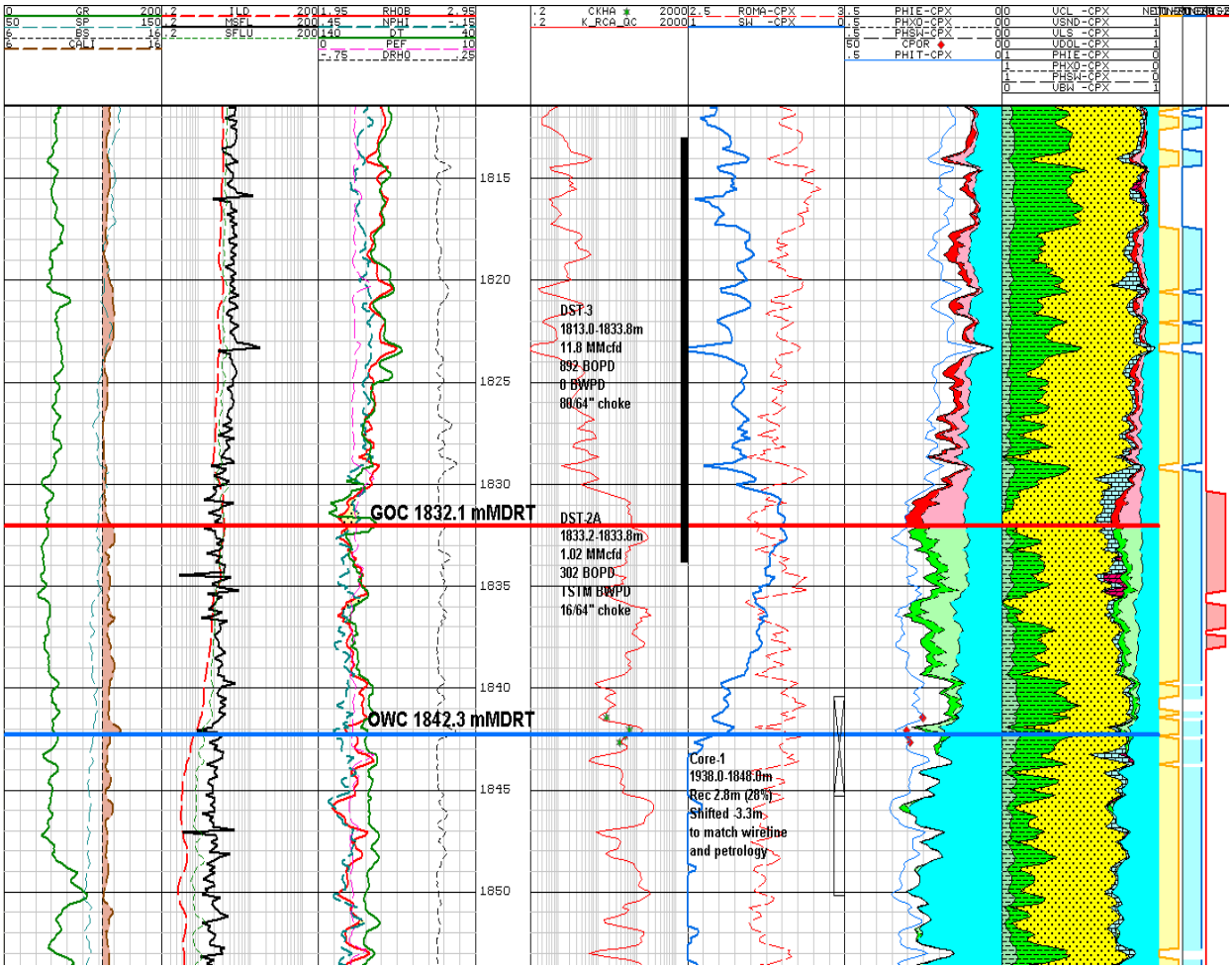

Figure 3.3: Petrophysical Summary Plot, upper EVCM.

The close proximity of Yolla-1 to a Tertiary volcano has resulted in the formation waters being highly saline, which will require careful planning for casing, logging, and cementing programmes in any future wells.

3.5 Fluid contacts

DST 2A provides the best evidence for the presence of a GOC in Yolla 1. This test initially produced oil and then subsequently gas. This is interpreted as gas

coning (see section 4.2) and places the GOC close to the top of the perforated interval i.e. 1832.2m KB in Yolla 1.

McCarthy (1995) reviewed RFT data from the upper EVCM in Yolla 1. The RFT data are ambiguous due to supercharging and tight sampling points and any precise determination of fluid contacts is extremely difficult. McCarthy (1995) concluded that the OWC lies between 1841m KB and 1856m KB. In addition, a GOC has been defined at 1832.9m. This estimate is based on the high gas flow on DST 3 and the apparent presence of gas at the 1832.5m KB sampling point (although no records of this sample can be found). McCarthy (1995) interprets a sonic kick in the interval 1830-1833m KB as due to the presence of free gas.

Petrophysical analysis (section 2.4) defines the OWC contact at 1831.1m SS (1842.2m KB Yolla 1). This appears to be the most accurate estimate for the OWC. No evidence for a gas cap is evident in this log analysis see section 3.4 and Appendix 2.

3.6 Structure

Depth maps were produced for the top of the TEV4 horizon. Conformable surfaces were then constructed for the other Upper EVCM horizons (see Table 3.1). The mapping shows that there is a shallow-dipping four-way dip southeast to northwest trending anticlinal structure at the TEV level. There is 24m of closure at the top TEV4 stratigraphic level (Fig. 3.4). The 1831.1m SS fluid contact coincides with the spill point for the TEV4 zone. The entire upper EVCM reservoir section is below the fluid contact in Yolla 2. Using this same fluid contact it is clear that there is no structural closure for all zones above the TEV4 (Fig. 3.4).

This data supports the petrophysical interpretation that there is no pay above the TEV4. This must clearly be the case if there is no trapping mechanism above this level.

3.7 Modelling methodology

The top TEV4 depth map was imported into Petrel 3D geological modeling software. Conformable surfaces were then constructed for all other upper EVCM horizons. Effective porosity curves for Yolla 1 and Yolla 2 were also imported. Fault polygons for the upper EVCM were imported and constructed within the software. A 100 x 100m horizontal grid scale was used to construct a pillar model. Eight stratigraphic zones were constructed TEV1, TEV1A, TEV2, TEV3, TEV4, TEV5, TEV6 and TEV7 (Fig. 3.1). These zones were subdivided into subzones of approximately 1m increments for the purposes of property modeling.

Porosity curves from Yolla 1 and Yolla 2 were upscaled and modeled using a stochastic sequential gaussian algorithm. As the lateral variability of the reservoir is not well understood, several different realizations using varying variogram ranges were undertaken. This allowed the sensitivity of OGIP to reservoir continuity to be examined.

Water saturation was calculated from porosity for the purposes of OGIP calculation using the following algorithm:

IF porosity < 0.31 then (Sw = -2.21575 x (porosity) + 1.07966)
IF porosity >= 0.31then (Sw = 0.38)

This algorithm was determined from the petrophysical interpretation from Yolla 1 above the transition zone (Fig 3.5).

Permeability was calculated from porosity using the equation outlined in section 3.3.

3.8 Hydrocarbons in place

Deterministic estimates of oil and gas in place were undertaken. The OWC was assumed to be 1831.1m SS and in the oil and gas case the GOC was assumed to be 1833.0 m SS. A Bo of 1.601 and a Bg of 0.00562 were used in these calculations. An all oil and an all gas case were also calculated for comparison.

A 8% effective porosity and 55% water saturation cutoff was applied to the model prior to calculating OGIP. Five cases of varying variogram ranges were used to examine the sensitivity of the OGIP to reservoir continuity. Figure 3.6 shows the effect this variation has upon the porosity grid within the model. The results of the volumetric calculations are shown in Table 3.4.

Case	Oil + Gas		Oil (mil bbls)	Gas (bcf)
	Oil (mil bbls)	Gas (bcf)		
3000m range	12.2	10.1	18.6	29.7
2000m range	13.0	10.5	19.6	31.3
1000m range	14.6	11.3	21.6	34.6
500m range	15.5	13.0	23.6	37.7
100m range	15.8	12.7	23.8	38.1

Table 3.4: Results from deterministic volumetric calculation for all gas, all oil and oil + gas cases. OWC/GWC of 1831.2m SS and a GOC of 1821.9mm SS.

The modeling indicates that the OGIP is almost totally contained within the TEV4 zone (Table 3.5).

Variogram range		100m		500m		1000m		2000m		3000m	
OIL CASE	TEV1	0		0		0		0		0	
	TEV1A	0		0		0		0		0	
	TEV2	0		0		0		0		0	
	TEV3	0		0		0		0		0	
	TEV4	22.9		22.9		20.9		18.5		17.4	
	TEV5	0		0		0		0		0	
	TEV6	0.9		0.7		0.7		1.1		1.2	
	TEV7	0		0		0		0		0	
	TEV1	0		0		0		0		0	
GAS CASE	TEV1A	0		0		0		0		0	
	TEV2	0		0		0		0		0	
	TEV3	0		0		0		0		0	
	TEV4	36.7		36.6		33.4		29.6		27.8	
	TEV5	0		0		0		0		0	
	TEV6	1.4		1.1		1.2		1.7		1.9	
	TEV7	0		0		0		0		0	
		Oil	*Gas*	*Oil*	*Gas*	*Oil*	*Gas*	*Oil*	*Gas*	*Oil*	*Gas*
OIL + GAS CASE	TEV1	0	0	0	0	0	0	0	0	0	0
	TEV1A	0	0	0	0	0	0	0	0	0	0
	TEV2	0	0	0	0	0	0	0	0	0	0
	TEV3	0	0	0	0	0	0	0	0	0	0
	TEV4	15.0	12.7	14.8	12.9	13.8	11.3	11.9	10.5	11.1	10.1
	TEV5	0	0	0	0	0	0	0	0	0	0
	TEV6	0.9	0	0.7	0	0.7	0	1.1	0	1.2	0
	TEV7	0	0	0	0	0	0	0	0	0	0

Table 3.5: Stratigraphic zone OGIP breakdown for each realization and hydrocarbon case. All gas volumes in bcf and oil volumes in MMstb.

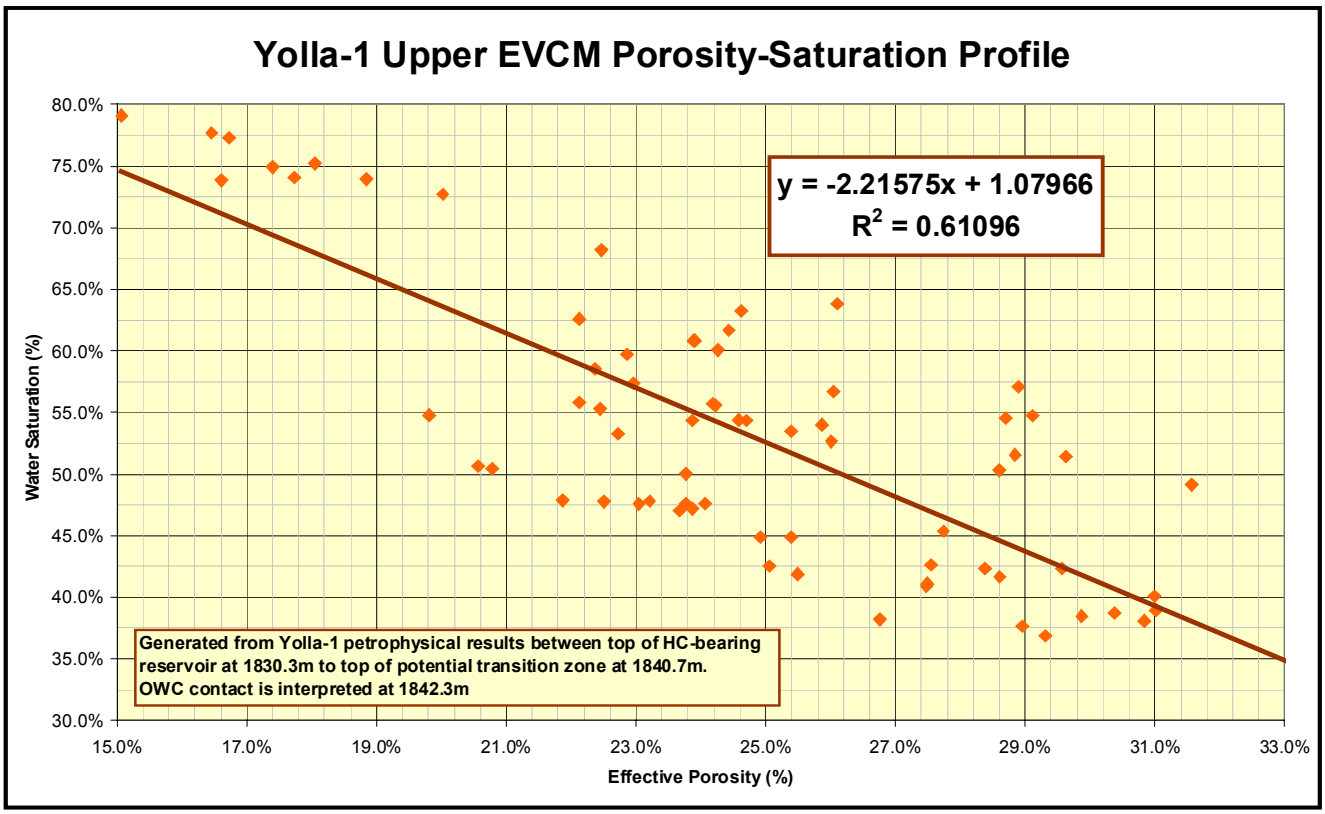

Figure 3.5: Porosity-Water Saturation crossplot for all data above fluid contact in Yolla-1. Trendline and corresponding equation is also shown.

TEV4
3000m Range

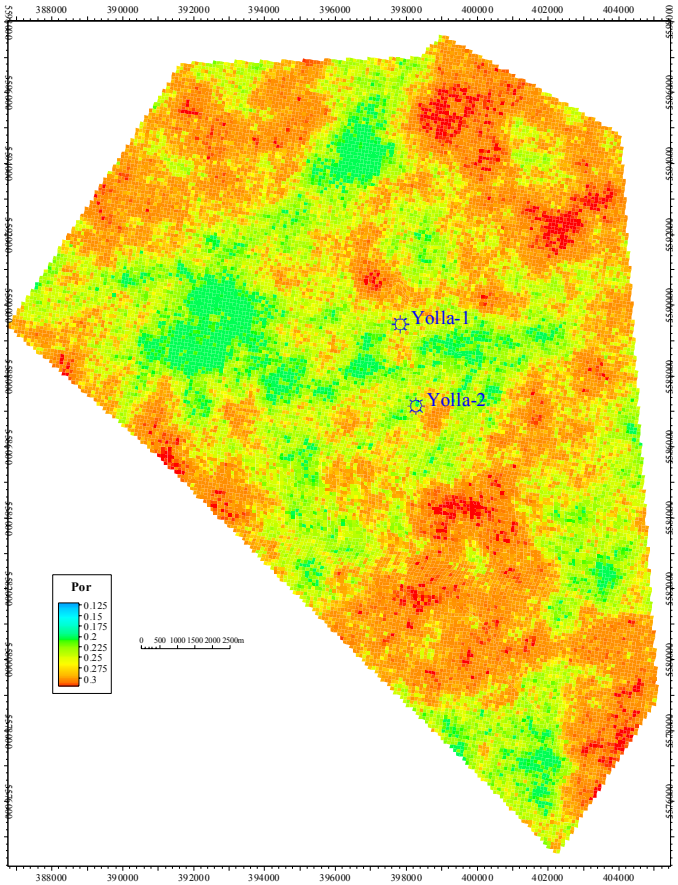

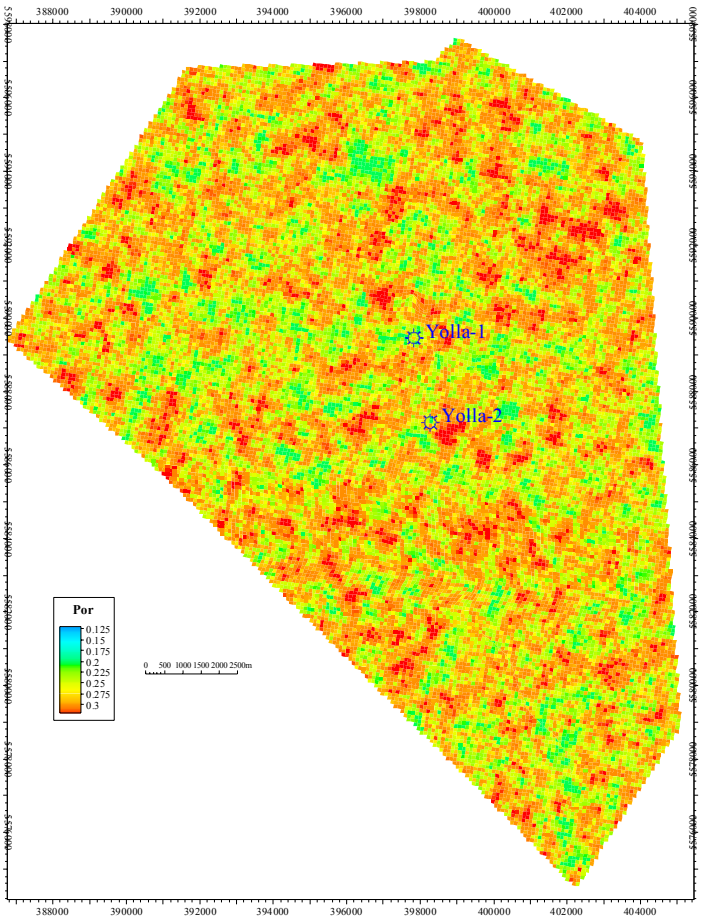

TEV4
500m Range

Figure 3.6: Comparison of porosity maps constructed in realisations where range of variogram has been altered. Porosity maps are derived from the TEV4 stratigraphic zone.

4 RESERVOIR ENGINEERING

Yolla 1 was drilled by AMOCO in 1985. The well encountered hydrocarbons in both the Intra EVCM and Upper EVCM formations. Evaluation of the gas development potential of the Intra EVCM was performed and documented on the report "Yolla Subsurface Development Plan", dated September 2001. This report reviews the 1830 Sand of the Upper EVCM formation, and studies the oil development potential of that reservoir.

The reservoir data reviewed for the 1830 Sand included RFT, DSTs 2, 2A and 3, and PLT Runs 1 and 2 performed during DSTs 2A and 3 respectively.

There are 11 and 6 valid data points available in the RFT Runs 1 and 4, respectively to evaluate the 1830 Sand. However the analysis on the Upper EVCM RFT data failed to determine the fluid type and the contacts in the 1830 Sand. No conclusive information can be drawn from the Upper EVCM RFT data.

DST 2 was considered to be invalid due to the extraneous water production. Therefore, no analysis was done on the test. The interval was subsequently squeezed and a smaller interval was perforated and re-tested as DST 2A

The well test interpretation on DST 2A appears unreliable. This is because the build-up data are still within the wellbore storage influenced region and the radial flow regime has not fully developed. Consequently, the reservoir parameters cannot be reliably calculated.

As there is significant oil and gas production during the DST 3, it is possible that the test interval straddled across a GOC with combined free gas and oil production. This postulation appears to be confirmed by the open-hole log interpretation results. There is some evidence of the existence of a free gas zone at the top of the 1830 Sand , based on the petrophysical interpretation on the Upper EVCM well logs.

Analysis of the DST 3 data indicates that ranges in the KH and P* values from 180 to 272 md-ft and 2606.4 to 2625.1 psia, respectively using the oil and gas properties. The Darcy skin ranges between –3.6 to 2.9 using oil and gas properties. This compares well with AMOCO's interpretation of 258 md-ft KH and 0.5 Darcy skin, but not the 2707 psia P*. The cause of the variation in the P* is mainly due to the use of different production time between this and AMOCO's analyses. As there is no detailed rate calculation information available, it is difficult to know how AMOCO's production time is derived.

The value of the P* is crucial in determining the extent of possible reservoir depletion and the possible range of the initial hydrocarbon in-place volumes. Based on this analysis, it is possible that there is reservoir depletion to some extent during DST 3.

PLT Run 1 was run during DST 2A. The analysis on File 3 (Pass 3) data of the PLT Run 1 indicates a small depth shift of about 2m, but that all production is from the perforated interval. The produced fluid is oil, possibly with gas entrained with a density of about 0.78 g/cc. The PLT enters sump brine immediately below the perforations, which may have approximately 3m of oil standing on the brine itself. There is no obvious free gas entering the wellbore, as there is no temperature cooling effect due to the gas expansion.

In File 5 (Pass 5) of the PLT Run 1, the production appears to be all from the perforations with a fluid density of 0.46 to 0.49 g/cc. In addition, a temperature anomaly of an abrupt decrease of 1.8 ^{o}F in temperature was observed across the top perforations. The lower fluid density and the temperature anomaly indicate a quantity of free gas was being produced and began entering the wellbore with the oil at the perforations between Passes 3 and 5. The cause of this late gas production is likely to be gas coning but the source of the free gas is unknown.

PLT Run 2 was run during DST 3. Files 4 to 8 (Passes 4 to 8) were performed prior to the end of the flow test. During and after File 4, the GR and CCL readings were very noisy and the gradiomanometer suffered a calibration shift near the perforations. The density of the produced fluids above the perforations is measured at about 0.04 to 0.06 g/cc from File 4. The GR response also varies among the various PLT passes. The cause of these anomalies is likely to be the high flow rate fluid (likely to be gas) from the perforations, which caused violent movement of the tool. Apart from the conclusion that the produced fluid is predominantly gas, little quantitative information about the produced fluid type and its gravity can be drawn from the PLT Run 2 gradiomanometer survey.

The results of the CCL and GR logs, and multi-pass single cable speed spinner survey of PLT Run 2 indicate that the perforations for DST 3 were most likely shot approximately 9 metres deep. The actual perforation interval during DST 3 is likely to be 1820.5 to 1840.5 m KB, after taking into account a PLT depth shift of about 1.5m. There appears to be two major zones of influx and they are 1825 to 1833 m and 1839 to 1840.5 m KB. The majority of the production is from the interval 1832 to 1833 m KB.

In summary, the full suite of engineering data is far from conclusive regarding fluid type and contacts. The best evidence points to:

- GOC close to the DST-2A perforation interval at around 1833.2 m KB given the rapid onset of gas production from that interval, and
- OWC possibly around 1840.5 m KB from the PLT density reading and the fact that DST-2 produced water from somewhere below 1835m

Productivity is low, and given the proximity of water, there appears to be a danger of early water production if the zone were to be completed. Pressure depletion observed during DST-3 suggests a limited accumulation of hydrocarbon.

Further appraisal is required for the Upper EVCM interval in conjunction with gas development drilling.

4.1 RFT Data Review

Reservoir pressure data for determining fluid gradient and contacts is available for the Upper and Intra EVCM intervals of Yolla 1. Valid data acquired from the RFT runs is listed in Table 4.1.

The RFT data were obtained from Volume 1 of the Yolla 1 final Well Completion Report (WCR). Runs 1 and 2 consisted of strain gauge pressure measurement while Runs 4 and 5 were conducted with a HP gauge.

Run 1 data between 1818 to 1946 m KB (11 points) and Run 4 data were used to evaluate the hydrocarbon zones within the Upper EVCM interval (1830 Sand). As HP gauge has higher accuracy than strain gauge, a -15 psi adjustment is required on the strain gauge data to line up Runs 1 and 4 data. The combined Runs 1 and 4 RFT points are used to establish a common water gradient line. The resulting RFT data plots for the 1830 Sand are presented in Figures 4.1 and 4.1A.

As observed in Figure 4.1, a common water gradient as 0.441 psi/ft (1.446 psi/m) can be inferred. DST-2A (1833.2 – 1833.8m KB) and DST-3 (1820.5 – 1840.5 m KB) appeared to produce predominantly oil and gas respectively (refer 4.2). Likewise, water production in DST-2 proved the existence of water somewhere below the interval tested by DST-3. However, there are insufficient reliable RFT points to be able to infer either a GOC or an OWC.

No conclusive information can be drawn regarding fluid contacts from the Upper EVCM RFT data.

Run No	Depth (m KB)	Pressure	
		(psi)	(psia)
Run 1	1818.0	2731.0	2745.7
	1833.0	2737.0	2751.7
	1832.5	2707.0	2721.7
	1839.0	2716.0	2730.7
	1843.0	2724.0	2738.7
	1846.5	2724.0	2738.7
	1856.0	2738.0	2752.7
	1868.0	2748.0	2762.7
	1905.0	2821.0	2835.7
	1921.0	2835.0	2849.7
	1946.0	2873.0	2887.7
	2034.0	3004.0	3018.7
	2125.0	3145.0	3159.7
	2215.0	3284.0	3298.7
	2327.0	3400.0	3414.7
	2428.0	3541.0	3555.7
	2725.0	4073.0	4087.7
	2756.0	4120.0	4134.7
	2760.0	4108.0	4122.7
	2763.3	4105.0	4119.7
	2811.0	4153.0	4167.7
	2813.0	4147.0	4161.7
	2819.0	4570.0	4584.7
	2820.0	4576.0	4590.7
	2820.5	4573.0	4587.7
	2823.5	4571.0	4585.7
	2845.5	4140.0	4154.7
Run 2	2725.0	4070.0	4084.7
	2760.5	4099.0	4113.7
	2763.3	4108.0	4122.7
	2811.0	4137.0	4151.7
	2820.0	4107.0	4121.7
	2821.0	4131.0	4145.7
	2823.5	4129.0	4143.7
	2545.5	4114.0	4128.7
Run 4	1845.0		2725.7
	1832.7		2710.1
	1830.0		2712.0
	1833.0		2709.3
	1837.0		2712.8
	1845.0		2722.4
Run 5	2724.0		4125.0
	2761.3		4156.0
	2820.0		4170.5
	2874.0		4238.0
	2952.5		4382.4
	2973.5		4387.2
	2988.0		4392.0

Table 4.1: Yolla 1 RFT Pressures

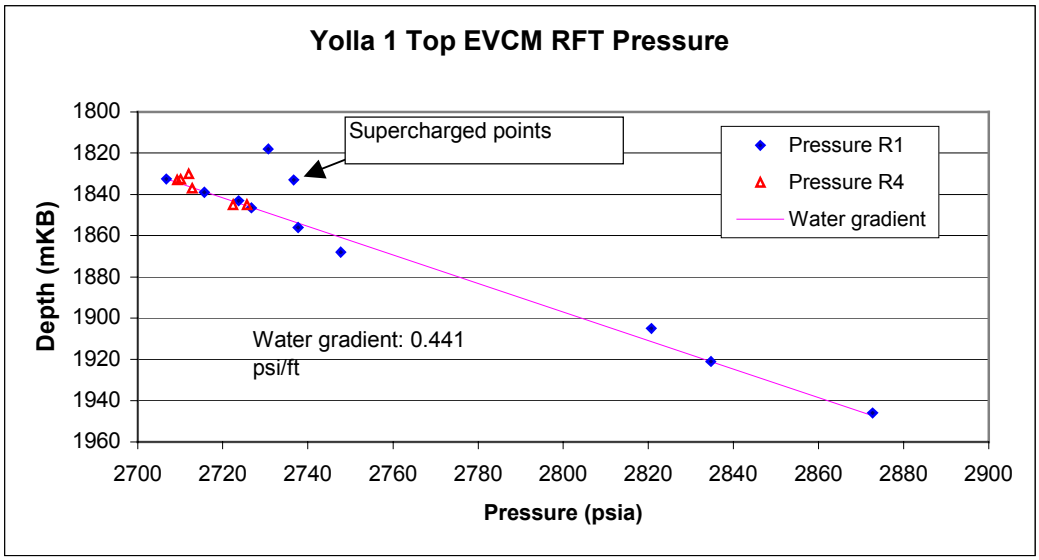

Figure 4.1: Yolla 1 1830 Sand RFT Pressure

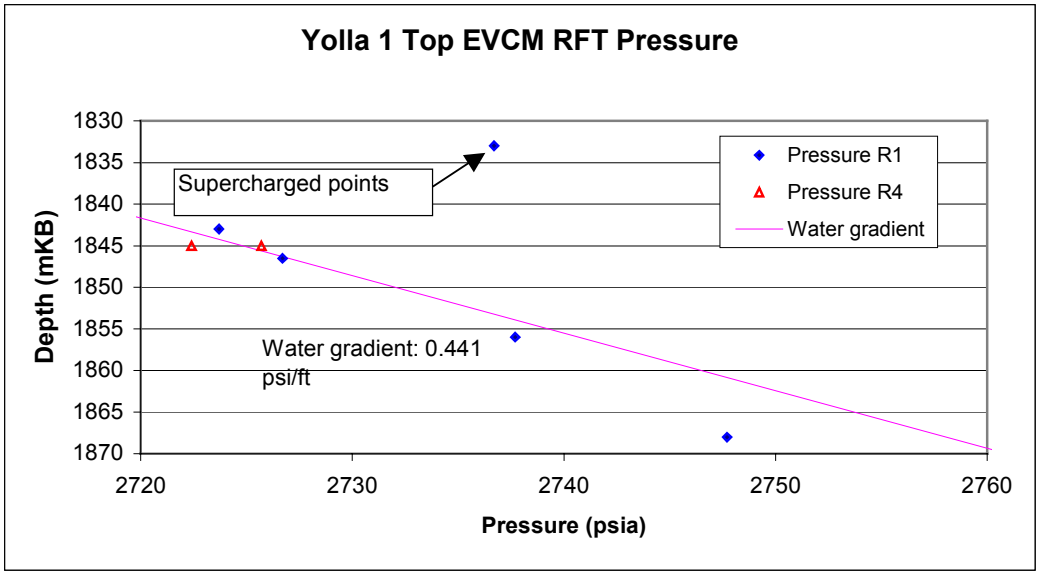

Figure 4.1A: Yolla 1 1830 Sand RFT Pressure - Detail

4.2 DST Data Review

Three DSTs (DST 2, 2A and 3) have been conducted on the 1830 Sand of Yolla 1. The testing results are summarised as follows in Table 4.2.

DST No	Test Interval (m KB)	Test Rate		
		Oil (bopd)	Gas (MMscfd)	Water (bwpd)
2	1830.0 – 1835.5	RTSTM	2.2	1675
2A	1833.2 – 1833.8	302	1.0	Nil
3	1820.5 – 1840.5	892	11.8	Nil

Table 4.2: 1830 Sand DST testing result summary

4.2.1 DST 2 Data Interpretation

DST 2 was considered to be invalid due to the extraneous water production. The source of the water is suspected to be from channeling behind the casing. Therefore, no analysis was done on the test. The interval was subsequently squeezed and a smaller interval was perforated and re-tested as DST 2A.

4.2.2 DST 2A Data Interpretation – Analytical Approach

DST 2A was perforated from 1833.2 to 1833.8 m KB. The test consists of 13.3 hours of flow and 5.5 hours of shut-in periods. Water production was negligible during the flow period, which suggests that the squeeze was successful.

Analysis of the DST data indicates the reservoir characteristics outlined below (Table 4.3). The analysis results from Sigma and AMOCO are also included for comparison.

	This Analysis	Sigma	AMOCO
Reservoir Model	Radial homogeneous	Dual layer & radial homogeneous	Radial homogeneous
Fluid Type	Oil	Oil & Gas	Gas
Permeability, md	101.4	67 – 141	28.6
Thickness, ft	5	30.8	2
KH, md-ft	507	2067 – 4330	57.2
Skin	18.2	25 – 62	5.7
Pi (psia)	2697.3	2679 – 2693	2713
Interpretation method	Analytical simulation	Analytical simulation	Horner analysis

Table 4.3: Comparison of interpretation results of Yolla 1 DST 2A

The log-log diagnostic plot of the build-up data is shown in Figure 4.2. As observed from the log-log plot, the build-up data is still affected by the wellbore storage effect and the radial flow regime is not fully developed. The analysis of the build-up data can only proceed by adapting a radial homogeneous, infinitely acting reservoir model. The reservoir parameters can only be determined from the analytical simulation process (auto match). The detailed DST 2A interpretation is presented in Appendix 3.

There are significant discrepancies among the different interpretations. This is mainly because the radial flow regime has not fully developed and the reservoir parameters cannot be reliably calculated. The use of different fluid properties also contributes to those discrepancies.

AMOCO's interpretation results may have a lower level of confidence, because their interpretation uses only Horner analysis. A fully developed infinite acting radial flow regime is required for Horner analysis.

4.2.3 DST 3 Data Interpretation – Analytical Approach

After DST 2A, the interval from 1813.0 to 1833.1 m KB of the Upper EVCM was perforated. However, there is strong evidence from PLT Run 2 (refer 4.2.6) during DST 3 that the perforations for DST 3 were shot approximately 9 meters deep. The actual perforation interval is estimated to be 1820.5 to 1840.5 m KB, after PLT depth shift correction (-1.5 m). Thus DST 3 tested the interval of 1820.5 to 1840.5 m KB (instead of the intended 1813.0 to 1833.8 m KB interval) with 6.6 hours of flow and 8.4 hours of shut-in periods.

As there is significant oil and gas production during the test, it is possible that the test straddled across a GOC with combined free gas and oil production. This postulation appears to be confirmed by the open-hole log interpretation results. There is some evidence of the existence of a free gas zone in the top of the 1830 Sand above 1833.2 m KB, based on the petrophysical interpretation on the Upper EVCM well logs.

As the analytical well test analysis package cannot handle the multi phase production, the analysis was performed using gas and oil properties separately, and the results were summarised below. A producing thickness of 20 feet (approx. 6 metres) was used consistent with the contributing interval indicated by the PLT run (refer 4.2.6). For comparison purposes AMOCO's interpretation has been included.

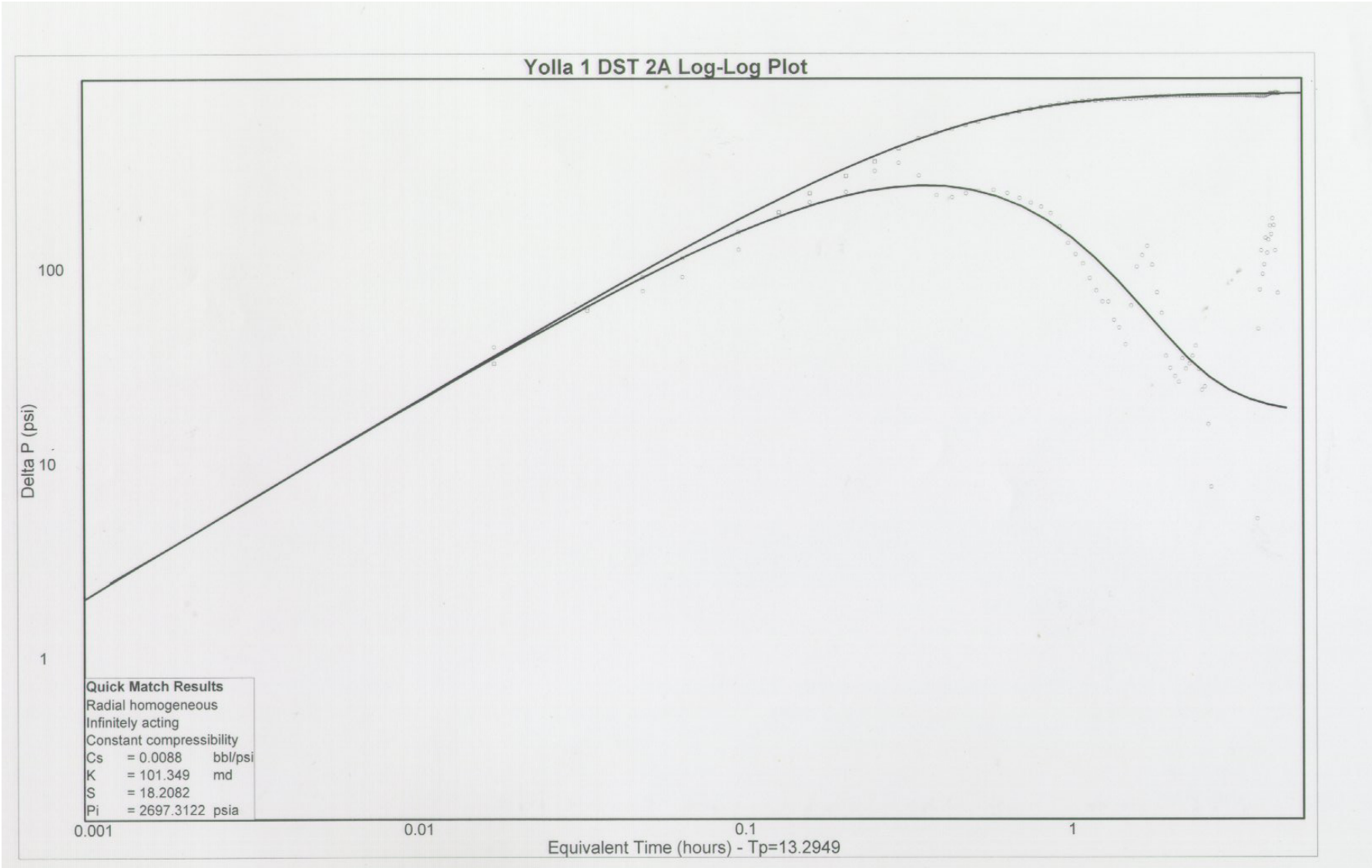
Yolla 1 DST 2A Log-Log Plot
100
10
1
Delta P (psi)
Quick Match Results
Radial homogeneous
Infinitely acting
Constant compressibility
Cs = 0.0088 bbl/psi
K = 101.349 md
S = 18.2082
Pi = 2697.3122 psia
0.001
0.01
0.1
1
Equivalent Time (hours) - Tp=13.2949

Figure 4.2

	This Analysis		AMOCO
Reservoir Model	Radial homogeneous		Radial homogeneous
Fluid Type	Oil	Gas	Gas
Permeability, md	13.6	9.0	16.1
Thickness, ft	20	20	16
KH, md-ft	271.7	180.4	258.2
Skin	2.9	- 3.6	0.5
Production time (hr)	6.6	6.6	12.5
Pi (psia)	2606.4	2625.1	2707
Interpretation method	Analytical simulation	Analytical simulation	Horner analysis

Table 4.4: Comparison of interpretation results of Yolla 1 DST 3

For analysis, a radial homogeneous, infinite acting model was selected for DST 3. The selection is based on the log-log diagnostic plot as shown in Figure 4.3. On the log-log plot, the pressure derivative leveled off and reached the radial flow regime after the wellbore storage effect. The pressure appears to have leveled off at the end of the test, however some scattering in the pressure derivatives was observed. The cause of this behaviour is unknown and may be due to the boundary effect. The determination of the boundary effect is inconclusive as the LTR (late time regime) pressure derivative trend is not stabilised and established. The detailed DST 3 interpretation is presented in Appendices 4 and 5 using oil and gas properties, respectively.

As the radial flow has been fully developed, the results of the analytical simulation and AMOCO's Horner analysis are comparable, except the extrapolated reservoir pressure (P*). This is mainly caused by the use of different production time between this and AMOCO's analyses. The 6.6 hours of production time used in this analysis is the time duration of the flow period. It is suspected that AMOCO used the equivalent production time (the cumulative production over the production rate just before closing in). As there is no detailed rate calculation information available, it is difficult to know how AMOCO's production time is derived.

Due to the uncertainty in the production time calculation and the limit of the analytical analysis on the multi phase flow, the determination of the extrapolated reservoir pressure and the extent of the reservoir depletion were inconclusive. However, it is possible that there is reservoir depletion to some extent during DST 3, which indicates a small initial hydrocarbon in-place volume.

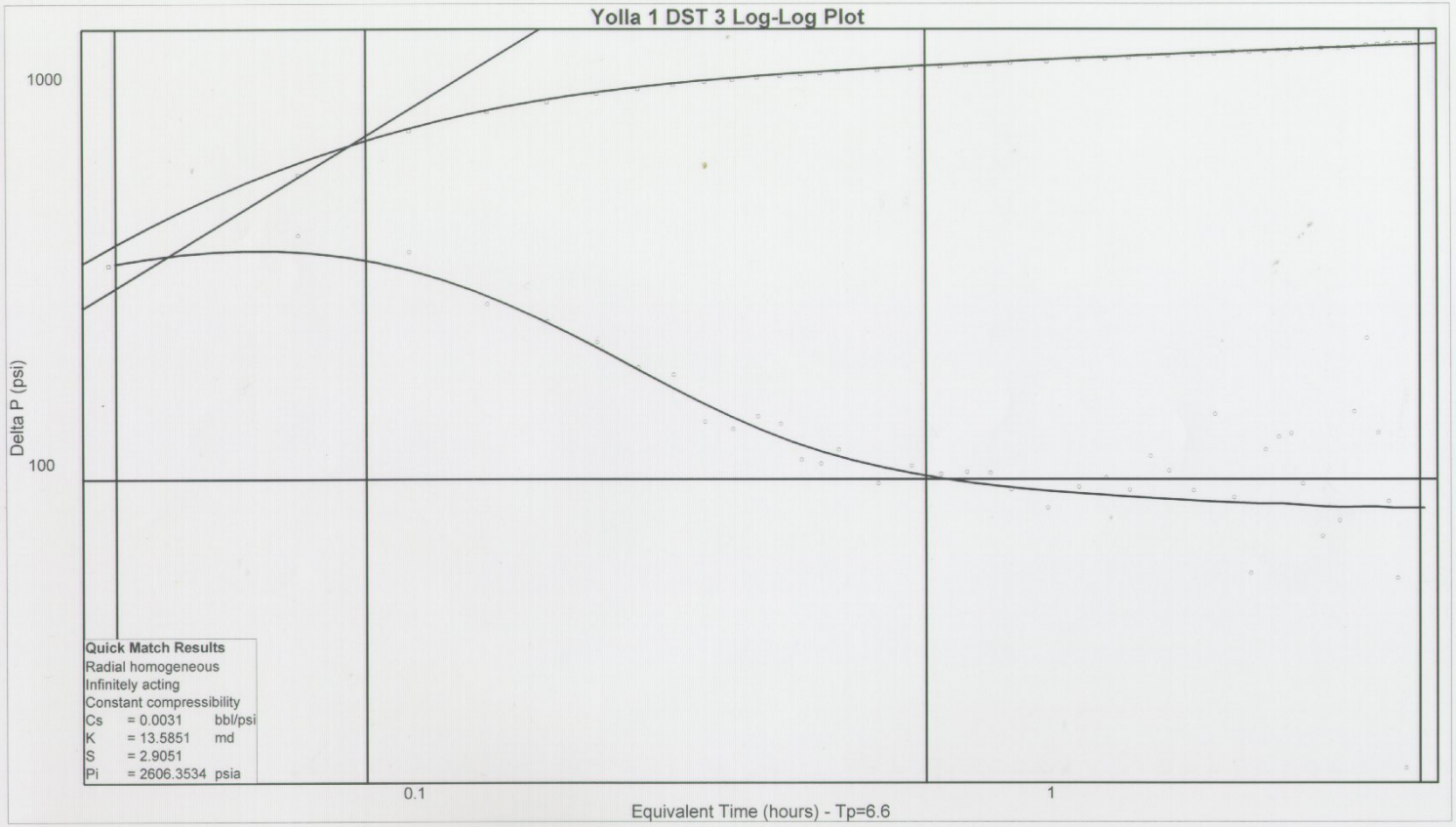
Yolla 1 DST 3 Log-Log Plot
1000
100
Delta P (psi)
0.1
1
Equivalent Time (hours) - Tp=6.6
Quick Match Results
Radial homogeneous
Infinitely acting
Constant compressibility
Cs = 0.0031 bbl/psi
K = 13.5851 md
S = 2.9051
Pi = 2606.3534 psia

Figure 4.3

4.2.4 PLT Data Review

PLT Runs 1 and 2 were conducted during DSTs 2A and 3 periods, respectively. The PLT tool consisted of GR, CCL, temperature, HP pressure and gradiomanometer sensors, with a flowmeter spinner added for DST-3. The objective of the PLT runs was to determine the type of the fluid produced, its gravity across the production interval, and in DST-3, the inflow contribution along the 20 metre perforated interval.

The PLT tool was also stationed below the perforations to measure the flowing bottomhole pressure during DST 2A, and flowing and shut-in bottomhole pressure during DST 3.

4.2.5 PLT Run 1 Review

PLT Run 1 was performed on the clean up flow period of DST 2A. The run sequence of event was summarised below.

Date	Time (hr)	Event	File (Pass) No
3 October, 1985	12:10	Rig up PLT	
	14:50	RIH PLT	1
	16:05	Flow well	
		Log FBHP	2
	19:53	Log under flow condition (down)	3
		Log FBHP	4
4 October, 1985	05:07	Log under flow condition (down)	5
	05:26	Well shut-in	
	06:30	POOH PLT/Rig down	6

Table 4.5: PLT Run 1 sequence of event summary

File 3 (Pass 3) was performed under flow conditions at about the middle and File 5 (Pass 5) at the end of the flow test. Based on the qualitative analysis on the temperature and gradiomanometer survey results of File 3 as shown in Figure 4.4, and allowing for an apparent depth shift of about 2 metres, all production is entering the perforations (1833.2 to 1833.8 m KB). The fluid density is about 0.78 g/cc, which suggests the fluid is oil. The PLT enters sump brine immediately below the perforations, which may have approximately 3m of oil standing on the brine itself. There is no obvious free gas entry point around the perforations as there are no temperature anomalies due to the gas expansion effect.

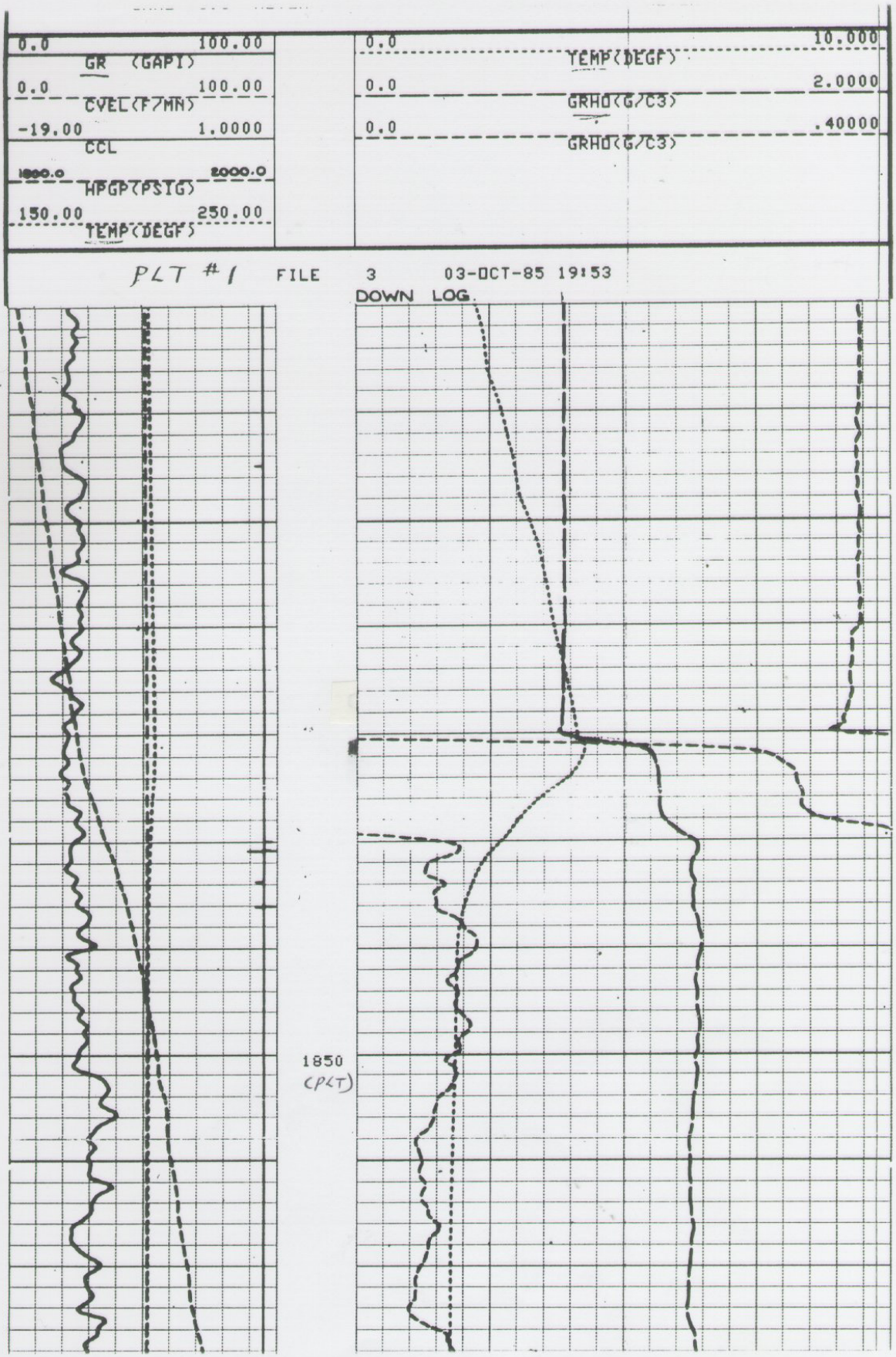
0.0
100.00
GR (GAPI)
0.0
100.00
CVEL(F/MN)
-19.00
1.0000
CCL
1000.0
2000.0
HPGP(PSIG)
150.00
250.00
TEMP(DEGF)
0.0
10.000
TEMP(DEGF)
0.0
2.0000
GRHO(G/C3)
0.0
.40000
GRHO(G/C3)
PLT #1
FILE 3
03-OCT-85 19:53
DOWN LOG.
1850
(PLT)

Figure 4.4

Later in the flow period of DST-2A, based on the File 5 results as shown in Figure 4.5, the production appears to be all from the perforations between 1833.2 to 1833.8 m KB, but now with a fluid density of 0.38 to 0.46 g/cc. There is no depth shift observed in File 5. In addition, a temperature anomaly of an abrupt decrease of 1.8 ^{o}F in temperature (gas cooling effect) was observed in top perforations. The change in fluid density (between Files 3 and 5) and the temperature anomaly indicates a quantity of free gas was being produced and began entering the wellbore with the oil at the perforations between Passes 3 and 5. The cause of this late gas production is likely to be gas coning but the source of the gas is unknown.

The PLT Run 1 result suggests a possible GOC existed above 1833.2 m KB.

4.2.6 PLT Run 2 Review

PLT Run 2 was performed on the clean up flow and shut-in periods of DST 3. The run sequence of event was summarised below in Table 4.6.

Date	Time (hr)	Event	File (Pass) No
4 October, 1985		Perforate 1813.0 to 1833.1 m	
	14:10	Rig up PLT	
	16:30	RIH PLT & log shut-in survey	1, 2
	17:55	Flow well	
		Log FBHP	3
5 October, 1985	00:11	Log under flow condition (down)	4
	00:14	Log under flow condition (up)	5
	00:25	Log under flow condition (down)	6
	00:29	Log under flow condition (up)	7
	00:30	Log under flow condition (down)	8
	00:30	Shut in well	
	00:37	Log under SI condition (up)	9
	00:41	Log under SI condition (down)	10
	00:44	Log under SI condition (up)	11
		Log SIBHP	12
	06:06	Log under SI condition (down)	13
	06:30	POOH PLT/Rig down	

Table 4.6: PLT Run 2 sequence of event summary

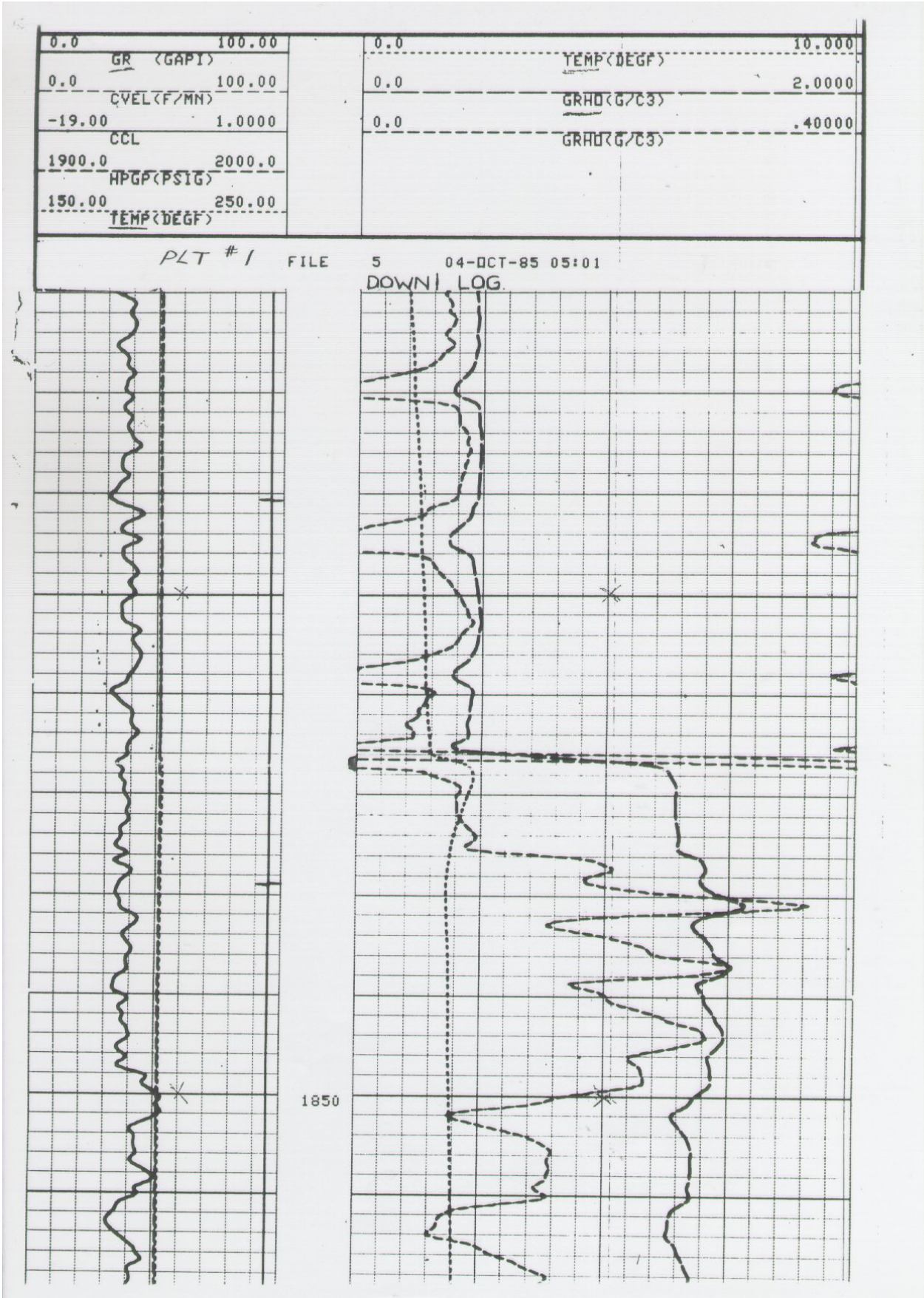
0.0
100.00
GR (GAPI)
0.0
100.00
CVEL(F/MN)
-19.00
1.0000
CCL
1900.0
2000.0
HPGP(PSIG)
150.00
250.00
TEMP(DEGF)
0.0
10.000
TEMP(DEGF)
0.0
2.0000
GRHO(G/C3)
0.0
.40000
GRHO(G/C3)
PLT #1
FILE 5
04-OCT-85 05:01
DOWN LOG
1850

Figure 4.5

PLT Run 2 was run during DST 3. Files 4 to 8 (Passes 4 to 8) were performed prior to the end of the flow test. During and after File 4, the GR and CCL readings were very noisy and the gradiomanometer appeared to suffer a calibration shift near the perforations (1834 to 1842 m KB log depth). The density of the produced fluids above the perforations is measured at about 0.04 to 0.06 in File 4. In later files, the gradiomanometer density reading appears to negative, and therefore obviously wrong. The GR response also varies among the various PLT passes. Figures 4.6, 4.7 and 4.8 illustrate the noisy PLT response and gradiomanometer shift near the perforations for Files 4, 5 and 6, separately. The cause of these anomalies is likely to be the high flow rate fluid (likely to be gas) from the perforations moving the tool violently, and in the case of the gradiomanometer, the tool possibly suffered damage due to direct impact from gas jets from the perforations. As a result, information about the produced fluid type and its gravity during DST-3 can be drawn solely from File 4 and is incomplete and inconclusive about entry into the wellbore of fluid other than gas.

There is strong evidence from PLT Run-2 during DST-3 that the perforations for DST-3 were shot approximately 9 metres deep. This would correspond to an error of 1 joint of casing in the CCL correlation prior to perforating. The evidence is as follows:

- CCL traces on the PLT log showing evidence of perforations between about 1822m and 1842 metres PLT log depth, rather than the intended 1813m to 1833.8m interval. Gamma ray correlations indicate that PLT traces are recorded approximately 1.5 metres deep, putting the actual perforation interval at 1820.5 – 1840.5m KB
- Elevated gamma ray readings down to 1842m metres PLT log depth, below the intended base of perforations at 1833.7m
- Extreme tool disturbance on the temperature and density curves between 1834 and 1842m PLT log depth, consistent with perforation influx jet impingement, but again below the intended base of the perforations at 1833.8
- Gamma ray curves away from the perforated interval are consistent with open hole readings implying that the PLT itself is within 1.5 to 2m of being on depth. The error is therefore in the perforations themselves.

The multi-pass single cable speed spinner survey is presented in Figure 4.9. Based on the spinner run results, and accounting for the true perforated interval of approximately 1820.5 – 1840.5 m KB, there appear to be two major zones of influx within the perforated interval. These are:

- 1825 – 1833m KB. The main influx is occurring in this region, with the majority occurring in the interval 1831.5 – 1833m. This is close to the zone flowed during DST-2A. Gradio and temperature disturbance evident in File 4 suggest that this interval is the source of the gas flow

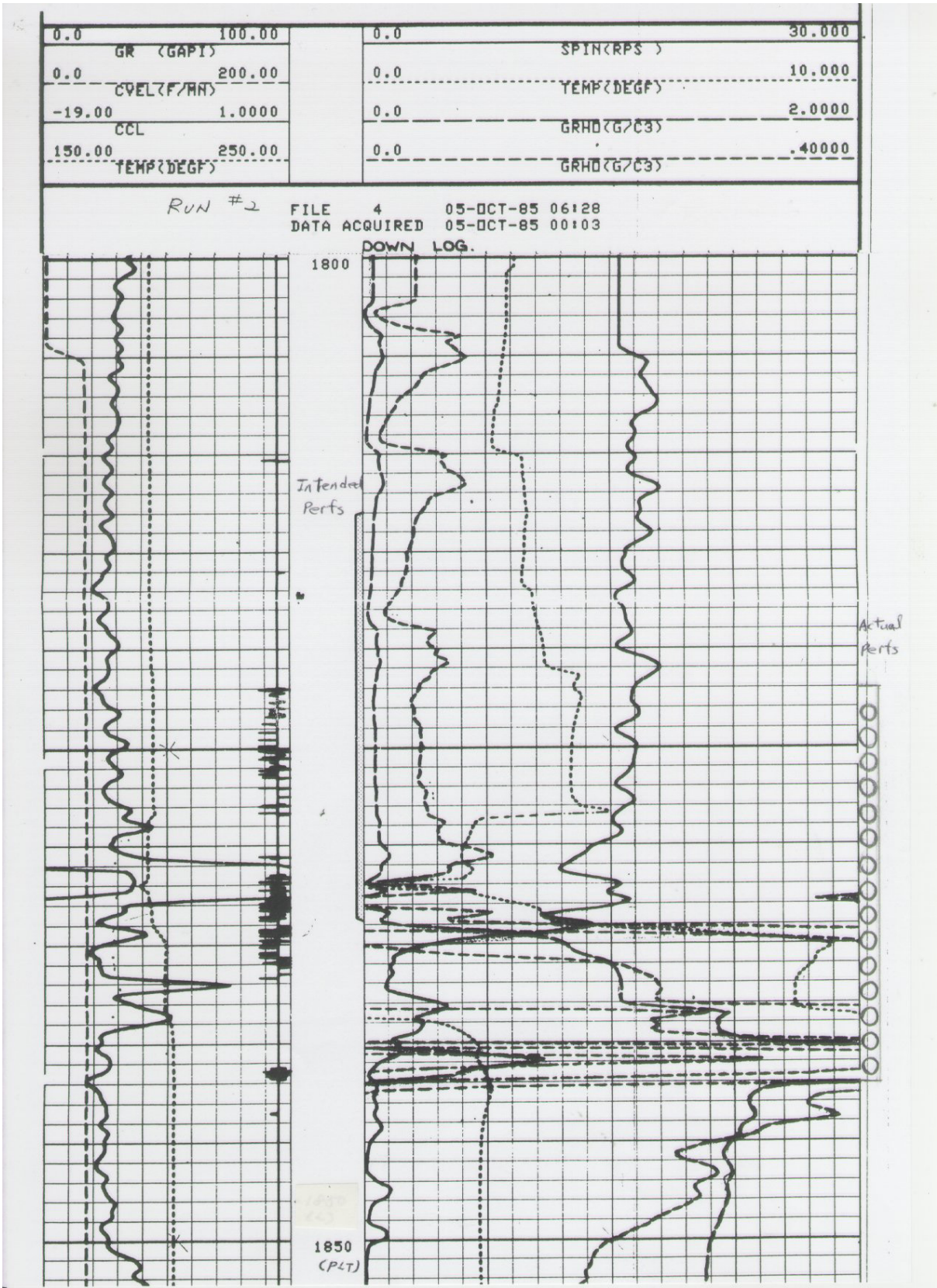
0.0
100.00
GR (GAPI)
0.0
200.00
CVEL(F/MN)
-19.00
1.0000
CCL
150.00
250.00
TEMP(DEGF)
0.0
30.000
SPIN(RPS)
0.0
10.000
TEMP(DEGF)
0.0
2.0000
GRHO(G/C3)
0.0
.40000
GRHO(G/C3)
RUN #2
FILE 4 05-OCT-85 06:28
DATA ACQUIRED 05-OCT-85 00:03
DOWN LOG.
1800
Intended Perfs
Actual Perfs
1850
(PLT)

Figure 4.6

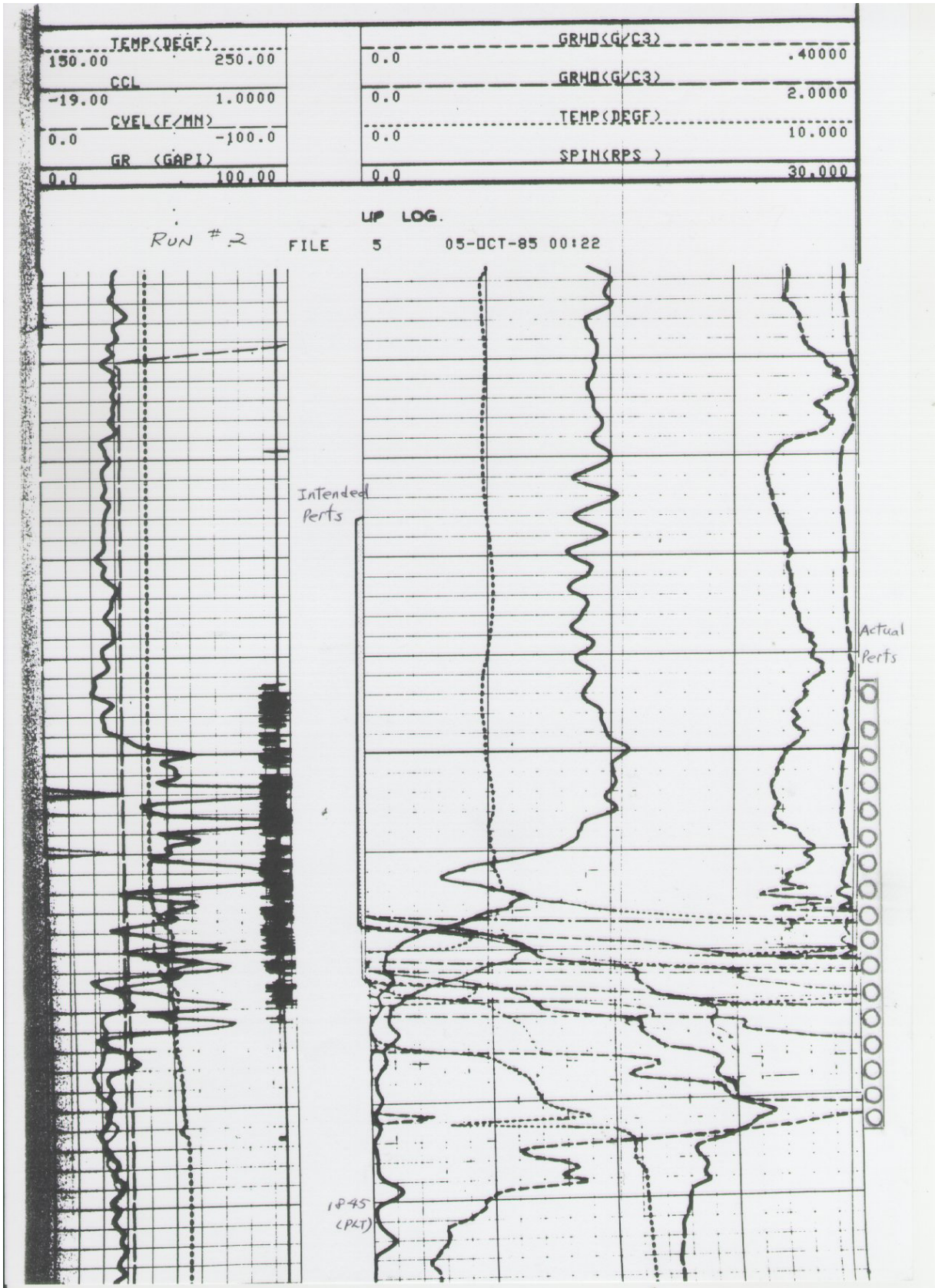
TEMP(DEGF)
150.00
250.00
CCL
-19.00
1.0000
CVEL(F/MN)
0.0
-100.0
GR (GAPI)
0.0
100.00
GRHD(G/C3)
0.0
.40000
GRHD(G/C3)
0.0
2.0000
TEMP(DEGF)
0.0
10.000
SPIN(RPS)
0.0
30.000
UP LOG.
RUN #2
FILE 5
05-OCT-85 00:22
Intended Perfs
Actual Perfs
1845 (PKT)

Figure 4.7

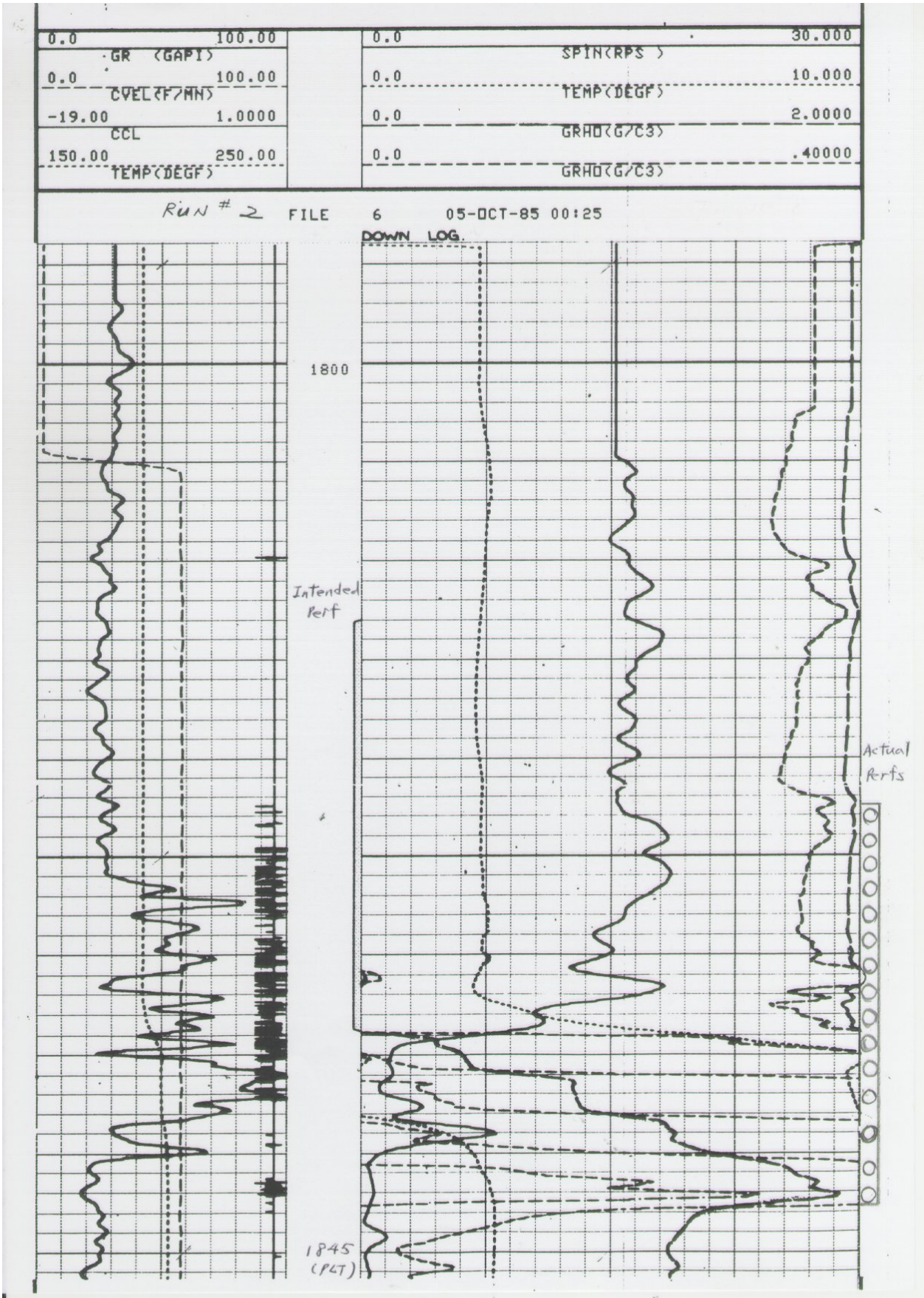
0.0
100.00
GR (GAPI)
0.0
100.00
CVEL(F/MN)
-19.00
1.0000
CCL
150.00
250.00
TEMP(DEGF)
0.0
30.000
SPIN(RPS)
0.0
10.000
TEMP(DEGF)
0.0
2.0000
GRHO(G/C3)
0.0
.40000
GRHO(G/C3)
RUN # 2 FILE 6 05-OCT-85 00:25
DOWN LOG.
1800
Intended Perf
Actual Perfs
1845 (PLT)

Figure 4.8

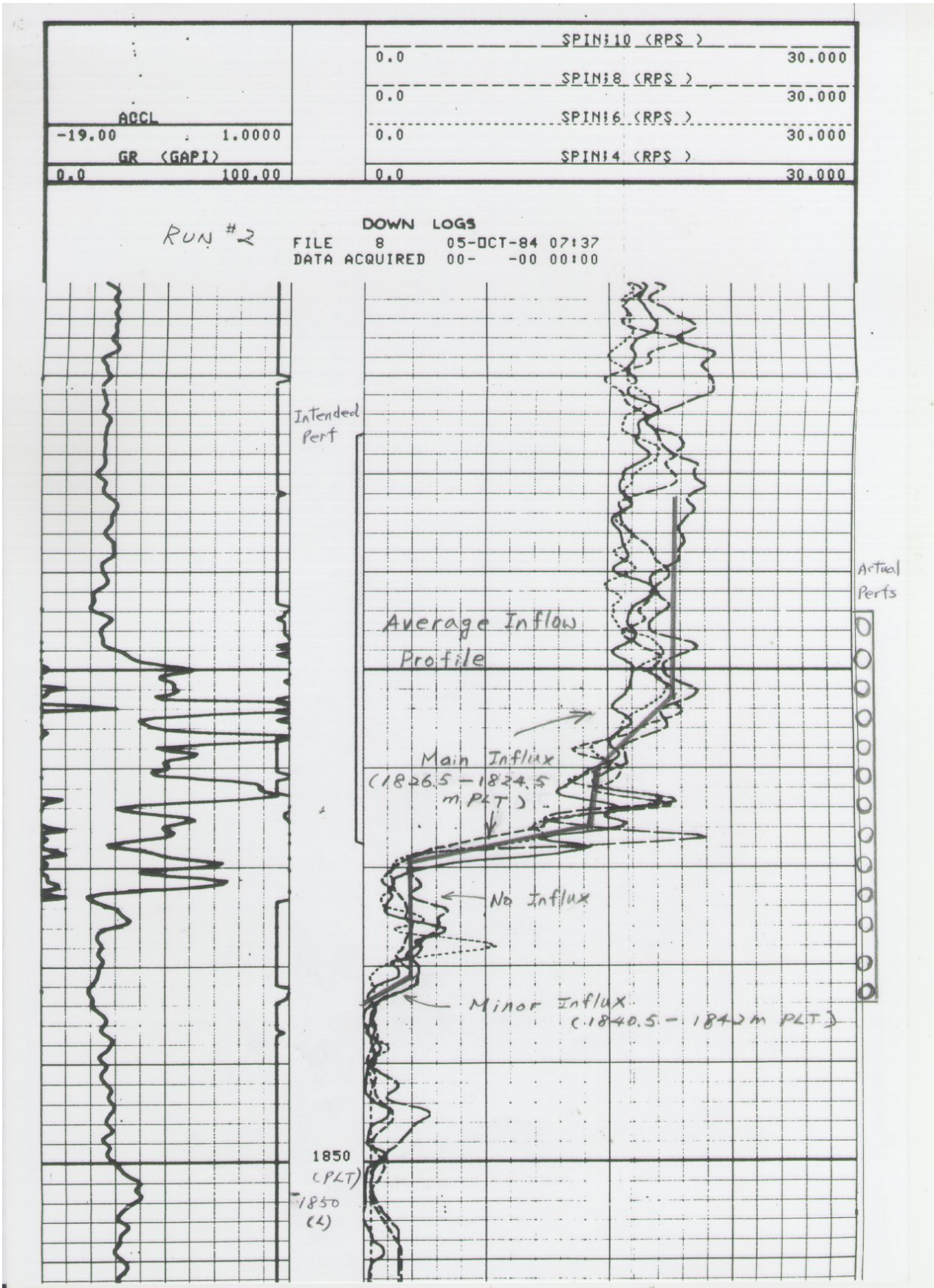
SPIN;10 (RPS)
0.0
30.000
SPIN;8 (RPS)
0.0
30.000
SPIN;6 (RPS)
0.0
30.000
SPIN;4 (RPS)
0.0
30.000
ACCL
-19.00
1.0000
GR (GAPI)
0.0
100.00
RUN #2
DOWN LOGS
FILE 8 05-OCT-84 07:37
DATA ACQUIRED 00- -00 00:00
Intended Perf
Actual Perfs
Average Inflow Profile
Main Influx (1826.5 - 1824.5 m PLT)
No Influx
Minor Influx (1840.5 - 1842 m PLT)
1850 (PLT)
1850 (4)

Figure 4.9

from the test, and that therefore gas has overrun the oil production seen at the start of DST-2A.

- 1839 – 1840.5m KB. A small influx contribution is coming from this interval. From gradio readings in File 4 taken before that instrument lost calibration, there is a short section of stable density measurement at 1836-1838m (PLT depth), between the contributing zones. The density reading is 1.04 g/cc suggesting liquid rather than gas. At that density, this liquid is presumably water. No water was reported from DST-3 so it is presumed that the water flow was very small and not evident in the separator readings taken at surface. Below the perforations, the density reading is 1.38 g/cc; high but consistent with mud in the sump.

The above spinner survey results compare well with petrophysical interpretation of:

- Top hydrocarbon bearing zone: 1824.5 m KB
- Bottom hydrocarbon bearing zone: 1838.1 m KB
- Best production interval (permeability streak): 1831.3 to 1832 m KB

The combined PLT Run 2 and DST 2 results suggest a possible OWC existed in proximity of 1840.5 m KB.

4.2.7 Engineering Data Conclusions

The full suite of engineering data is far from conclusive regarding fluid contacts. The best evidence points to:

- GOC close to the DST-2A perforation interval at around 1833.2 m KB given the rapid onset of gas production from that interval, and
- OWC possibly around 1840.5 m KB from the PLT density reading and the fact that DST-2 produced water from somewhere below 1835m

Productivity is low, and given the proximity of water, there appears to be a danger of early water production if the zone were to be completed.

Pressure depletion observed during DST-3 suggests a limited accumulation of hydrocarbon.

It is recommended that the Upper EVCM be further evaluated in proposed gas development wells prior to any decision being taken to develop the zone for production. The main priorities for appraisal of the zone are:

- Confirmation of fluid contacts by high resolution logging and by taking further pressure data
- Confirmation of productivity through some form of production test conducted over a period of no less than several days

5 Yolla 1 1830m Sand Simulation

As the information derived from Yolla 1 Upper EVCM RFT, DST and PLT review are limited, computer simulation modelling was used to resolve some of the data uncertainty, especially the reservoir permeability and reservoir pressure, and to estimate the hydrocarbon production potential of the 1830m Sand.

A two dimensional, three phase conceptual single well radial model was selected to perform the study. The model was constructed using the best estimate of the required reservoir and fluid data, based on the results of the Yolla 1 Upper EVCM reservoir engineering data review. Then the key parameters in the model were tuned by history matching the DST rates and pressures as observed during DSTs 2A and 3. Finally, future single well production trend can be generated using the calibrated conceptual model, to evaluate the hydrocarbon production potential of the 1830m Sand.

5.1 Model Description

The dimensions of the radial model are 40 x 1 x 40. The inner ring radius was 0.4 ft (representing 9.625" wellbore) and outer ring radius 2591.4 ft. The radius expansion factor is 1.25. The GOC is assumed to be 1833m KB and 1842.5m KB for the WOC. The vertical layering system is presented in Table 5.1 below.

Layer	Fluid	Thickness	Layer Depth	
		(m)	From (m)	To (m)
1	Gas	1.00	1827.00	1828.00
2		1.00	1828.00	1829.00
3		1.00	1829.00	1830.00
4		1.00	1830.00	1831.00
5		1.00	1831.00	1832.00
6		1.00	1832.00	1833.00
7	Oil	0.20	1833.00	1833.20
8		0.15	1833.20	1833.35
9		0.15	1833.35	1833.50
10		0.15	1833.50	1833.65
11		0.15	1833.65	1833.80
12		0.20	1833.80	1834.00
13		0.50	1834.00	1834.50
14		0.50	1834.50	1835.00
15 - 27		0.50	1835.00	1841.50
28		0.50	1841.50	1842.00
29		0.50	1842.00	1842.50
30	Water	0.50	1842.50	1843.00
31		0.50	1843.00	1843.50
32 - 38		0.50	1843.50	1847.00
39		0.50	1847.00	1847.50
40		0.50	1847.50	1848.00

Table 5.1: Layering system of the 1830m sand radial model

The porosity is assumed to be 0.25 uniformly for all the grid blocks. The reservoir temperature was taken as 209 ^{o}F. The solution oil gas ratio, oil formation factor and gas volume factor were obtained from page 24 of the reservoir fluid PVT study of Yolla 1, DST 2A. The oil and gas viscosity were estimated using PVT correlations. The Upper EVCM fluid properties are summarised in Table 5.2.

Pressure (psia)	Gas PVT Properties		Oil PVT Properties		
	Bg (rb/Mscf)	Vg (cp)	Rs (Mcf/stb)	Bo (rb/stb)	Vo (cp)
315	10.380	0.0123	0.154	1.181	0.284
615	5.169	0.0130	0.253	1.234	0.264
915	3.386	0.0137	0.344	1.278	0.252
1215	2.492	0.0145	0.437	1.322	0.240
1515	1.957	0.0154	0.528	1.366	0.228
1815	1.603	0.0163	0.634	1.415	0.214
2115	1.355	0.0172	0.747	1.468	0.201
2415	1.179	0.0182	0.872	1.530	0.187
2725 (BP)	1.041	0.0192	0.998	1.601	0.175
3500	0.796	0.0220	0.998	1.582	0.187
4500	0.608	0.0261	0.998	1.557	0.203

Table 5.2: Fluid properties for Upper EVCM

Hysteresis options in Eclipse 100 were activated to describe the imbibition and drainage process in the thin reservoir. Capillary pressure data were chosen to create a water-oil transition zone up to top 1 metre of the oil zone. The relative permeability and capillary pressure hysteresis used in the model are shown in Figure 5.1 for oil-water system, Figure 5.2 for and oil-gas system, and Figure 5.3 for capillary data.

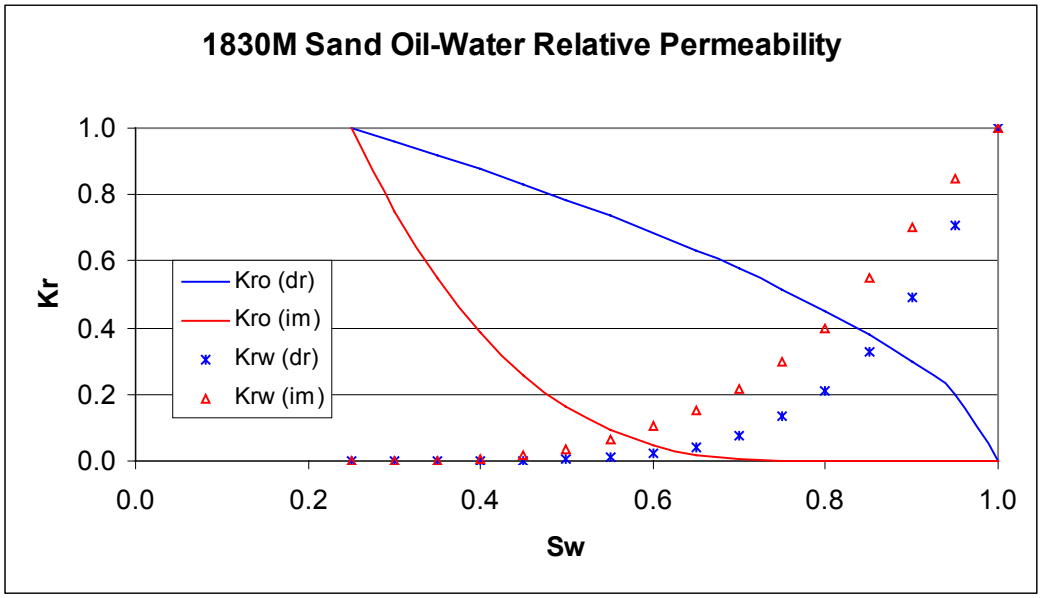

Figure 5.1: 1830m Sand oil-water relative permeability hysteresis curves

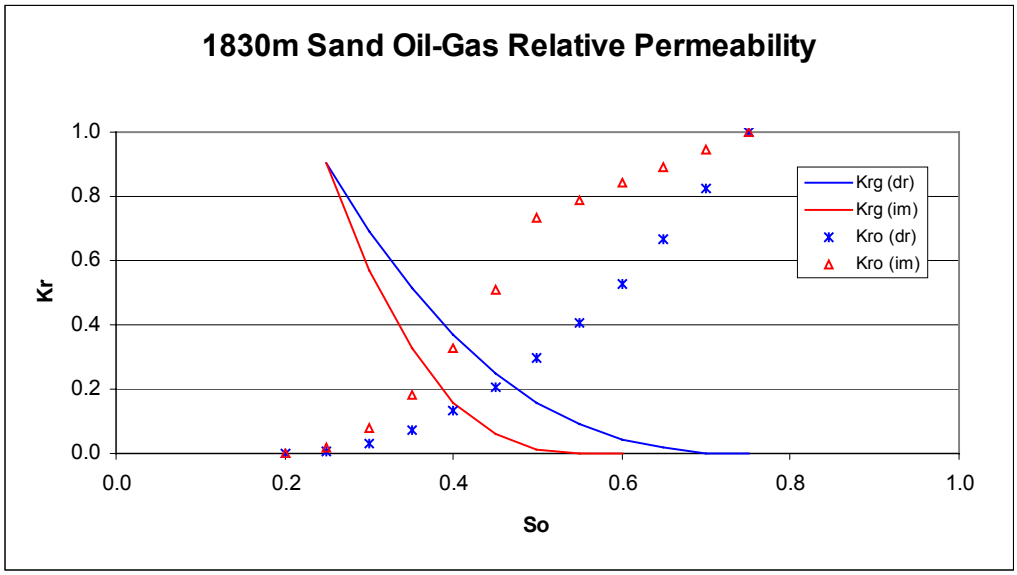

Figure 5.2: 1830m Sand oil-water relative permeability hysteresis curves

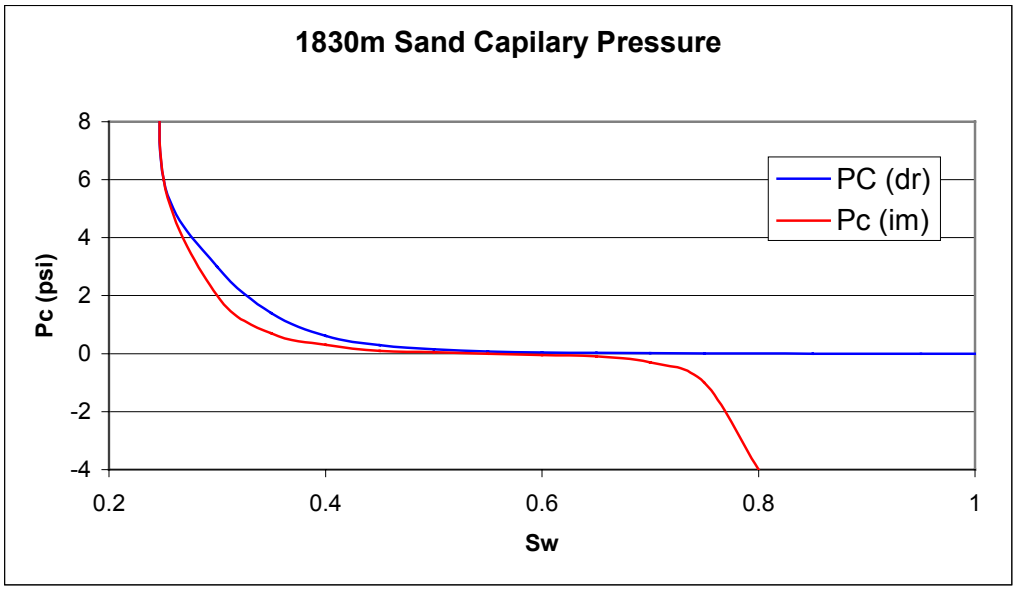

Figure 5.3: 1830m Sand capillary pressure hysteresis curves

After the initialisation, the initial fluid in-place volume in the model includes 12.34 MMstb of oil, 12.68 Bcf of free gas, 11.77 Bcf of solution gas, and 30.97 MMbbl of water. The detailed model set up and data entry can be found in Appendix 6.

5.2 DST 2A & 3 Results Matching – Numerical Simulation Approach

As the analytical well test analysis model cannot handle the multi phase flow effect, the numerical simulation approach was used. To determine the key reservoir parameters such as the formation permeability and the reservoir pressure, the single well radial model was calibrated to history match DSTs 2A and 3 results.

In the history matching DSTs 2A and 3 results, the control parameter was the DST oil rate and the matching parameters were the bottomhole pressure and the gas rate. The formation permeability in the gas and oil zones, and the initial reservoir pressure were varied to achieve the match. The Darcy and non-Darcy skins are assumed to be zero to improve the confidence level of the mach. This assumption appears to be reasonable especially in history matching DST 3 results as the skin in DST 3 is negligible.

The matching results were reasonable as shown in Figures 5.1 and 5.2 for DSTs 2A and 3, respectively.

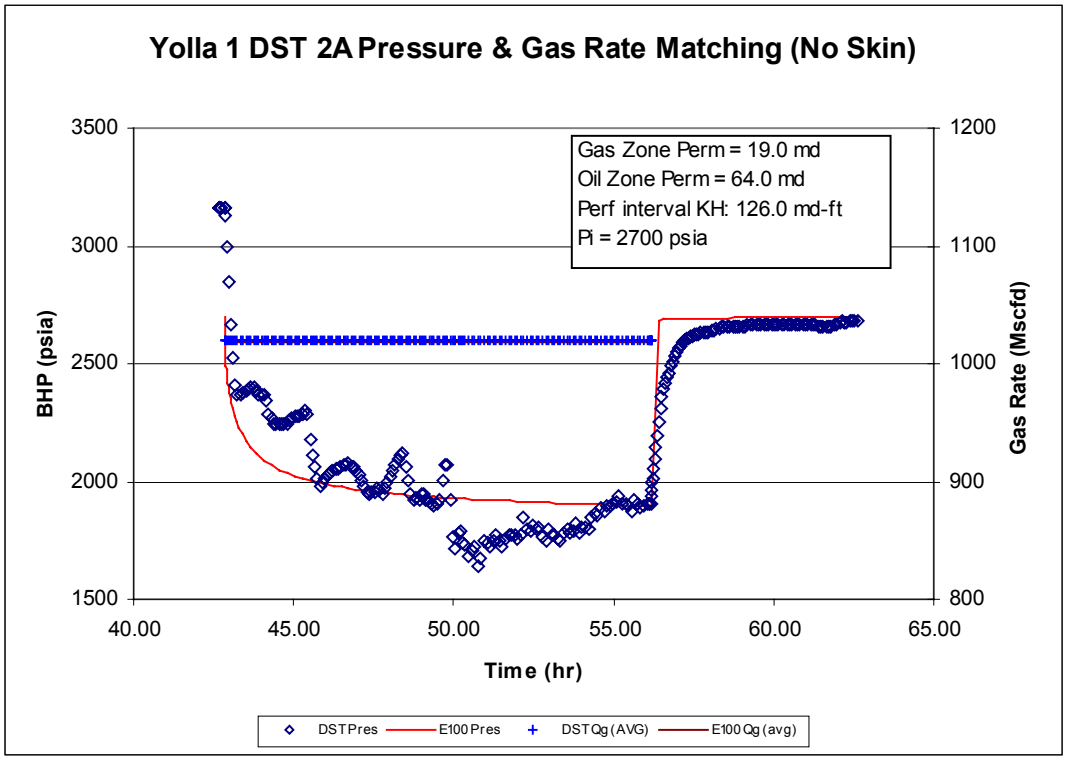

Figure 5.4: Yolla 1 DST 2A matching

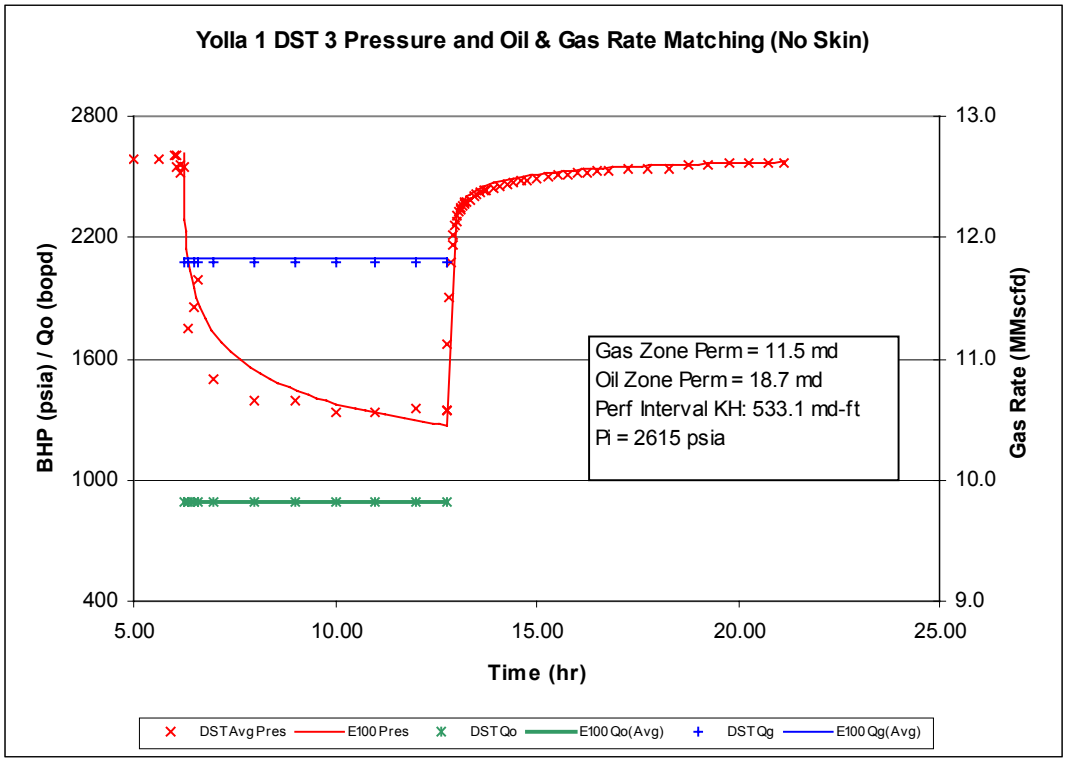

Figure 5.5: Yolla 1 DST 3 matching

The reservoir productivity (KH) of DST 2A from the history matched model is 126.0 md-ft, which is lower that from the analytical estimation (507 md-ft). The possible explanations are:

- A high skin was determined from the analytical approach while the skin is assumed to be zero in the numerical approach. The KH from the simulator would be higher if the actual skin is larger than that in the simulator. This skin was subsequently minimised by the additional perforations during DST 3.
- The production contribution in DST 2A may extend beyond the perforated interval. The 126.0 md-ft productivity in the numerical model only took into account the perforated interval.
- The DST 2A parameters cannot be reliably determined in the analytical approach, as the radial flow has not fully developed.

The reservoir productivity of DST 3 estimated by the model is 533.1 md-ft, which is higher than that from the analytical estimation (180 – 272 md-ft). The result is expected as the numerical model can handle the multi-phase flow effect accurately. It also seems sensible, as the KH from DST 3 should be higher than DST 2 because DST3 tested a significantly larger perforation interval.

The reservoir pressure during DST 3 was estimated to be 2615 psi. This compares well with the analytical interpretation results and indicates possible pressure depletion of over 100 psi during DST 3. Therefore, the hydrocarbon in-place volume and potential in the Upper EVCM is likely to be limited.

5.3 Production Forecast

Three runs were performed compared oil and gas recoveries as a function of THP, using the history matched conceptual single well radial model of DST 3. The objective of the production forecast is to determine the oil and gas recoveries that could be expected from an 1830m Sand well.

A porosity multiplier of 1.15 was applied to the oil and water zones so that the initial oil in-place in the model would match that from the volumetric estimation of 14.2 MMstb of oil.

The THPs under investigation are 1200, 725 and 430 psi. The tubing size is selected as 2 3/8" with a 1.25 km step out. This small tubing size is required to provide a stable vertical lift performance over a 5 to 10 year production life under the multi phase flow. The perforation interval is assumed to be 1827 to 1834 m (6 m of gas and 1 m of oil, Layers 1 to 12).

The results of THP sensitivity forecast are summarised in Table 5.3 and presented in Figures 5.6 and 5.7.

Case	1	2	3
THP	1200	725	430
Years on production	4.3	7.5	10
Oil – OOIP: 14.19 MMstb			
- Initial rate (bopd)	141.9	169.9	188.1
- Cum Prod (Mbbl)	82.9	157.1	224.0
- RF (%)	0.58	1.11	1.58
Gas – OGIP: 26.2 Bcf			
- Initial rate (MMscfd)	5.20	7.04	7.42
- Cum Prod (Bscf)	0.62	1.12	1.55
- RF (%)	2.35	4.28	5.93

Table 5.3: Hydrocarbon production potential of 1830m Sand

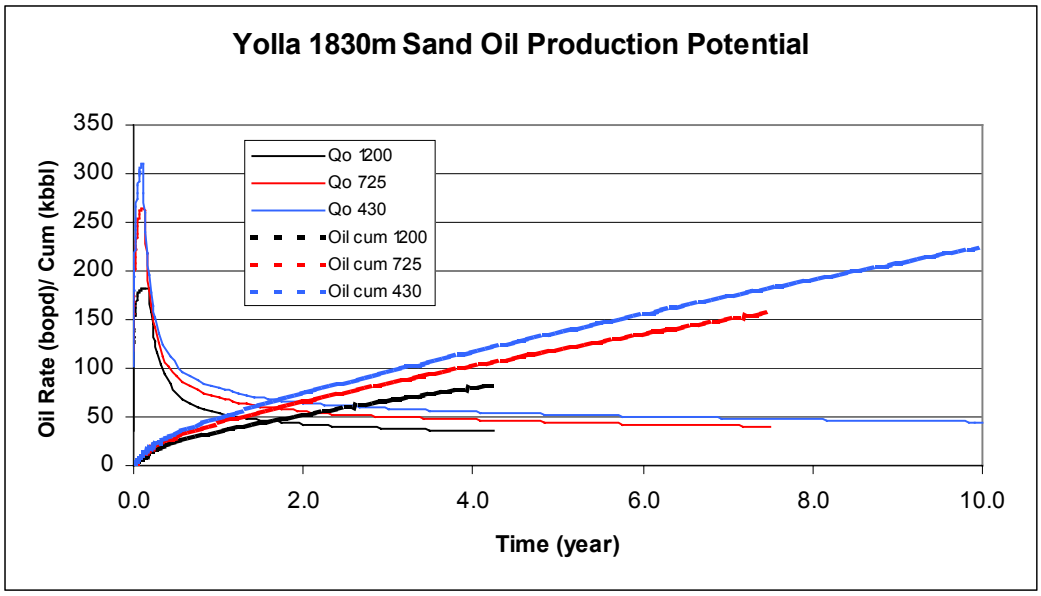

Figure 5.6: Yolla 1830m Sand Oil Production Potential

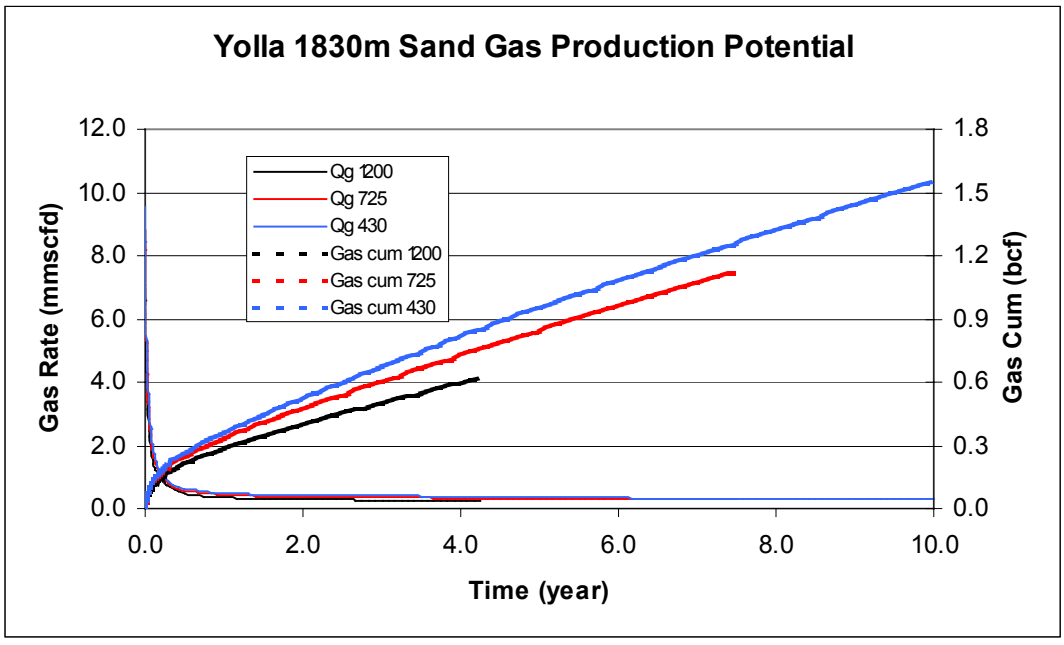

Figure 5.7: Yolla 1830m Sand Gas Production Potential

As observed from the above results, the field life extends progressively with a higher oil and gas recoveries when the THP is lowered from 1200 to 430 psi. The results are expected as the reservoir abandonment pressure will be reduced if the THP has lowered.

However the field recovery is extremely low. The best recovery under the 430-psi THP is only at 1.6% of oil and 5.9% of gas. This low recovery is resulted from the sharp production decline as shown in Figures 5.6 and 5.7. The possible causes of such severe production decline are:

- The depletion drive mechanism assumed in the model (no active aquifer),
- The three phase relative permeability effect due to the oil and water coning into the gas zone,
- High friction pressure loss in the wellbore due to the multi phase flow.

The field life for each THP case will be shortened if a larger tubing size is used. The oil recovery may be improved if a larger wellbore in the oil zone is included in the perforation interval, but potentially at the expense of water production and loss of the wellhead pressure.

5.4 Simulation Conclusion

The key finding from the simulation study is that low hydrocarbon recovery with sharp production decline can be expected from the 1830m Sand. Small tubing such as 2 3/8" is required to provide long-term wellbore production stability.

Without undertaking economic analysis, these low recoveries do not appear to justify any consideration of development on the basis of current understanding.

REFERENCES

McCarthy P. 1995. Yolla Petroleum Engineering Review. Internal report for Sagasco Resources Ltd.

Taylor, R. (in prep). Yolla 3D 2000 Reprocessing Interpretation Report (Origin Energy Resources Ltd internal report).

APPENDIX 1

UPPER EVCM PETROLOGY REPORT

RESERVOIR SOLUTIONS PTY LTD
QUEENSLAND CENTRE FOR ADVANCED TECHNOLOGIES
TECHNOLOGY COURT, PULLENVALE, 4069, QLD
ABN 27 088 995 073

PETROLOGY, DIAGENESIS AND RESERVOIR QUALITY OF CORE SAMPLES FROM YOLLA-1

Julian C. Baker PhD

A report to:

Origin Energy Resources Ltd.
339 Coronation Drive
Milton QLD 4064

11 September, 2001

C O N T E N T S

Page

1. INTRODUCTION

Petrological analysis was carried out on four, closely spaced core samples from the Upper Eastern View Coal Measures between 1845.35m and 1847.50m in Yolla-1. The main aim of the study was to determine why, despite being highly porous, the sampled section has low permeability. Samples are listed in Table 1.

2. ANALYTICAL PROGRAM

2.1 THIN-SECTION ANALYSIS

Thin-sections were cut in kerosene and impregnated with blue dyed epoxy resin. Mineral composition and visible porosity were determined by a count of 400 points in each thin-section. Grain size was estimated with the aid of an eyepiece graticule. Photomicrographs were taken to illustrate clay distribution, diagenetic effects and porosity characteristics.

2.2 X-RAY DIFFRACTION ANALYSIS

Bulk-rock X-ray diffraction (XRD) analysis was carried out on two samples (1845.35m, 1846.60m) in order to quantify mineral abundance. The XRD analysis used a finely ground whole rock powder sample, and the SIROQUANT processing technique was used to calculate mineral abundance.

Quantitative XRD analyses complement the thin-section analyses but cannot be compared directly. This is because the thin-section detrital clay component includes quartz and the various clay minerals (mainly kaolinite) that are recorded as these phases by XRD. In addition, thin-section authigenic clay, detrital clay and siderite include microporosity, and therefore total thin-section clay and siderite are elevated relative to other grain types. Finally, XRD analyses do not include visible porosity. Therefore, given that the analysed sandstones contain some macroporosity, component abundances as determined by XRD analysis will be higher than those determined by thin-section analysis.

2.3 SCANNING ELECTRON MICROSCOPY

Scanning electron microscopy (SEM) was carried out on the same two samples that were analysed by XRD in order to provide information on porosity characteristics and the nature and distribution of clays within pore systems. An energy dispersive spectrometer (EDS) was used to determine the elemental composition of clays and carbonate cements during SEM analyses.

Thin section composition, texture and QFR ratios are given in Table 1, and QFR compositions are plotted in Figure 1. Quantitative XRD analyses are given in Table 2, and annotated XRD traces are presented in Appendix 1. Annotated photomicrographs are presented in Appendix 2.

3. TEXTURE

Samples are grain supported, moderately bioturbated, variably argillaceous, well sorted, lower very fine grained sandstones with a mean grain size of 0.07-0.08mm (Table 1). Detrital clay and associated siderite are concentrated into irregular patches and laminae, the distribution of which has been influenced by bioturbation, and there is also widespread, finely dispersed detrital clay matrix. Common sandy burrows are up to at least 7mm in length and are locally lined by clay. Quartz grains are mainly angular to subangular.

4. THIN-SECTION COMPOSITION

Samples are argillaceous quartzarenites (quartzwackes) with a mean QFR ratio of 99:0:1 (Table 1). Quartz content ranges from 46.2% to 54.8% and varies mainly according to detrital clay + siderite content. As expected given the very fine grain size, quartz is almost entirely monocrystalline. In the cleaner areas, quartz grains are locally partly enveloped by incipient euhedral quartz overgrowths.

Feldspar content is less than 0.4%. All feldspar is K-feldspar (orthoclase) that is fresh to slightly altered and mostly partly dissolved.

Lithics do not exceed 0.8% and consist of micaceous metamorphic rock fragments (mainly quartz/muscovite schist) and cherty felsic volcanic rock fragments.

Other detrital grains include very minor (<1%) to rare chert, muscovite, biotite, fine organic fragments and heavy minerals (zircon, monazite, brown tourmaline, rutile, sphene, leucoxene).

Besides organic fragments and leucoxene, opaques include fine framboidal/euhedral pyrite that is mainly associated with detrital clay and organic fragments.

Monazite grains are locally rimmed by radiogenically immobilised bitumen.

Brown detrital clay ranges from 12.6% to 20.5% and forms irregular patches, laminae and dispersed matrix, the distribution of which has been controlled by bioturbation. Detrital clay is extensively replaced by siderite at 1846.60m and 1847.50m.

Authigenic clay ranges from 9.5% to 17.0% and has formed by alteration of micaceous grains and probably also by recrystallisation of finely dispersed detrital clay matrix. Authigenic clay mainly consists of extremely fine grained kaolinite and minor illitic clay and has commonly dispersed to form microporous pseudomatrix. There are also mica-like grains of kaolinite that are the remnants of completely altered mica (Plate 1). Most micaceous grains are partly altered to kaolinite, and illitic remnants of precursor micaceous grains locally occur within authigenic kaolinite. Authigenic clay commonly has a blue hue (Plate 7) as a result of being sufficiently microporous for impregnation by epoxy resin.

All carbonate is siderite, the amount of which varies from less than 3% at 1845.35m and 1846.00m to 15-17% at 1846.60m and 1847.50m. In the two deepest samples, siderite forms irregularly distributed clusters of intergrown rhombic/scalenohedral crystals up to 0.2mm long that extensively replace detrital clay, particularly where the clay is concentrated into patches and laminae. In the other two samples, fine rhombic siderite crystals are disseminated within patches of detrital clay matrix and also locally replace altered biotite grains. Detrital clay at

TABLE 1. THIN-SECTION ANALYSES AND QFR RATIOS

Depth (m)	1845.35	1846.00	1846.60	1847.50
Quartz (monocrystalline)	53.0	54.8	46.2	50.1
Quartz (polycrystalline)	0.3	-	-	-
Chert	0.3	-	-	-
K-feldspar	0.3	0.3	-	-
Plagioclase	-	-	-	-
Igneous rock fragments	0.3	-	-	-
Metamorphic rock fragments	0.5	0.5	-	0.3
Sedimentary rock fragments	-	-	-	-
Mica	0.8	0.3	0.3	0.3
Heavy minerals	0.3	-	0.3	0.5
Opaques	1.5	0.8	1.2	1.0
Siderite	1.3	2.8	16.8	15.8
Authigenic clay	15.3	17.0	11.8	9.5
Detrital clay	12.6	20.5	17.0	15.2
Visible primary porosity	11.0	2.0	3.4	6.0
Visible secondary porosity	2.5	1.0	3.0	1.3
Q (quartz + chert)	98.0	98.6	100.0	99.4
F (feldspar)	0.5	0.5	0.0	0.0
R (rock fragments)	1.5	0.9	0.0	0.6
Mean grain size (mm)	0.08	0.08	0.08	0.07
Sorting	well	well	well	well

FIGURE 1. QFR COMPOSITIONS

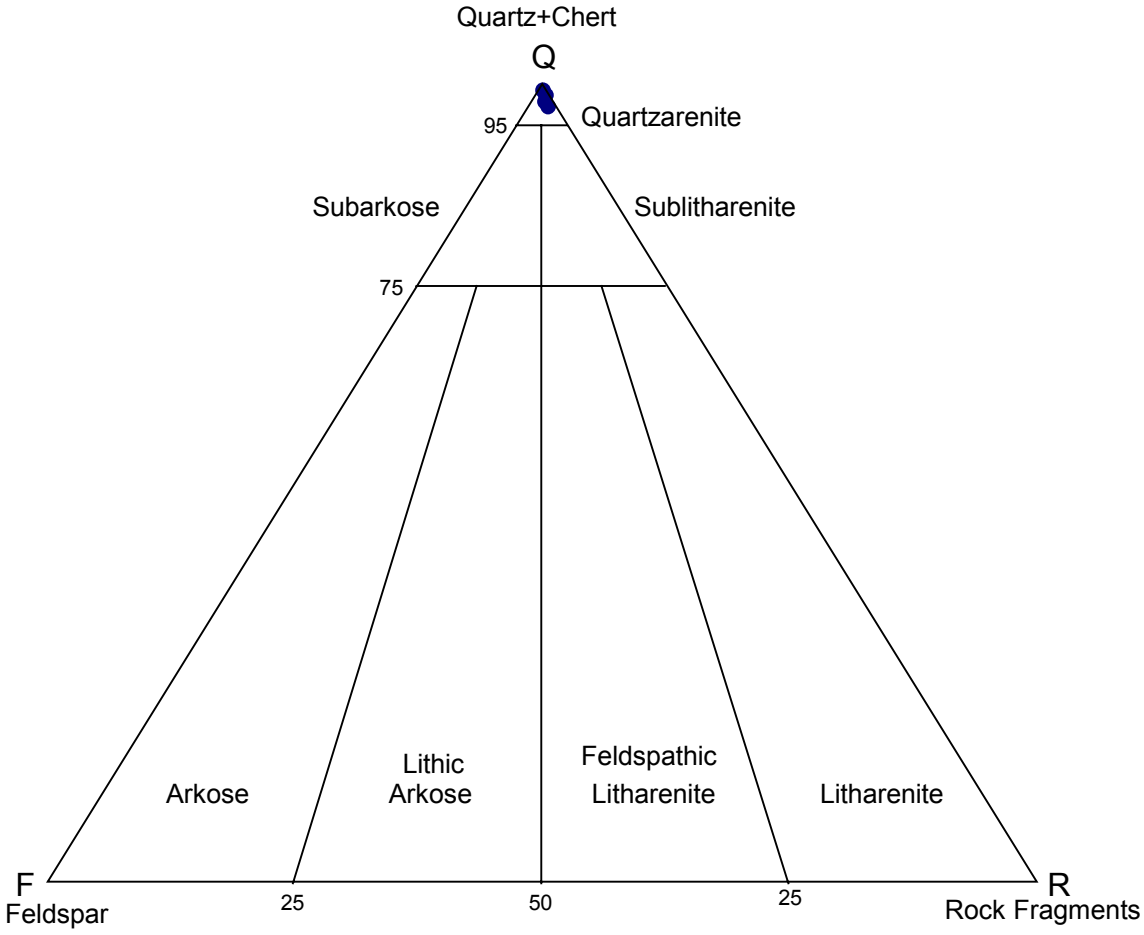

1845.35m and 1846.00m is far less sideritised than at 1846.60m and 1847.50m.

Visible porosity ranges from 3.0% to 13.5% and varies mainly according to clay + siderite content. Where the sandstones are relatively clean, abundant primary intergranular porosity is preserved between loosely packed and poorly cemented framework grains. However, such macroporous areas tend to be localised (largely as a result of bioturbation), with most areas being microporous due to pore filling by clay and associated siderite, particularly in the three deepest samples. Primary porosity is supplemented by scattered secondary pores that occur where K-feldspar grains have completely dissolved.

5. XRD ANALYSES

Bulk rock XRD analyses of samples from 1845.35m and 1846.60m indicate a simple mineralogy, with the only detected minerals being quartz, kaolinite, illite/mica and siderite (Table 2). Feldspar is present in insufficient amounts for detection by XRD.

Kaolinite dominates over illite, indicating, given that both detrital clay and authigenic clay are abundant, that kaolinite is the main clay mineral component of both detrital clay and authigenic clay.

SEM revealed the presence of authigenic illitic clay with a morphology typical of illitic mixed-layer illite/smectite. Accordingly, clay fraction XRD analyses of the same samples would probably indicate that the illite detected by bulk rock XRD analysis is actually a mixture of discrete illite and illitic mixed-layer illite/smectite.

TABLE 2. QUANTITATIVE XRD ANALYSES (%)

Depth (m)	1845.35	1846.60
Quartz	80.3	71.5
Kaolinite	16.0	15.5
Illite/mica	3.1	2.0
Siderite	0.6	11.0

6. DIAGENESIS

Labile micaceous grains, which were common in the sandstones at the time of accumulation, have partly to completely altered to kaolinite and minor illitic clay that, in many areas, have compactionally deformed and dispersed to form pseudomatrix (Plate 5; Plate 8, Fig. 1). Authigenic kaolinite also appears to have formed by recrystallisation of finely dispersed detrital clay matrix. SEM showed that most intergranular areas are occupied by authigenic kaolinite that is made up of stacks (locally vermicular) of loosely packed, pseudohexagonal plates, most of which are less than 10µm in length (Plate 4; Plate 9, Fig. 2).

In the two deepest samples (1846.60m, 1847.50m), detrital clay is extensively replaced by siderite that forms clusters of intergrown rhombic/scalenohedral crystals up to 0.2mm long (Plate 7; Plate 9, Fig. 1). In the other two samples (1845.35m, 1846.00m), fine rhombic siderite crystals are disseminated within patches of detrital clay matrix (Plate 5) and also

locally replace altered biotite grains. EDS showed that the siderite is enriched in magnesium and calcium.

Scattered secondary mouldic/intergranular pores occur where labile grains have completely dissolved (Plates 1, 6, 7). The presence of rare, partly dissolved K-feldspar grains (Plate 2) shows that at least some of the dissolved labile grains were K-feldspar.

Other diagenetic effects include compaction of authigenic clay and ductile grains (mica, micaceous rock fragments, organic fragments) (Plate 11), minor grain welding by grain contact dissolution (Plate 2), incipient quartz overgrowth cementation (Plates 9, 11), and, particularly within argillaceous areas, the precipitation of fine pyrite framboids/euhedra (Plate 1). Sutured grain contacts occur in some of the argillaceous areas where grain contact dissolution has been promoted by thin films of detrital clay.

Pyrite is included within siderite, indicating that pyrite predates siderite. Both pyrite and siderite are likely to have formed during shallow burial. Secondary mouldic pores are surrounded by siderite and compacted authigenic kaolinite, indicating that secondary porosity formed after siderite and at least some compaction and authigenic kaolinite. Quartz overgrowths most likely formed during deep burial.

If siderite precipitated during shallow burial, then its relatively high magnesium and calcium content would be consistent with siderite precipitation from marine porewater.

7. RESERVOIR QUALITY

Intergranular porosity has been severely reduced by pore filling by authigenic clay (mainly kaolinite) and erratically distributed, variably sideritic detrital clay, particularly at 1846.00m and 1846.60m, where primary intergranular porosity does not exceed 3.4%. Relatively clean burrow infills, where framework grains are loosely packed and poorly cemented, contain abundant primary intergranular porosity (Plates 1, 10, 11), but the porosity in these areas is not conducive to high permeability because surrounding areas are largely microporous due to pore filling by clay and siderite. Most primary intergranular porosity is confined to localised macroporous areas that have an erratic distribution due to the effects of bioturbation. Hence, even where there are large amounts of primary intergranular porosity (e.g., at 1845.35m), permeability remains low.

Primary intergranular porosity is supplemented by scattered, grain-sized secondary pores that have formed by K-feldspar dissolution (Plates 1, 6, 7). These pores, many of which are mouldic, would not enhance reservoir quality because they tend to be isolated by clay-rich, microporous sandstone and consequently would have little or no interconnectivity with any macropores in the vicinity.

SEM confirmed that pores and pore throats are largely occupied by clay, most of which is authigenic kaolinite that has formed by alteration of micaceous grains and probably also by recrystallisation of finely dispersed detrital clay matrix (Plate 3; Plate 8, Fig. 1). The kaolinite is extremely fine grained, with most kaolinite plates being less than 10μm in length, and is highly microporous (Plate 4, Fig. 2; Plate 9, Fig. 2). Detrital clay matrix is also highly microporous (Plate 8, Fig. 2). SEM and thin-section analyses both showed that even where there is abundant primary intergranular porosity, pore throats are still commonly

choked by authigenic kaolinite (Plate 9, Fig. 2) and finely dispersed kaolinitic detrital clay matrix (Plate 2).

The other major factor besides high clay content that results in low permeability is the very fine grain size (permeability decreases with decreasing grain size). The sandstones are not much coarser than coarse silt. In such very fine grained sandstones, clay becomes even more effective in reducing permeability due to the very small size of intergranular pores and pore throats.

In summary, the sandstones would have high measured porosity because they contain abundant, highly microporous clay and, particularly within relatively clean burrow infills, abundant primary intergranular porosity that is preserved on account of framework grains in these areas being loosely packed and poorly cemented. Permeability remains low because of the high authigenic clay and sideritised detrital clay content, the erratic distribution of macroporous areas (which would result in macropores having a low degree of interconnectivity through the sands on a centimetre scale) and the very fine grain size.

8. SUMMARY AND CONCLUSIONS

- Core samples from between 1845.35m and 1847.50m in Yolla-1 are bioturbated, variably argillaceous, well sorted, lower very fine grained quartzarenites in which framework grains besides quartz include very minor to rare K-feldspar, rock fragments, variably altered mica, organics and accessory heavy minerals.

- Detrital clay forms irregular patches, laminae and finely dispersed matrix, the distribution of which has been controlled by bioturbation.

- Abundant fine grained, microporous authigenic clay has formed by alteration of labile micaceous grains and probably also by recrystallisation of finely dispersed detrital clay matrix. Authigenic clay pseudomatrix is common.

- The detrital and authigenic clay mineral suite is dominated by kaolinite and also includes illite and probably illitic mixed-layer illite/smectite.

- Detrital clay is extensively replaced by early-diagenetic siderite at 1846.60m and 1847.50m. Minor siderite is associated with detrital clay at 1845.35m and 1846.00m.

- Diagenetic effects besides authigenic clay and siderite formation include authigenic clay/ductile grain compaction, minor grain contact dissolution, incipient quartz overgrowth cementation, and pyrite precipitation.

- Primary intergranular porosity is abundant within relatively clean, sandy burrow infills, where framework grains are loosely packed and poorly cemented. Elsewhere, intergranular porosity has been severely reduced by pore filling by authigenic clay and sideritic detrital clay. Minor secondary porosity has formed by K-feldspar dissolution.

- High measured porosity would reflect the abundance of highly microporous clay and, within localised areas, primary intergranular porosity. Low permeability reflects the high content of clay and associated siderite, the erratic distribution of macropores (due to bioturbation) and the very fine grain size.

APPENDIX 1.
X-RAY DIFFRACTOGRAMS

Key to abbreviations:

I = illite/mica

K = kaolinite

Q = quartz

S = siderite

1845.35m
Bulk rock

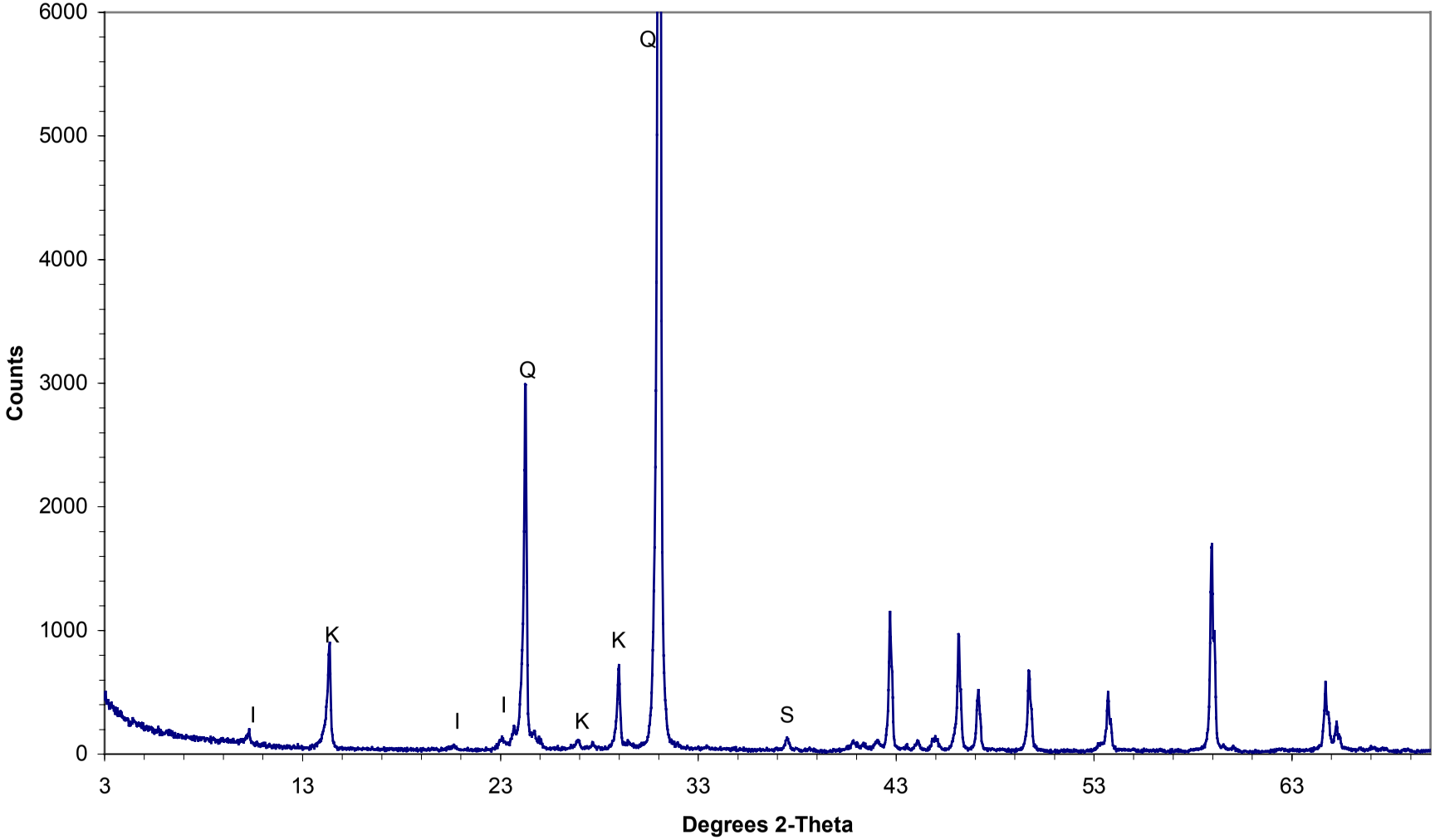

1846.60m
Bulk rock

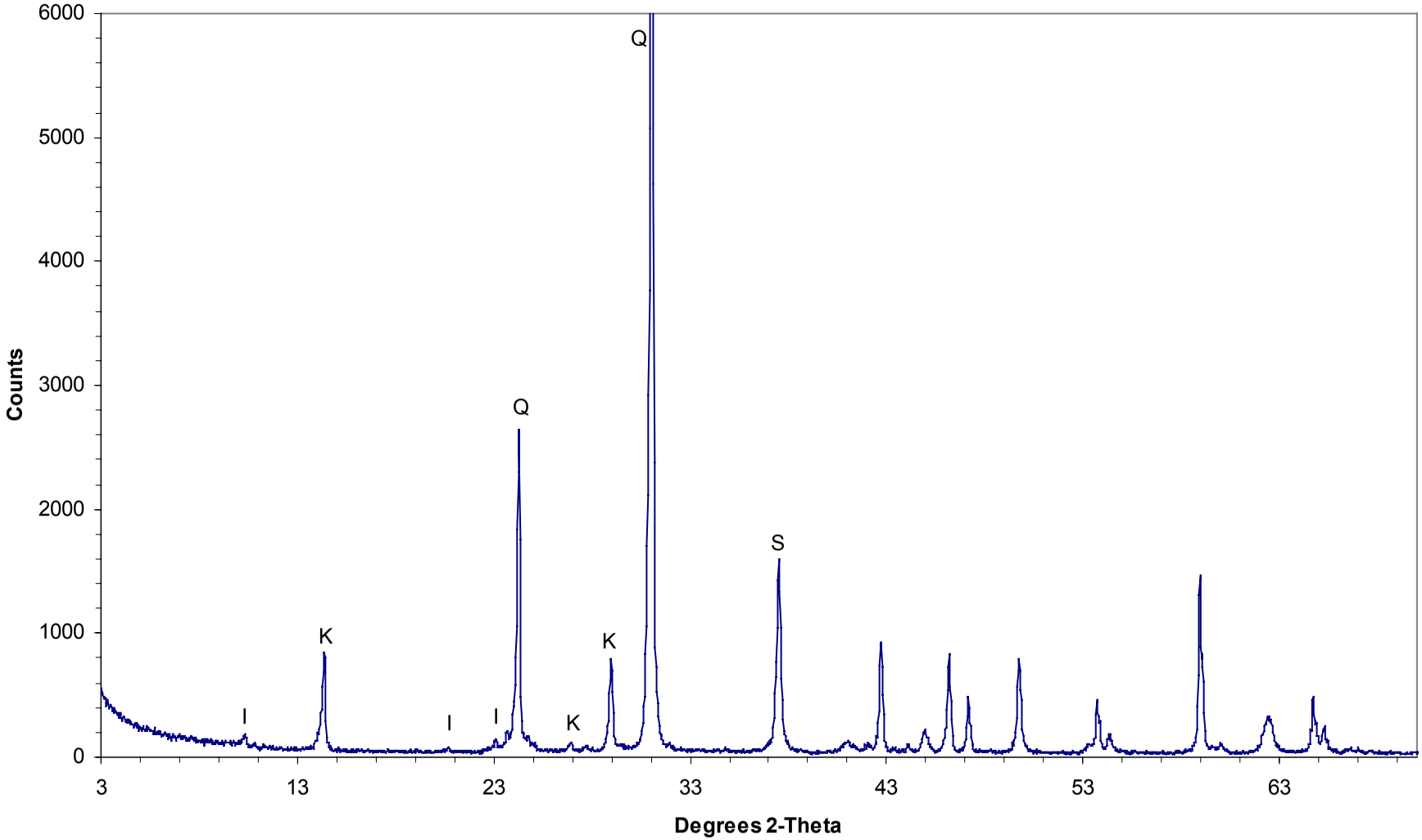

APPENDIX 2.
PHOTOMICROGRAPHS

PLATE 1: 1845.35m

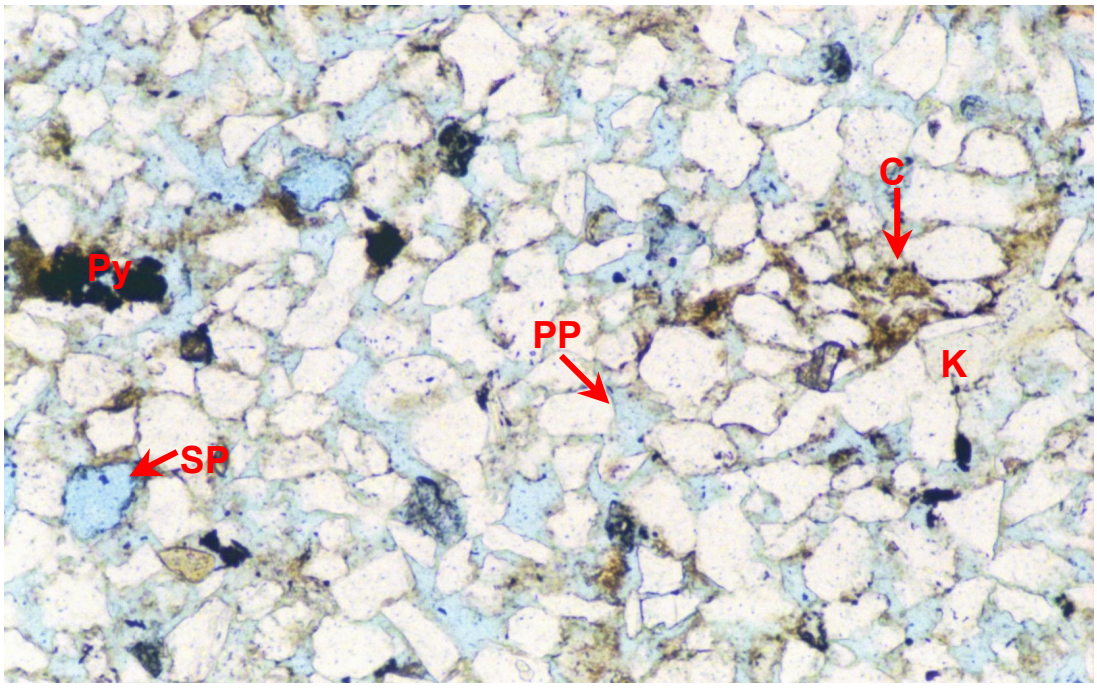

FIGURE 1 Plane polarised light

FIGURE 2 Crossed polarisers

0.2mm

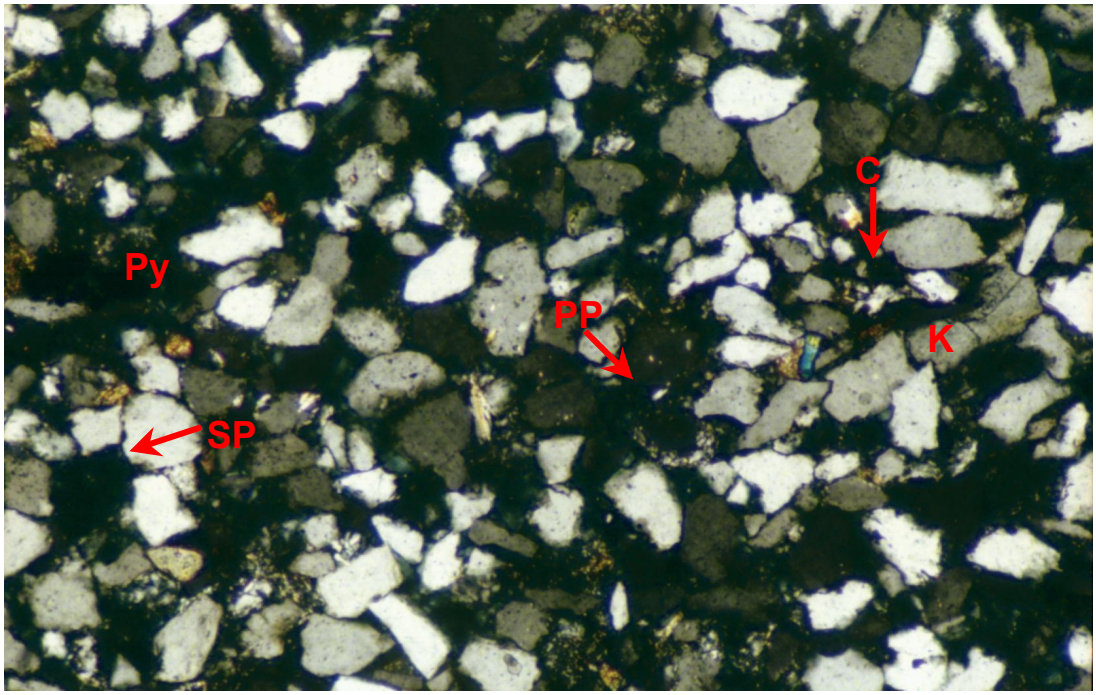

Within a relatively clean, sandy burrow infill, abundant primary intergranular porosity (PP) is preserved between loosely packed, poorly cemented quartz framework grains, except where intergranular spaces are filled by patchy brown detrital clay (C) and associated fine pyrite (Py). A secondary pore (SP) has formed by K-feldspar dissolution, and a mica-like grain of kaolinite (K) occurs where biotite has altered.

PLATE 2: 1845.35m cont.

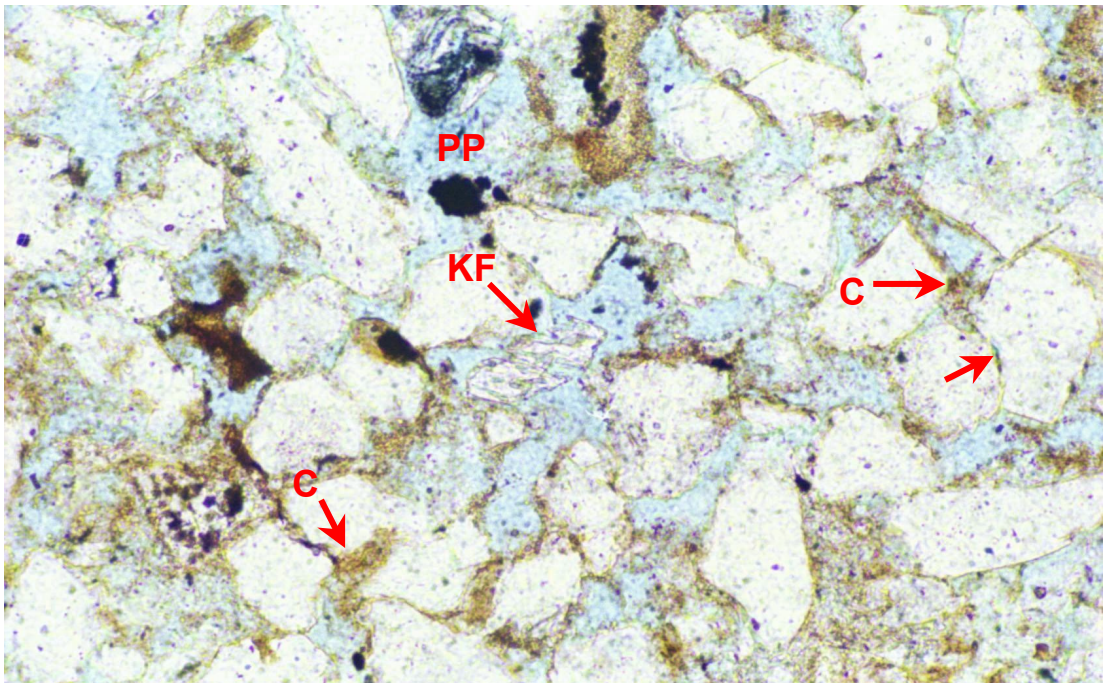

FIGURE 1 Plane polarised light
FIGURE 2 Crossed polarisers

0.1mm

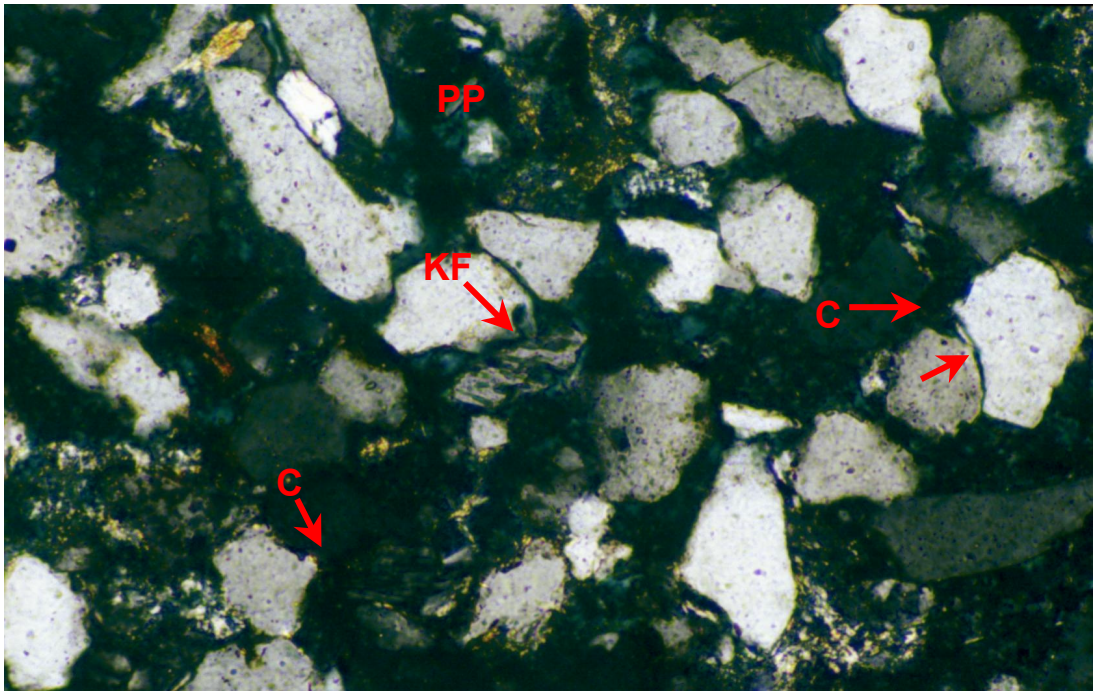

Even in areas where there is abundant primary intergranular porosity (PP), pore throats are commonly clogged by thinly dispersed, kaolinitic detrital clay matrix (C). Framework grains include rare, partly dissolved K-feldspar grains (KF). Some juxtaposed quartz grains have welded grain contacts (arrow) that are the result of minor grain contact dissolution.

PLATE 3: 1845.35m cont.

FIGURE 1

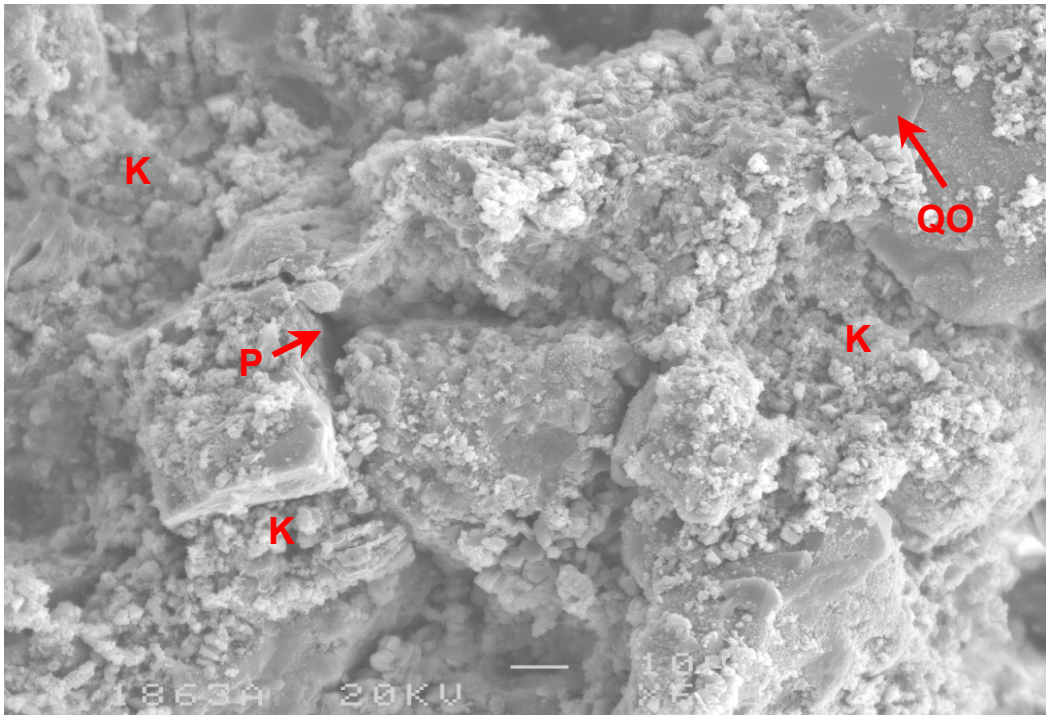

Representative area in which an intergranular pore (P) would not be conducive to permeability on account of adjacent pores and pore throats being clogged by fine grained authigenic kaolinitic clay (K). Thin quartz overgrowths (QO) partly envelop quartz grain surfaces that were not totally covered by clay.

FIGURE 2

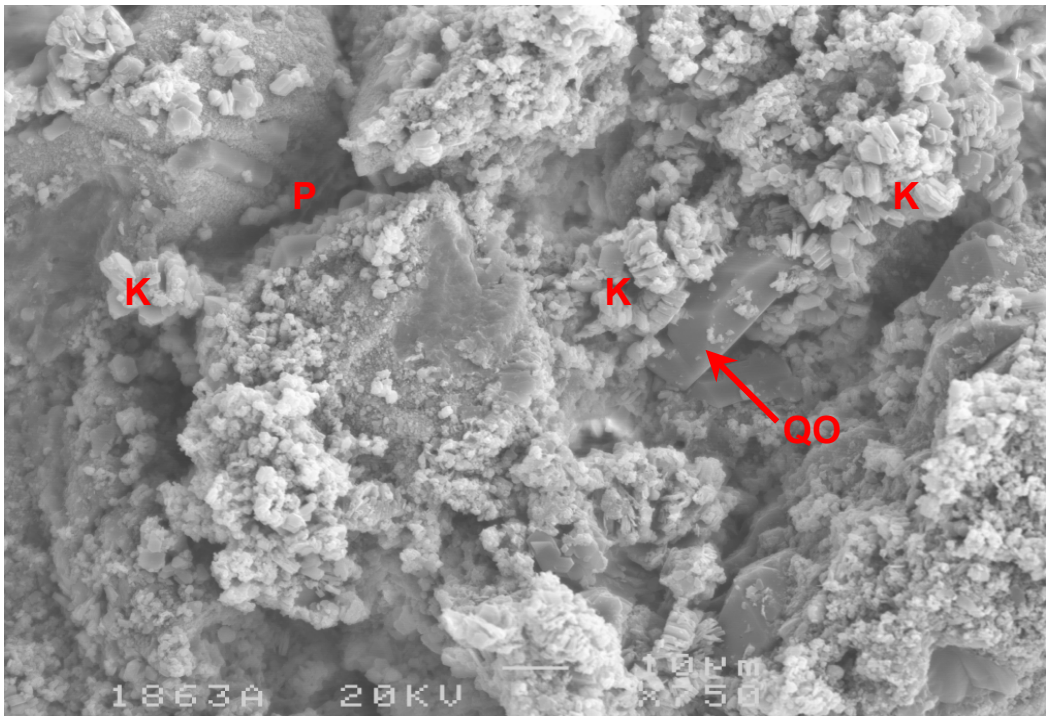

Intergranular spaces are commonly occupied by loosely packed, very fine grained authigenic kaolinite (K). Low permeability would reflect the small size of intergranular pores (P) coupled with the abundance of clay throughout most of the intergranular pore system. Quartz overgrowths (QO) are insufficiently well developed to reduce permeability.

PLATE 4: 1845.35m cont.

FIGURE 1

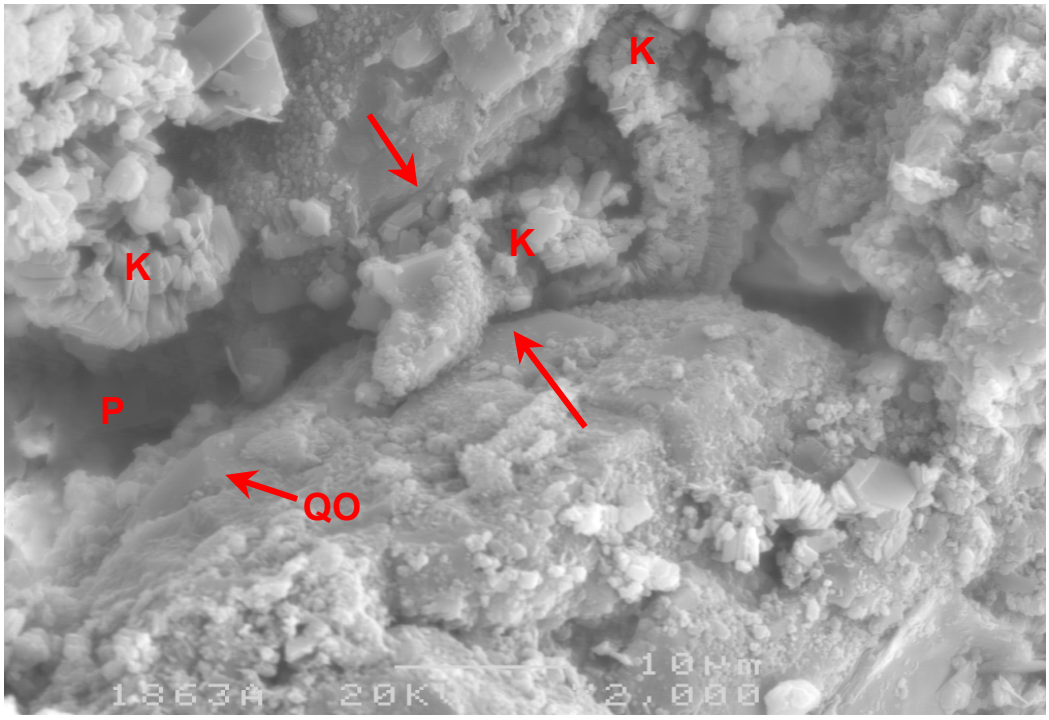

A pore throat (between arrows) is choked by authigenic kaolinite (K), which also partly fills adjacent intergranular pores (P). Incipient quartz overgrowths (QO) have developed on free quartz grain surfaces.

FIGURE 2

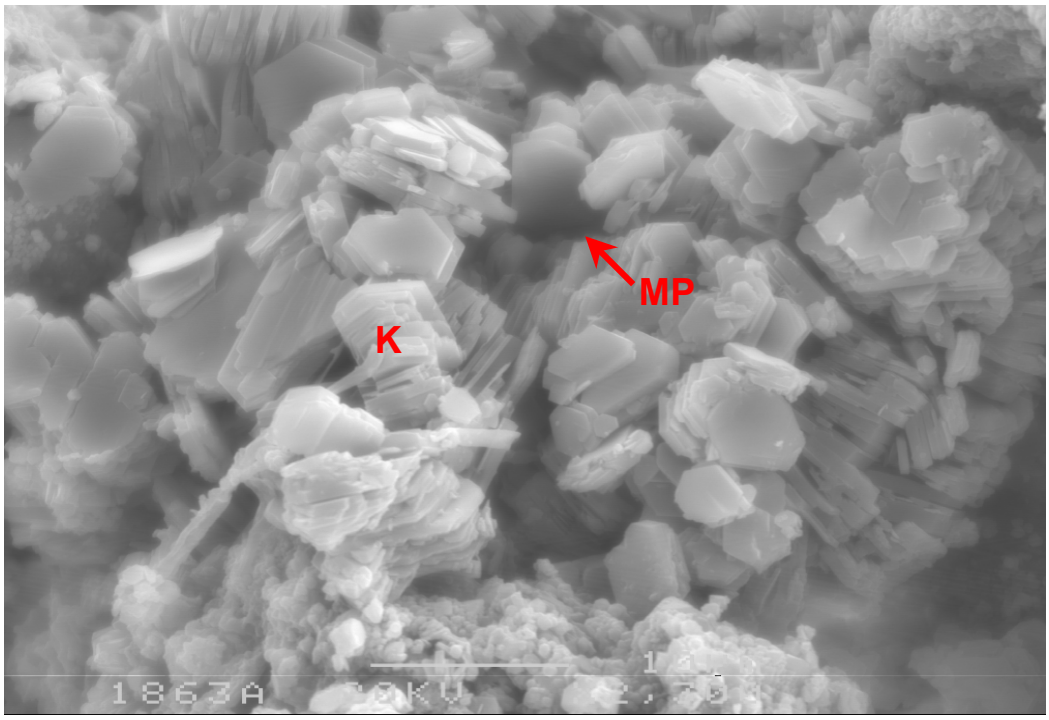

Detail of typical pore filling authigenic kaolinite (K). The kaolinite is very fine grained, with most plates being less than 10µm long, and is highly microporous (MP). The presence of such kaolinite within intergranular spaces transforms macroporosity into microporosity, thereby drastically reducing permeability.

PLATE 5: 1846.00m

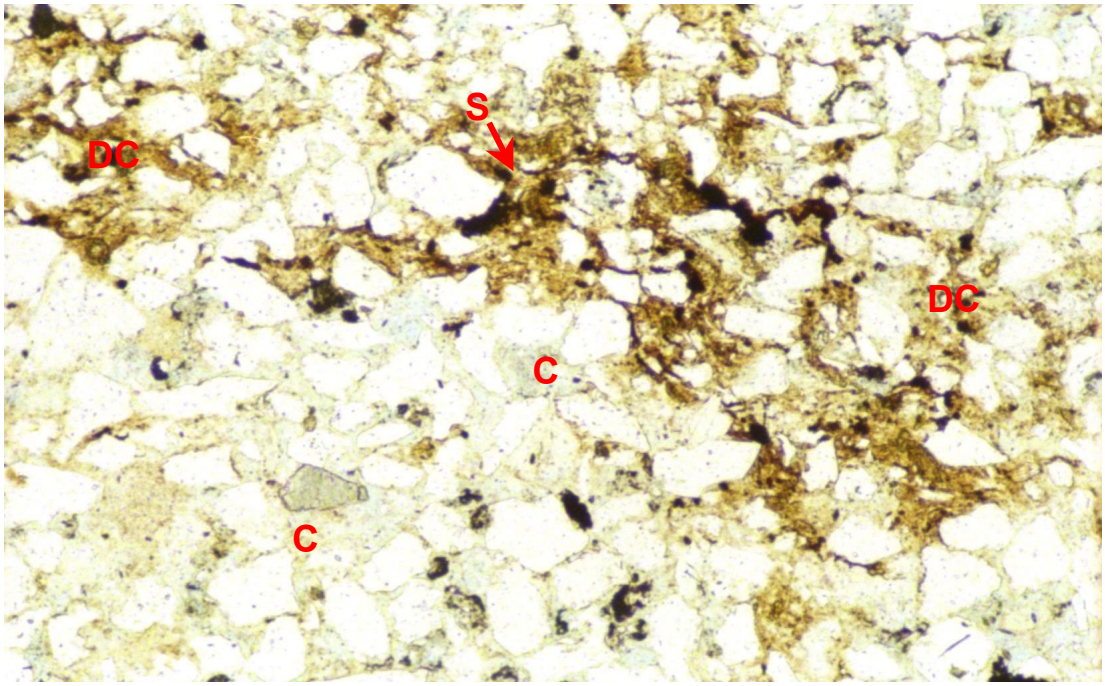

FIGURE 1 Plane polarised light
FIGURE 2 Crossed polarisers

0.2mm

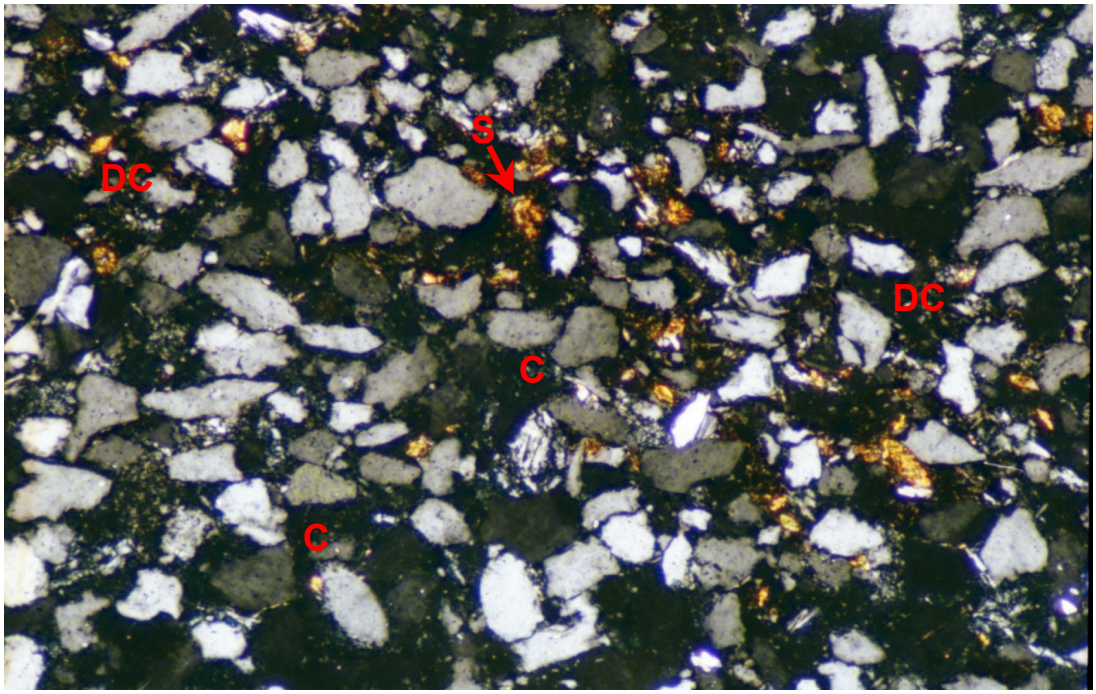

This sample is the least macroporous of the four samples. In the field of view, intergranular areas are filled by authigenic kaolinitic/illitic clay pseudomatrix (C) and patchy brown detrital clay matrix (DC) and associated fine siderite (S).

PLATE 6: 1846.60m

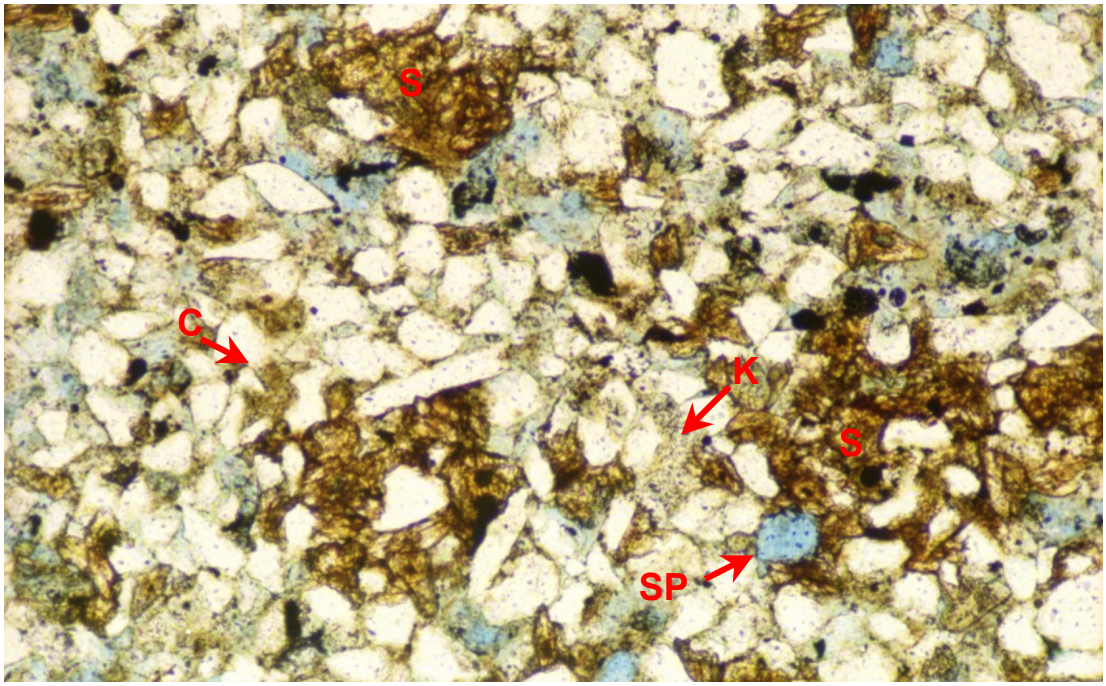

FIGURE 1 Plane polarised light
FIGURE 2 Crossed polarisers

0.2mm

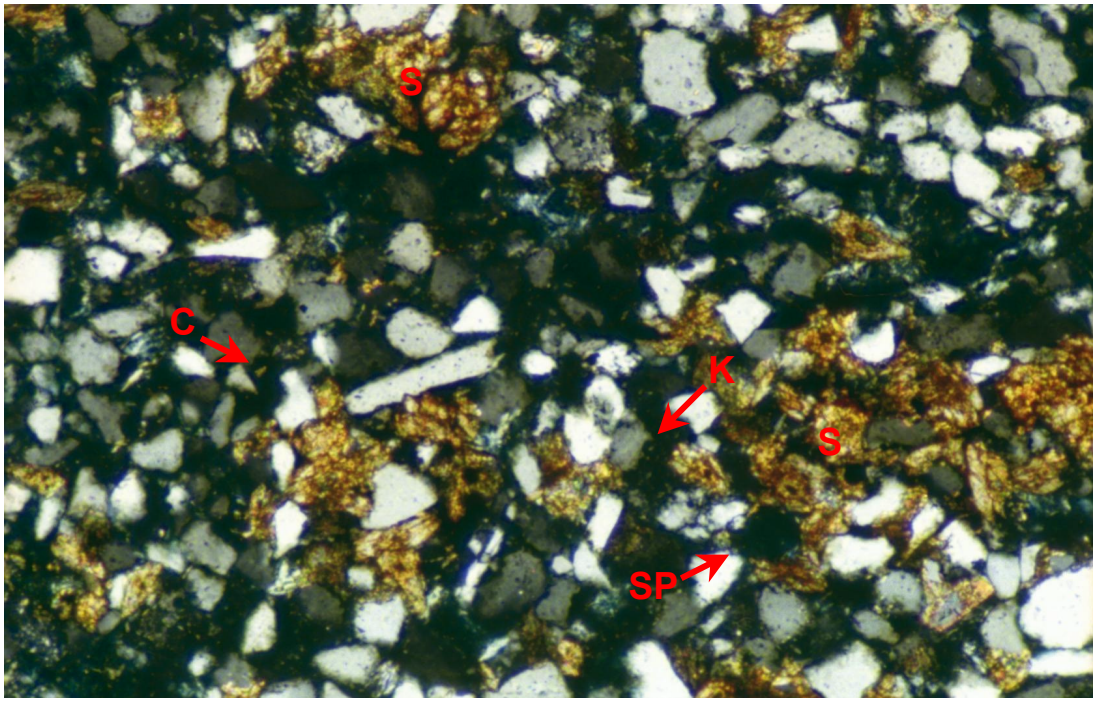

Most intergranular spaces are filled by authigenic kaolinitic clay (K) and by detrital clay (C) that has been extensively replaced by siderite (S). Scattered secondary mouldic pores (SP) occur where K-feldspar has dissolved.

PLATE 7: 1846.60m cont.

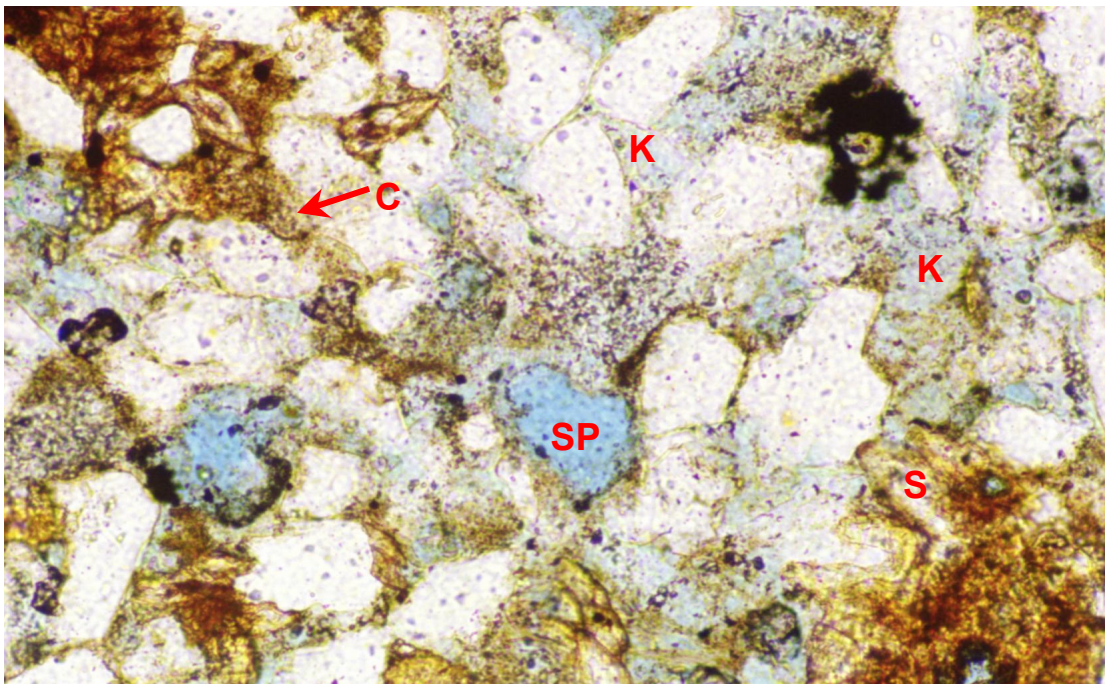

FIGURE 1 Plane polarised light
FIGURE 2 Crossed polarisers

0.1mm

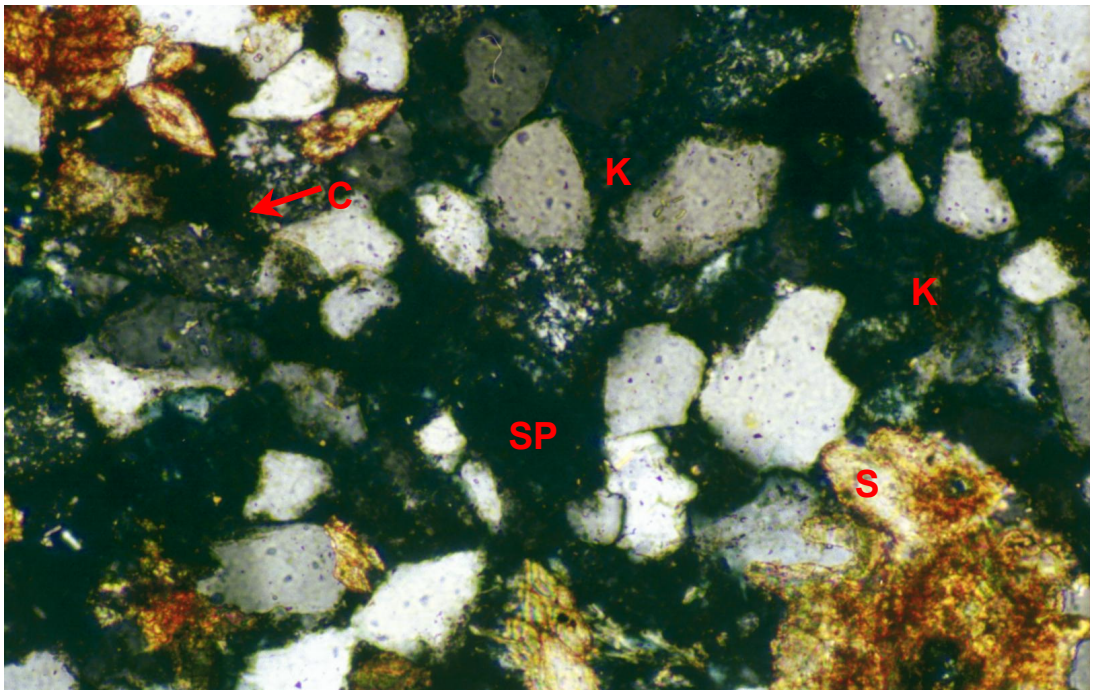

Detail of pore filling authigenic kaolinitic clay (K) and detrital clay (C), the presence of which would result in very low permeability. Detrital clay is extensively replaced by siderite (S). Authigenic clay has a blue hue, showing that it is sufficiently microporous for impregnation by epoxy resin. Being totally surrounded by microporous sandstone, secondary mouldic grain dissolution pores (SP) would not be conducive to permeability.

PLATE 8: 1846.60m cont.

FIGURE 1

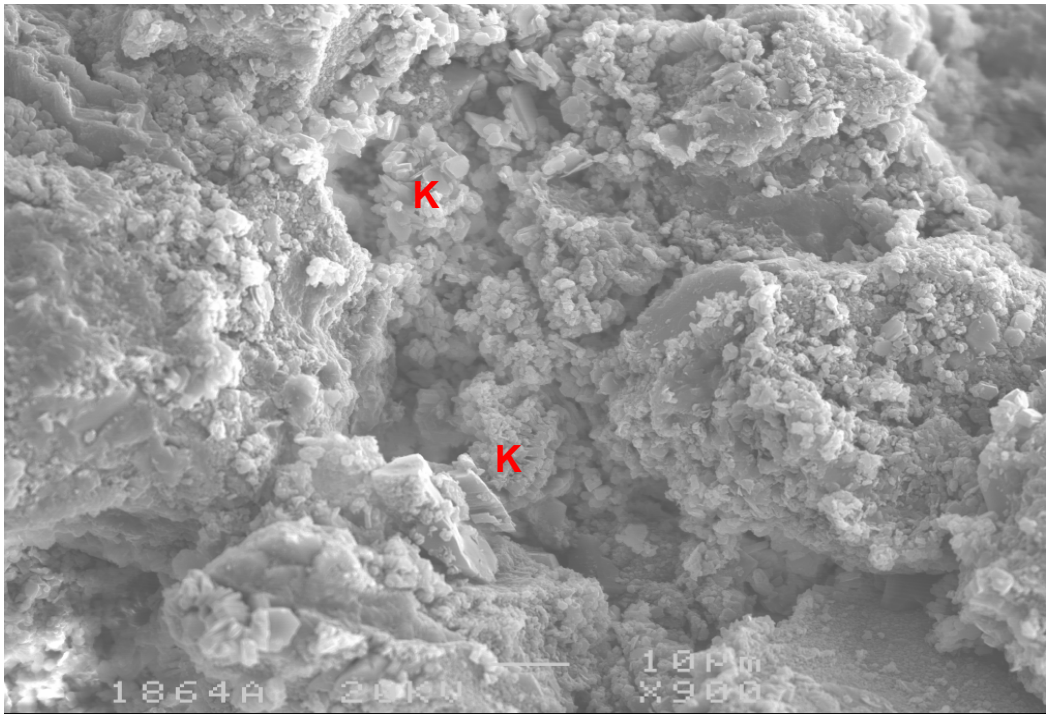

Throughout much of the sample, fine grained, microporous kaolinitic pseudomatrix (K) fills all intergranular spaces. The pseudomatrix has formed by compaction and alteration of micaceous grains.

FIGURE 2

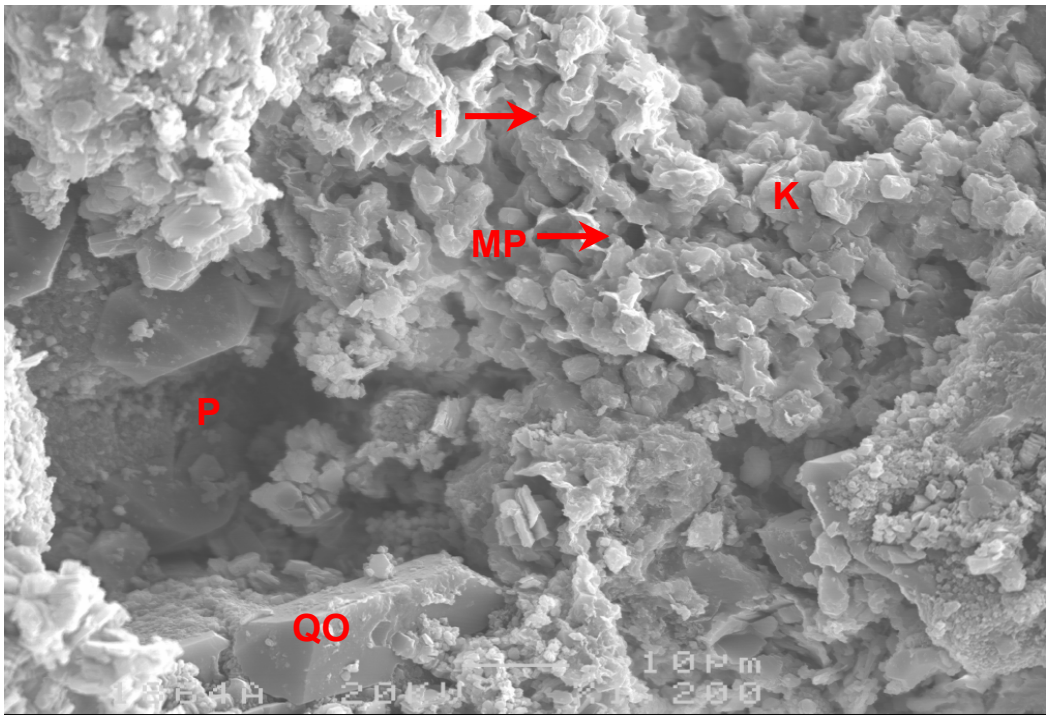

An intergranular pore (P) would be sealed from any adjacent intergranular pores by the presence of microporous (MP) detrital clay matrix composed mainly of kaolinite (K) and illitic clay (I). Quartz overgrowths (QO) are poorly developed and thus only fill a small portion of the pore.

PLATE 9: 1846.60m cont.

FIGURE 1

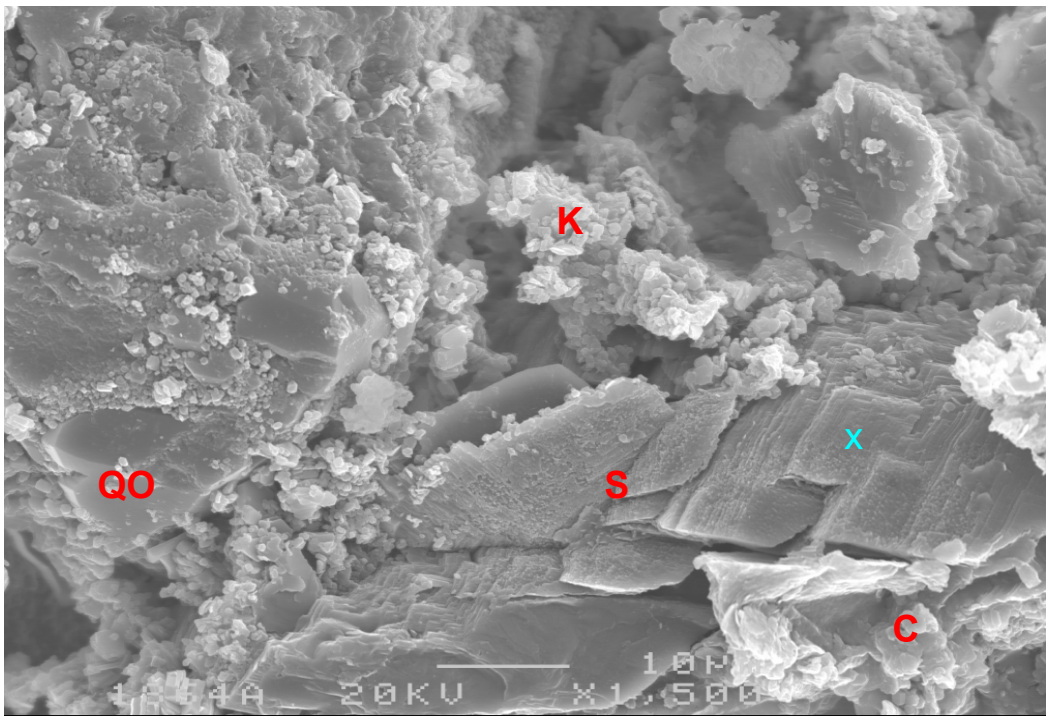

In addition to authigenic kaolinite, the presence of patchy detrital clay (C) and associated siderite (S) greatly reduces permeability. EDS analyses for point "x" revealed that the siderite contains significant amounts of magnesium and calcite, consistent with siderite precipitation from marine porewater. Fine kaolinitic clay (K) and incipient quartz overgrowths (QO) are also marked.

FIGURE 2

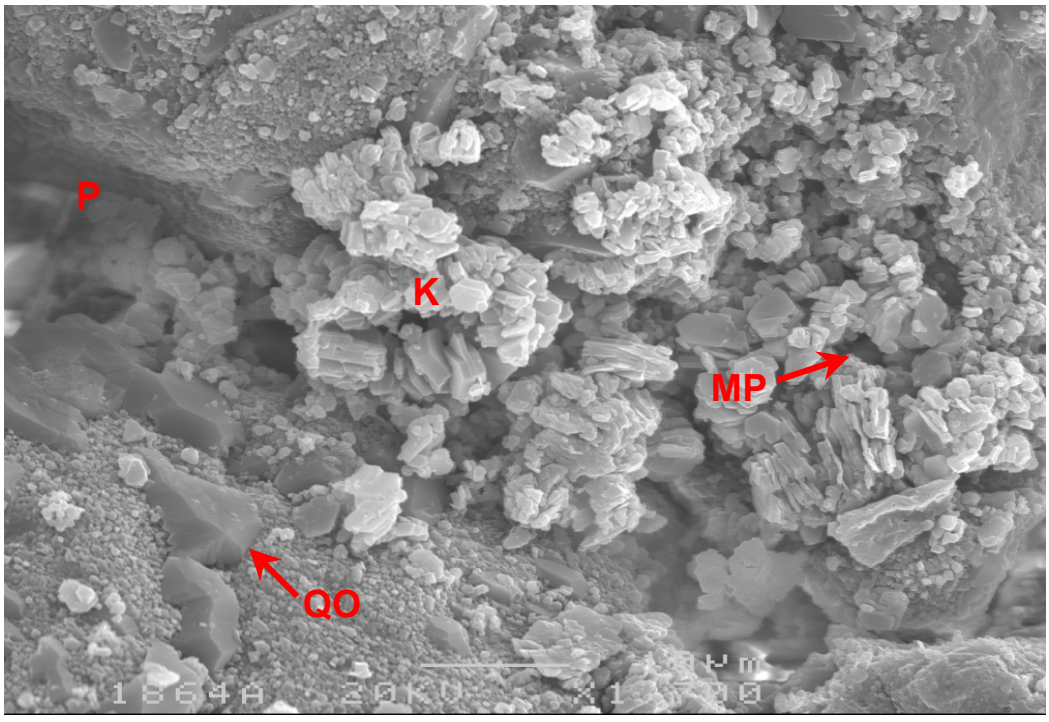

High porosity and low permeability are largely explained by the presence of loosely packed, hence highly microporous (MP) authigenic kaolinite (K) within most intergranular pores and pore throats, even in areas where there are common intergranular macropores (P). Incipient quartz overgrowths (QO) have developed on free quartz grain surfaces.

PLATE 10: 1847.50m

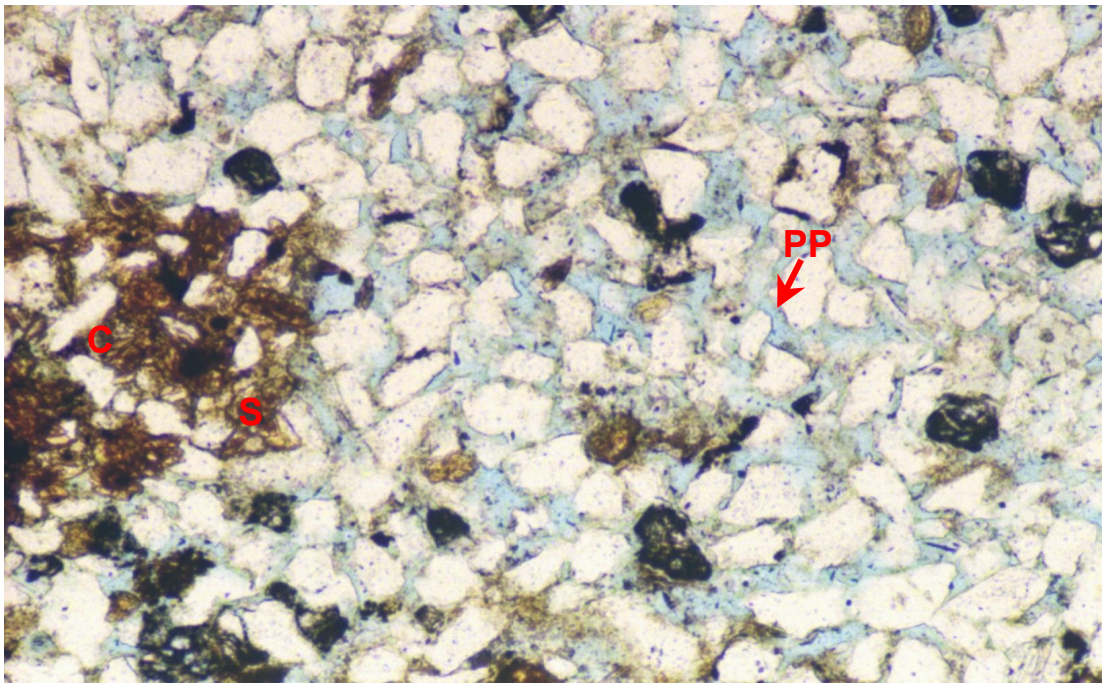

FIGURE 1 Plane polarised light
FIGURE 2 Crossed polarisers

0.2mm

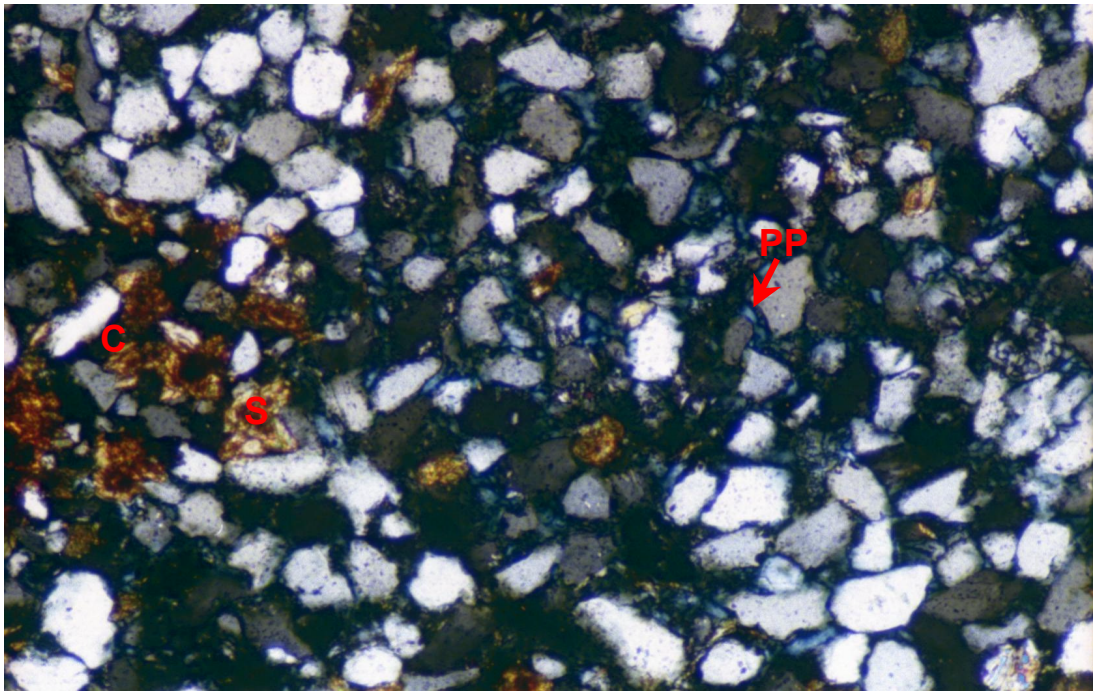

A relatively clean, sandy burrow infill contains abundant primary intergranular porosity (PP). Detrital clay (C) and associated siderite (S) have an irregular distribution throughout the sample due to the effects of bioturbation.

APPENDIX 2

PETROPHYSICAL ANALYSIS

TRL/1, BASS BASIN, TASMANIA

YOLLA - 1

PETROPHYSICAL REVIEW

UPPER EASTERN VIEW COAL MEASURES

1765-1965 mMDRT

Origin Energy Resources Limited
Second Floor, South Court, John Oxley Centre
339 Coronation Drive
MILTON QLD 4064

Chris Shield, January 2002
N:\chris\bass\yolla\Yolla-1\Yolla-1 Petro Report.doc

EXECUTIVE SUMMARY

This report details a review of the reservoir quality and hydrocarbon charge potential of the upper EVCM Formation sediments intersected whilst drilling the exploration well, Yolla-1 in TR/L1 in the Bass Basin, Tasmania. The study entails an analysis of all available lithological data, an evaluation of the quality of the hydrocarbon shows, and a complete petrophysical analysis (Table 1).

Very-fine grained, quartzose sandstones with a high (20-40%) volume of clay, interbedded with, claystones, and coals were intersected within the upper EVCM Formation. Porosity, measured from core analysis and derived from log analysis, is higher than expected for sandstones with such a large volume of clay. Petrology indicates that the kaolinitic clay present contributes a significant amount of secondary micro-porosity, which would not contribute to recovery. Calculated permeabilities are moderate in the sandstones that are hydrocarbon-bearing (TEV3 and 4). The reservoir would be expected to flow hydrocarbons at moderate rates.

Lower reservoirs (TEV5, 6, and 8) have less clay, and would be expected to have better deliverability. These reservoirs are below the hydrocarbon-water contact at Yolla-1.

A gas-oil contact is postulated at 1832.1 mMDRT, but its exact location may be questioned due to the high clay content within the reservoirs masking any potential density-neutron effect. An oil-water contact is apparent from the logs at 1842.3 mMDRT, and occurs at the base of a claystone bed. The top of the transition zone is interpreted at 1840.7 mMDRT.

The close proximity of Yolla-1 to a Tertiary volcano has resulted in the formation waters being highly saline, which will require careful planning for casing, logging, and cementing programmes in any future wells.

Zonation					Gross Rock	Net Reservoir						Net Pay		
Name	Top		Base		Thickness	Thickness	Av. Clay Volume	Av. Eff. Porosity	Av. Permeability	Ave. kH	Net Res/Gross	Thickness	Av. Water Sat.	Net Pay/Gross
	mKB	mSS	mKB	mSS	metres	metres	%	%	mD	mD.ft	%	metres	%	%
TEV0	1765	1753.9	1800	1788.9	35.0	1.2	30.2	21.4	29.66	118.7	3.5	0		0.0
TEV1	1800.0	1788.9	1807.0	1795.9	7.0	0.0	----	----	----	----	0.0	0.0		0.0
TEV1A	1807.0	1795.9	1817.5	1806.4	10.5	2.7	33.2	11.7	0.81	7.3	26.1	0.0		0.0
TEV2	1817.5	1806.4	1823.1	1812.0	5.6	5.3	28.6	14.0	1.71	29.9	95.2	0.0		0.0
TEV3	1823.1	1812.0	1829.5	1818.4	6.4	5.8	23.2	16.8	3.46	65.7	90.5	0.0		0.0
TEV4	1829.5	1818.4	1839.6	1828.5	10.1	10.1	17.7	25.0	53.59	1775.8	100.0	6.7	46.6	66.4
TEV5	1839.6	1828.5	1843.0	1831.9	3.4	2.4	33.2	20.4	38.50	308.2	71.8	0.0		0.0
TEV6	1843.0	1831.9	1857.8	1846.7	14.8	13.9	21.6	24.2	57.84	2632.0	93.7	0.0		0.0
TEV7	1857.8	1846.7	1866.5	1855.4	8.7	0.2	36.8	14.1	0.61	0.3	1.7	0.0		0.0
TEV8	1866.5	1855.4	1871.4	1860.3	4.9	5.0	5.1	25.0	13.47	222.3	102.7	0.0		0.0
TEV9	1871.4	1860.3	1911.4	1900.3	40.0	9.5	26.9	17.2	2.73	84.6	23.6	0.0		0.0
TEV10	1911.4	1900.3	1929.0	1917.9	17.6	15.5	13.9	21.6	9.53	485.9	88.3	0.0		0.0
Total	1800.0	1788.9	1880.0	1869.6	164.0	71.7	19.6	21.6			43.7	6.7	46.6	4.1
DST-2A	1833.2	1822.1	1833.8	1822.7	0.6	0.6	20.9	24.4	112.26	221.0	100.0	0.6	47.2	100.0
DST-3	1822.0	1810.9	1842.0	1830.9	20.0	17.1	20.4	22.1	17.12	958.6	85.4	6.7	46.6	33.6
Best Sand	1830.3	1819.2	1833.3	1822.2	3.0	3.0	9.6	27.7	74.26	730.9	100.0	3.0	41.4	100.0

Table-1. Petrophysical Summary

TABLE OF CONTENTS

Figures

Tables

Appendices

Enclosure

INTRODUCTION

Yolla-1 is an exploration well located close to the crest of the structure containing the Yolla Gas Field in TRL/1.

The well intersected moderate to good quality sandstones with moderate fluorescence and gas shows in the upper Eastern View Coal Measures. This report addresses the hydrocarbon indications and potential of all strata intersected within the upper Eastern View Coal Measures, between 1765 and 1965 mMDRT.

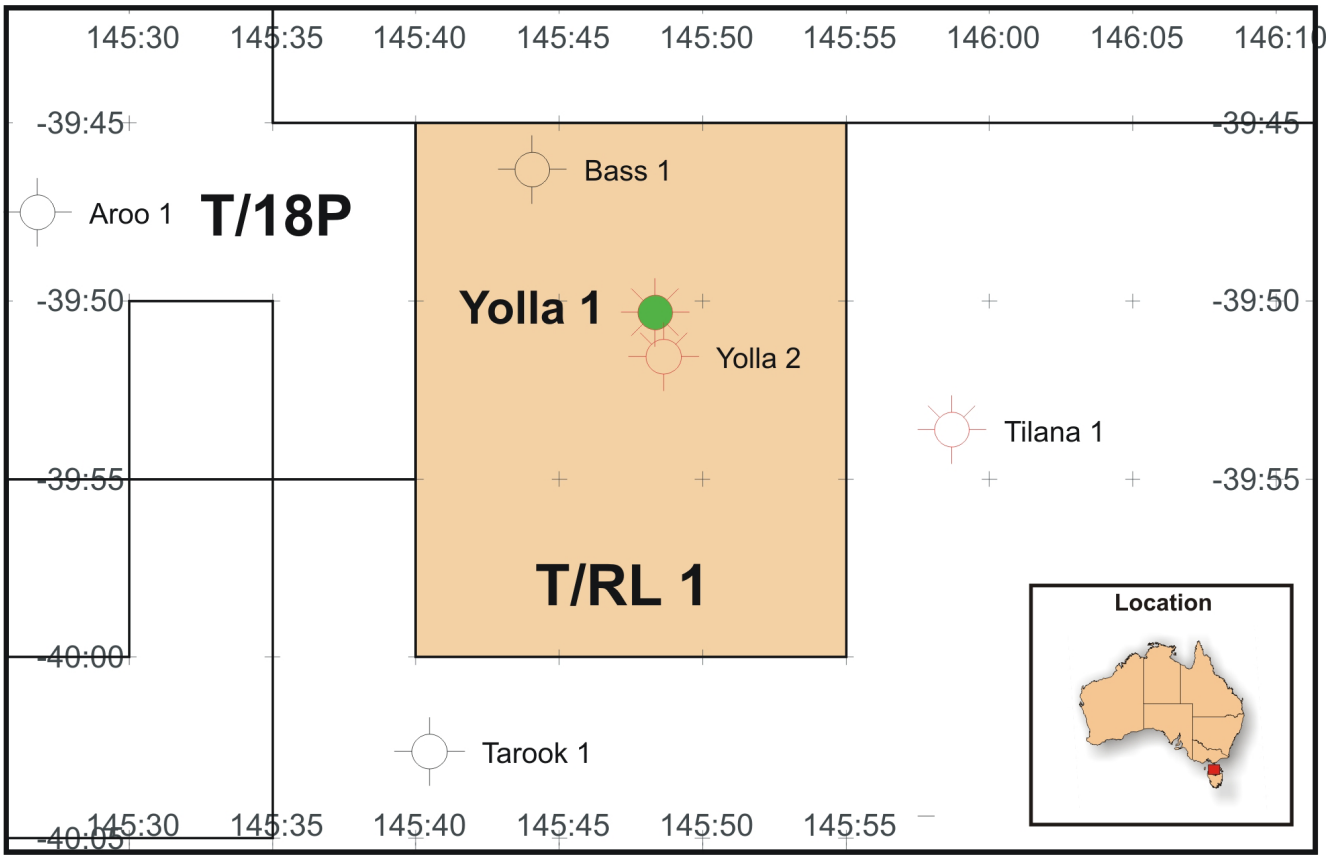

Figure 1. Location Map

DATA AVAILABILITY AND QUALITY

Lithological Data

One 10 metre conventional core was attempted between 1838 and 1848 mMDRT. The core barrel recovered only 2.8 metres of core, much of which is broken-up and has been severely

washed by mud into rounded pieces. It is assumed that the recovered core represents the basal section cored, and that the remaining rock has been flushed away by the action of the coring process. Correlating wireline log coverage with available core photos, petrological, and core analysis data, it has been possible to depth-match the core to the wireline data with a –3.3m depth-shift required. Lithology information is provided by this core, sidewall core descriptions, and cuttings descriptions of samples recovered at 3 metre intervals.

Wireline Log Data

Yolla-1 was wireline logged by Schlumberger (Table 2) in three suites. Suite-1 was logged in the 17½-inch mud-filled hole, and suites 2 and 3 were logged in a 12¼-inch mud-filled hole. The section encompassing the upper EVCM was logged twice, approximately one month apart. The logs utilised in this study are from the suite-2 logging pass, as the borehole should be in better condition and mud filtrate invasion should be minimised.

The wireline log data for suite-2 is of a moderate quality. The porosity logs conform and perform as expected in the clean and porous sandstones between 1867 and 1871 mMDRT. Resistivity logs overlie and track in the argillaceous section overlying the TEV3 sand.

Gaps of less than 0.5 metre are present in the recorded data for the micro-spherically focussed (MSFL) tool. The origin of these gaps uncertain, if the data had been transposed from analogue to digital formats, then these gaps may represent the pen skipping. As the gaps in the log data are small, there is minimal effect to the log analysis results.

The photo-electric factor (PEF) log is responding anomalously high, possibly due to poor calibration, and required a static shift to allow the complex lithology model to define the relative percentage of quartz, limestone, and dolomite.

The spontaneous potential (SP) tool displays very poor bed resolution and definition, and is erratic in nature. This is suggestive of the formation water resistivity (Rw) being similar to the mud filtrate resistivity (Rmf), which is not true, or the SP fish is improperly grounded electrically. There may be an additional effect of mechanical rig noise, causing the “chatter” in the log’s appearance. As a result, the SP log was not used in this interpretation.

Suite/Run	Tool String	Interval (mMDRT)	BHT (degC)
1/1	ISF-BHC-MSFL-GR-SP-CALS	399-1759	75.0
2/1	ISF-BHC-MSFL-GR-SP-CALS	1755-1984	72.0
2/2	LDL-CNL-GR-CALI	1755-1985	79.0
3/1	ISF-BHC-MSFL-GR-SP-CALS	1755-3350	121.0
3/2	LDL-CNL-NGT-EPT-CALI	1755-3350	
3/3	HDT-GR	1755-3350	
3/4	RFT-GR	1819-2845	
3/5	RFT-GR	1807-2988	
3/6	RFT-GR		
3/7	RFT-GR		
3/8	RFT-GR		
3/9	CST-GR		
3/10	VSP		

Table-2. Log Data Acquired

Additional logs, acquired as part of suite-3 and not utilised in this interpretation, include the natural gamma ray spectrometry tool (NGT) and the electro-magnetic propagation tool (EPT). The EPT may be of use in the identification of thin beds. The NGT will be of use for the purposes of clay-typing and mineralogy determination. The NGT tool may also be useful in optimising the permeability calculation from the logs, once matched to valid routine core analysis (RCA) data. Unfortunately the core acquisition was poor, leading to a reduced confidence in the available RCA data. Only five valid RCA plugs are available from Yolla-1, which makes the inclusion of the NGT data statistically invalid in assisting to derive permeability. Should quality RCA data be collected from wells in the future and merged with the valid data from Yolla-1, then the NGT data should be re-visited.

Formation Test Data

Four cased-hole drill-stem tests (DST) were conducted during the drilling of the 12.25” hole section (Table 3). The high water production recorded in DST-2 was the result of water entering through channels in the cement surrounding the casing. DST-2A and DST-3 were conducted following several cement squeezes. Both these latter valid DSTs in the upper EVCM flowed oil and gas to surface.

Test	Interval (mRT)	Formation	Flow	Choke Size
1	2809.1-2814.2 2817.9-2824.6	EVCM	GTS @ 15.1MMcfd OTS @ 580 bcpd	40/64”
2	1830.0-1835.2	Upper EVCM	GTS @ 2.2 MMcfd WTS @ 1675 bwpd	32/64”
2A	1833.2-1833.8	Upper EVCM	GTS @ 1.02 MMcfd OTS @ 302 bopd	16/64”
3	1813.0-1833.8	Upper EVCM	GTS @ 11.8 MMcfd OTS @ 892 bopd	80/64”

Table-3. Formation Tests

BOREHOLE DATA

Hole Conditions

The borehole is in excellent condition, with no washouts exceeding 0.5 inches over-gauge except above 1769 mMDRT up to the 13.375” casing shoe. The hole rugosity in the upper EVCM section is low throughout. Above 1810 mMDRT and within claystone units, there are highly conductive stringers present on the MSFL that coincide with slight increases in caliper (CALI). These features may represent fractures, but without image logs it is not possible to determine if their origin is drilling-induced or natural.

Mud Properties

The section encompassing the upper EVCM was drilled with a freshwater-gel-polymer mud (Table 4), where the mudweight and solids entrapment were minimised. This mud system provided an in-gauge hole that was optimised to allow for high quality wireline logs to be acquired.

Depth	Mud Type	Mud Weight (g/cc)	R_{mf} @ Temp (Ωm @ °C)	Viscosity (sec/litre)	Chlorides (ppm)
1982.5	Water-Poly	1.07	0.627 @ 17	49	4,000
Solids (%)	**Sand (%)**	**R_m @ Temp (Ωm @ °C)**	**R_{mc} @ Temp (Ωm @ °C)**	**Fluid Loss (cc)**	**Barite (%)**
4	Tr	0.682 @ 20	0.980 @ 16	6.0	0.0

Table-4. Mud Properties

Bottom Hole Temperature

A Horner temperature plot of the results of the two logging passes in suite-2 (Figure 2), provides an extrapolated bottom hole temperature (BHT) of 94.0 degrees Celsius. The maximum-recorded temperatures from the individual logging runs were used to environmentally correct the wireline log data.

RESERVOIR QUALITY

The upper EVCM contains two potential reservoir sections (1814.0-1858.0, 1866.5-1883.0 mMDRT).

The upper reservoir represents a thinly-bedded sequence of interbedded argillaceous sandstones and siltstones, which fines upwards into a siltstone and claystone dominated lithology. The sandstones are described from core, sidewall cores, and cuttings, as light to medium brown, very fine-grained sandstone containing moderately well sorted, angular grains. The sandstones contain common argillaceous matrix, and trace mica and carbonaceous fragments. Good visual porosity, moderate fluorescence, and good gas shows were recorded from the sandstones.

A short core was recovered within this zone. Routine core analysis (RCA) conducted on plugs cut from this core, recorded good porosities but low permeabilities. Recent petrological studies have revealed that these sandstones contain 20-40% kaolinitic clay. The measured core plug porosity is being artificially enhanced by the presence of large quantities of micro-porosity present within the clay structure. In addition, many of the sandstones are intensely bioturbated, which destroys the internal fabric of the rock, increases the tortuosity, and decreases the permeability in the samples. These sandstones would be expected to be poor reservoirs and flow at low rates due to the very-fine grain-size, low permeability, and high clay content.

HORNER TEMPERATURE PLOT

WELL:	Yolla-1	**LOG SUITE:**	2
PERMIT:	TR/L1	**DATE:**	19-Jul-85
NOTES:	Sensor measure points estimated.	**T.D.:**	1986.0 (Logger)
	Circulation time assumed to be 1.0 Hours.		

LOG TYPE	BOTTOM DEPTH OF LOGGED INTERVAL mRT {Sensor Measure Point}	Tx (hrs)	T (hrs)	T/(Tx+T)	Max. TEMP Deg C	Eq. Max TEMP Deg C
ISF-MSFL-BHC-GR-SP-CALS	1976	1.00	5.50	0.846	72	72.00
LDT-CNL-GR-CALI	1980	1.00	8.17	0.891	79	79.16

Where: Tx = CIRCULATION TIME
T = TIME SINCE CIRCULATION STOPPED

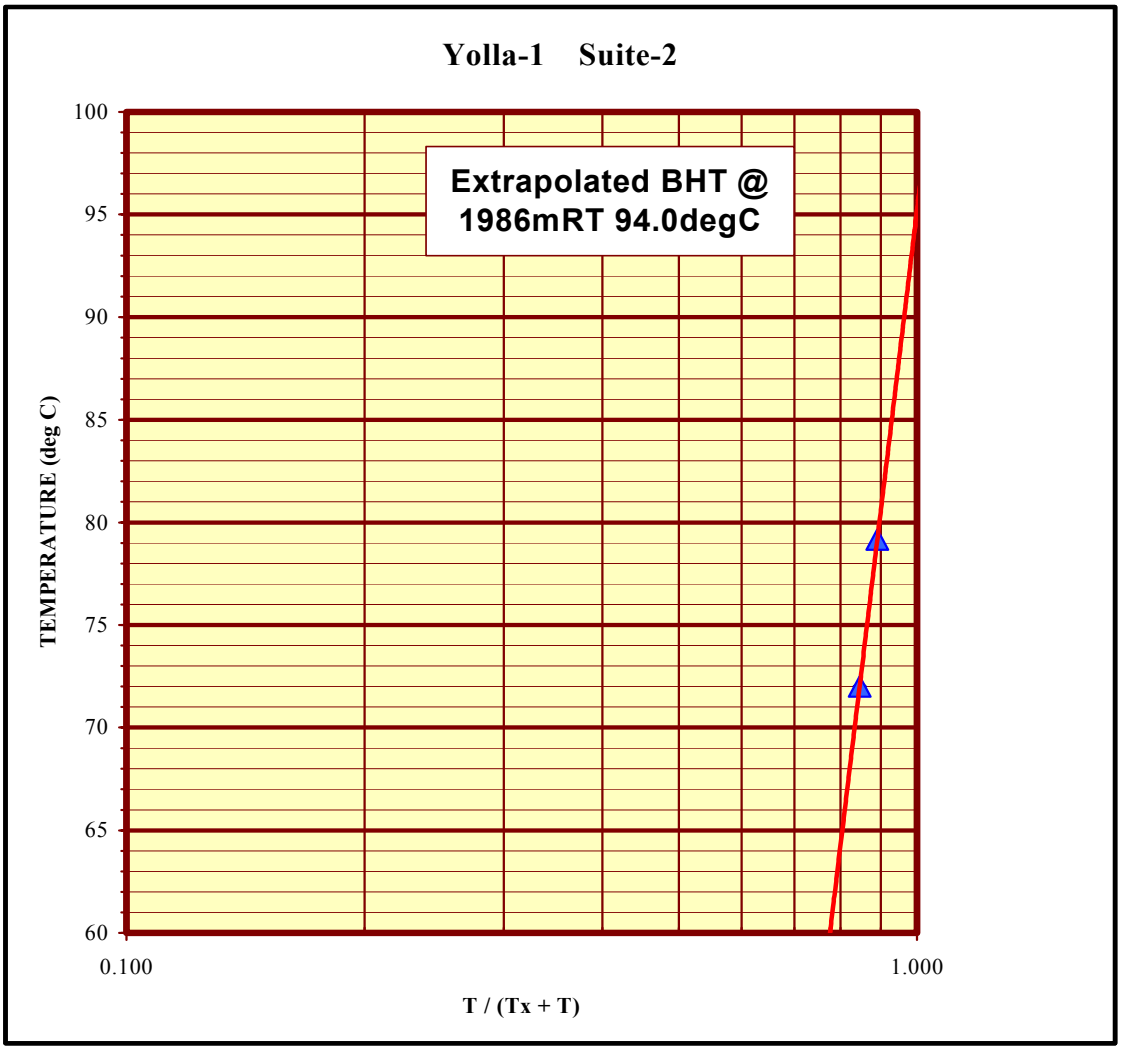

Figure-2. Suite-2 Extrapolated Borehole Temperature Plot

The lower reservoir section (1866.5-1883.0 mMDRT) is an interbedded sequence of moderately clean sandstones, arenaceous claystones, and coals at the base of the reservoir. From sidewall cores and cuttings, the sandstones are light to medium brown, very fine to fine-grained sandstone containing poorly sorted, angular to sub-angular quartz grains. The sandstones contain trace argillaceous matrix and carbonaceous fragments. Good visual porosity, poor fluorescence, and nil gas shows were recorded from the sandstones.

The reservoir quality is higher in this lower section, predominantly due to the decreased clay content within the sandstones. In particular, a sandstone bed between 1866.5 and 1871.5 mMDRT, is interpreted with minimal clay content and its blocky GR character is suggestive of a shore-face or fluvial depositional environment.

HYDROCARBON SHOW EVALUATION

The upper EVCM in Yolla-1 has been sub-divided into three zones based upon the quality of the hydrocarbon shows present (1815.0-1830.0, 1830.0-1845.25, 1845.25-1856 mMDRT). The show for each zone has been evaluated using a show evaluation procedure developed for the onshore Surat, Bowen, Eromanga, and offshore Carnarvon Basins. This procedure has not been calibrated for the offshore Bass Basin, and therefore the recorded scores should be used as qualitative, rather than quantitative guides. This procedure does provide an efficient means of comparing and contrasting the shows recorded in the upper EVCM, and assists in arriving at conclusions as to the interpreted nature of the show (i.e. movable, residual, etc).

Natural fluorescence was first noted in an argillaceous sandstone sidewall core from 1815 mMDRT. The interval 1815-1830 mMDRT can be summarised to contain a trace to 20% faint, uneven, yellow-brown fluorescence, with a slow, very pale yellow crush cut, and a trace of very dull yellow residual ring. The maximum gas peak of 400 units of C1-C4 gas was recorded at 1812 mMDRT. This zone has been interpreted as containing only trace hydrocarbons, which have probably leaked up into the poorer quality reservoirs present in this zone over geological time (Figure-3). This zone is unlikely to contain significant quantities of recoverable hydrocarbon.

HYDROCARBON SHOW EVALUATION FORM

WELL: Yolla-1 FORMATION: Upper EVCM					INTERVAL 1815-1830 mRT				INTERPRETATION Trace Hydrocarbon				
POINTS	**1**	**2**	**3**	**4**	**5**	**6**	**7**	**8**	**9**	**10**	**Factor**	**Points**	**Source**
Mud Weight Overbalance (SG)	0.024	0.048	0.072	0.096	0.120	0.144	0.168	0.192	0.216	>0.24	x3	**6**	Mudlog
Increase in ROP into Show Interval		x1.5			x2			x2.5			x3	**6**	
Increase in Total Gas over Background	x2	x3	x4	x5	x6	x7	x10	x20	x40	>x80		**3**	
Increase in C1 over Background	x2	x3	x4	x5	x6	x7	x10	x20	x40	>x80		**3**	
Increase in C2 over Background	x2	x3	x4	x5	x6	x7	x10	x20	x40	>x80		**6**	
Increase in C3 over Background	x2	x3	x4	x5	x6	x7	x10	x20	x40	>x80		**4**	
Increase in C4 over Background	x2	x3	x4	x5	x6	x7	x10	x20	x40	>x80		**4**	
Visual Estimated Porosity (%)	<5			5 - 10		10 - 15		15 - 20		>20	x3	**15**	SWC Desc
Show Lithology with Fluorescence (%)	Trace	10	20	30	40	50	60	70	80	>90	x2	**4**	
Fluorescence Colour		Brown		Orange	Gold	Yellow	Cream		White	Blue White		**4**	
Fluorescence Distribution	Pinpoint			Spotted			Patchy			Uniform		**4**	
Fluorescence Intensity	Faint			Dull			Dim			Bright		**1**	
Dominant Cut Fluorescence Type		Slow Crush	Crush	Fast Crush			Slow Stream	Streaming	Fast Stream	Instant	x2	**4**	
Hydrocarbon Residue on Spot Dish	Trace		Thin Ring	Ring	Thick Ring		Thin Film	Film	Thick Film	Solid		**1**	
											Total	**65**	

Figure-3. Hydrocarbon Show Evaluation, 1815-1830 mMDRT.

The next zone, between 1830 and 1845.25 mMDRT, is bounded by an increase in show quality and quantity in a sidewall core recovered from 1830 mMDRT, and the top of the recovered core at 1845.25 mMDRT. The core itself is described with minimal fluorescence, but associated rubble interpreted to be remnants of rock making up the non-recovered upper portion of the cored interval, contains the best fluorescence noted in the upper EVCM in this well. The show in this section can be summarised as 40-80% moderately bright, even, yellow to occasionally blue-white fluorescence, with a slow, light yellow, streaming cut, and a light yellow residual ring. The interval 1829-1835 mMDRT contains a maximum gas peak of 15,000 units of C1-C4 gas. This zone has been interpreted as containing movable hydrocarbons (Figure-4), with the interval 1829-1835 mMDRT having the potential to flow at high rates.

HYDROCARBON SHOW EVALUATION FORM

WELL: Yolla-1 FORMATION: Upper EVCM					INTERVAL 1830-1845.25 mRT				INTERPRETATION Movable Hydrocarbon				
POINTS	**1**	**2**	**3**	**4**	**5**	**6**	**7**	**8**	**9**	**10**	**Factor**	**Points**	**Source**
Mud Weight Overbalance (SG)	0.024	0.048	0.072	0.096	0.120	0.144	0.168	0.192	0.216	>0.24	x3	**6**	Mudlog
Increase in ROP into Show Interval		x1.5			x2			x2.5			x3	**12**	
Increase in Total Gas over Background	x2	x3	x4	x5	x6	x7	x10	x20	x40	>x80		**10**	
Increase in C1 over Background	x2	x3	x4	x5	x6	x7	x10	x20	x40	>x80		**10**	
Increase in C2 over Background	x2	x3	x4	x5	x6	x7	x10	x20	x40	>x80		**10**	
Increase in C3 over Background	x2	x3	x4	x5	x6	x7	x10	x20	x40	>x80		**10**	
Increase in C4 over Background	x2	x3	x4	x5	x6	x7	x10	x20	x40	>x80		**10**	
Visual Estimated Porosity (%)	<5			5 - 10		10 - 15		15 - 20		>20	x3	**27**	SWC Desc
Show Lithology with Fluorescence (%)	Trace	10	20	30	40	50	60	70	80	>90	x2	**14**	
Fluorescence Colour		Brown		Orange	Gold	Yellow	Cream		White	Blue White		**7**	
Fluorescence Distribution	Pinpoint			Spotted			Patchy			Uniform		**8**	
Fluorescence Intensity	Faint			Dull			Dim			Bright		**9**	
Dominant Cut Fluorescence Type		Slow Crush	Crush	Fast Crush			Slow Stream	Streaming	Fast Stream	Instant	x2	**14**	
Hydrocarbon Residue on Spot Dish	Trace		Thin Ring	Ring	Thick Ring		Thin Film	Film	Thick Film	Solid		**4**	
											Total	**151**	

Figure-4. Hydrocarbon Show Evaluation, 1830-1845.25 mMDRT.

The basal zone (1845.25-1856 mMDRT) encompasses the top of the recovered core interval down to the base of any natural fluorescence noted in the sidewall cores and cuttings. The shows in this zone can be summarised as 20-40% faint, uneven, yellow-brown fluorescence, with a moderately fast, yellow, crush cut, and a thin, yellow residual ring. The interval 1846.5-1850 mMDRT contains a maximum gas peak of 650 units of C1-C3 gas. This gas peak coincides with the base of the cored interval, and may be artificially enhanced by swabbing fluids into the hole while extracting the core barrel, and via the increased time that the formation was left open to the borehole while tripping in and out of the hole. Consequently, although included in the hydrocarbon show evaluation (Figure-5), little confidence is placed in the reliability of this gas peak. This basal zone has been interpreted as containing residual hydrocarbons, and would not be expected to flow any hydrocarbons.

LOG ANALYSIS METHODOLOGY

A complete listing of all reservoir zonations, petrophysical models, constants, and parameters applied in the interpretation are included as Appendix 1.

HYDROCARBON SHOW EVALUATION FORM

WELL: Yolla-1 FORMATION: Upper EVCM					INTERVAL 1845.25-1856 mRT				INTERPRETATION Residual Hydrocarbon				
POINTS	**1**	**2**	**3**	**4**	**5**	**6**	**7**	**8**	**9**	**10**	**Factor**	**Points**	**Source**
Mud Weight Overbalance (SG)	0.024	0.048	0.072	0.096	0.120	0.144	0.168	0.192	0.216	>0.24	x3	**6**	Mudlog
Increase in ROP into Show Interval		x1.5			x2			x2.5			x3	**15**	
Increase in Total Gas over Background	x2	x3	x4	x5	x6	x7	x10	x20	x40	>x80		**10**	
Increase in C1 over Background	x2	x3	x4	x5	x6	x7	x10	x20	x40	>x80		**10**	
Increase in C2 over Background	x2	x3	x4	x5	x6	x7	x10	x20	x40	>x80		**8**	
Increase in C3 over Background	x2	x3	x4	x5	x6	x7	x10	x20	x40	>x80		**8**	
Increase in C4 over Background	x2	x3	x4	x5	x6	x7	x10	x20	x40	>x80		**2**	
Visual Estimated Porosity (%)	<5			5 - 10		10 - 15		15 - 20		>20	x3	**18**	SWC Desc
Show Lithology with Fluorescence (%)	Trace	10	20	30	40	50	60	70	80	>90	x2	**8**	
Fluorescence Colour		Brown		Orange	Gold	Yellow	Cream		White	Blue White		**4**	
Fluorescence Distribution	Pinpoint			Spotted			Patchy			Uniform		**4**	
Fluorescence Intensity	Faint			Dull			Dim			Bright		**1**	
Dominant Cut Fluorescence Type		Slow Crush	Crush	Fast Crush			Slow Stream	Streaming	Fast Stream	Instant	x2	**6**	
Hydrocarbon Residue on Spot Dish	Trace		Thin Ring	Ring	Thick Ring		Thin Film	Film	Thick Film	Solid		**2**	
											Total	**102**	

Figure-5. Hydrocarbon Show Evaluation, 1845.25-1856 mMDRT

Preparation

Schlumberger wireline were loaded from digital field tape copies into the Crocker Data Processing (CDP) Petrolog v8.13 software.

Due to time constraints and the focussed nature of this study, only logs from suite-2 were utilised, and were referenced to the casing shoe. No high resolution logging data was acquired.

Environmental Corrections

The GR curve from the resistivity pass was corrected for borehole size using the micro resistivity caliper, and Potassium Chloride (KCl) concentration.

The Deep Induction (ILD) log was corrected for hole size and stand-off. The Micro Spherically Focussed Log (MSFL) log was corrected for mudcake thickness. The spherically focussed induction (SFLU) log was corrected for hole size and mudcake thickness. The invasion diameter correction was applied and the true formation resistivity (Rt) and invaded zone resistivity (Rxo) were calculated.

The density (RHOB) log data was corrected for borehole size and mud density at the wellsite.

The Compensated Neutron (NPHI) log was corrected in the field for borehole size. The following corrections were applied within Petrolog: borehole salinity, formation salinity, formation temperature, formation pressure, mudcake thickness, and mud density.

Clay Volume and Porosity

Clay volume (VCl) was defined by application of a linear GR, RHOB-NPHI cross-plot, RHOB-DT cross-plot, and DT models. The minimum VCl calculated from all techniques was applied as the VCl in the interpretation. VCl parameters were set to ensure that the average values calculated from logs matched the sidewall cores and cuttings descriptions. Clay parameters for the upper EVCM unit were set from an argillaceous claystone-bearing interval (1765.0-1807.2 mMDRT; Figure-6)), which acts as the seal for the hydrocarbon-bearing reservoirs. The sand parameters were set from the best reservoir quality sandstones lower in the section, 1866.6-1871.2 mMDRT (Figure-7).

A linear density-neutron model was applied to derive porosity, with a Wyllie sonic porosity model being applied in badhole areas. Badhole was defined using cut-offs for differential caliper, DRHO, and hole rugosity.

Formation Water Resistivity

DST-2 (1830.0-1835.2 mMDRT) recovered water at an average of 1675 BWPD. Following several squeeze jobs, the interval was re-tested (DST-2A) and produced no water. The top of the re-drilled section above the final cement plug, above which DST-2A was recorded was 1887.3 mMDRT. The first good quality, porous, water-bearing sandstones below 1887.3 mMDRT are present between 1910 and 1960 mMDRT, and it is these sandstones that are assumed to be producing the water produced in DST-2. Table-5 summarises the water resistivity of this sample.

The confidence in the water analysis resistivity can be indicated by a water analysis quality rating, with one representing an excellent analysis, and eleven representing an unacceptable result. The water analysis rating is affected by the volume and type of fluid recovered, the length of the flow period, the chemical balance of anions and cations and ratios thereof, the pH of the sample, and difference between Rw and Rmf.

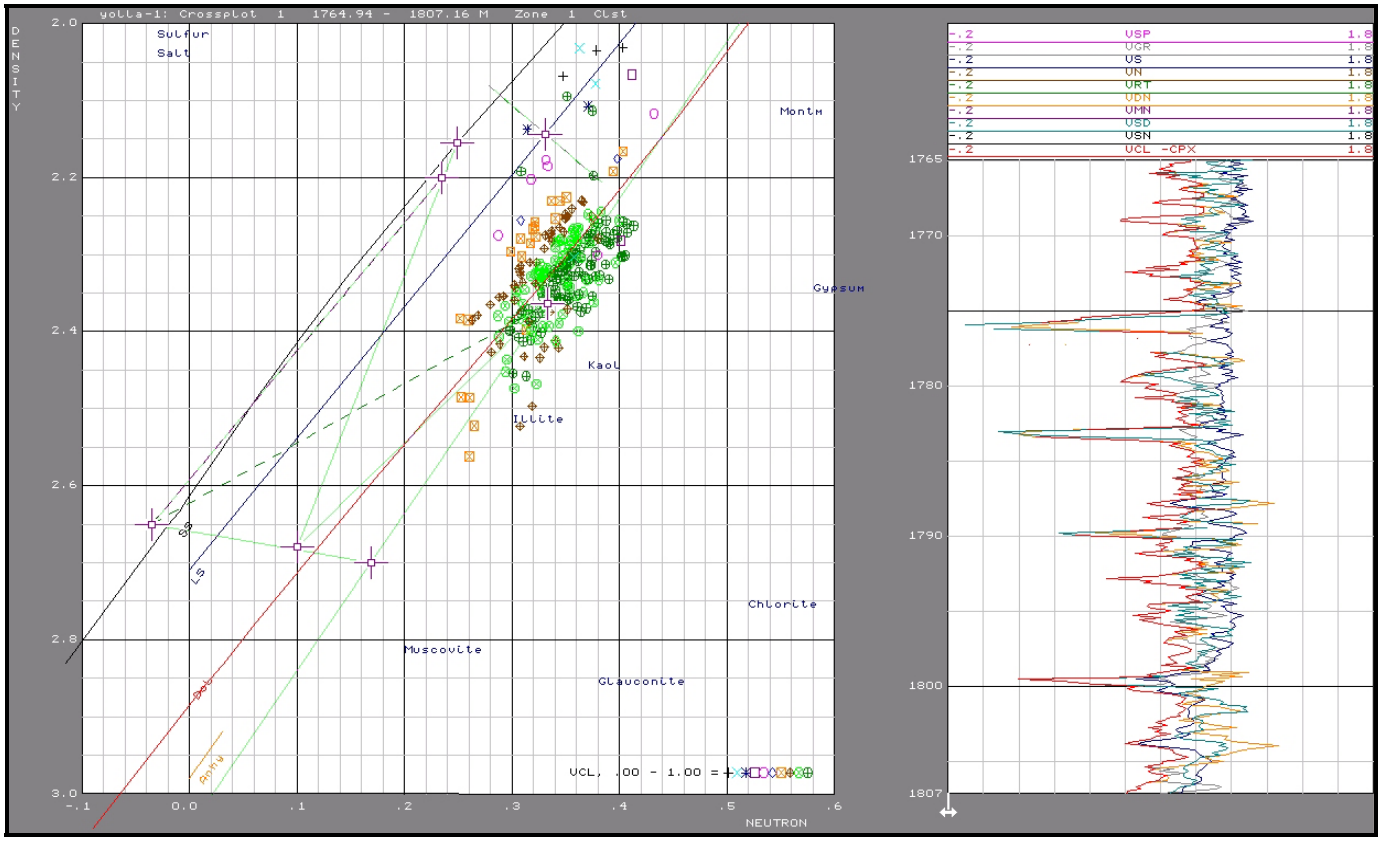

Figure 6. Clay volume determination, RHOB-NPHI, upper EVCM, 1765.0–1807.2 mMDRT

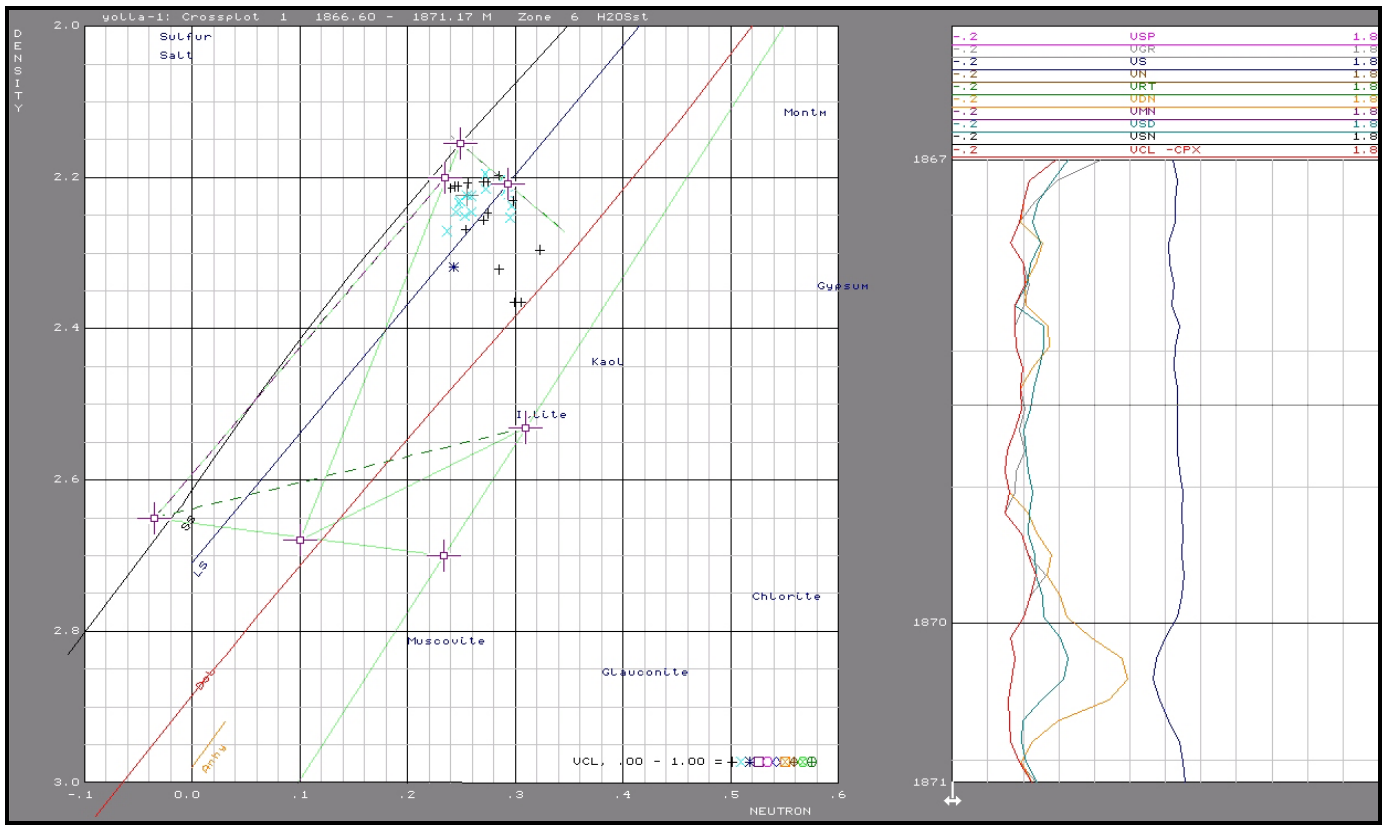

Figure 7. Sand volume determination, RHOB-NPHI, upper EVCM, 1866.6 1871.2 mMDRT

Formation	Well	Quality Rating	R_w @ Temp (Ωm @ °C)	Salinity (ppm NaCl Eq)	Source
Upper EVCM	Yolla-1	1	0.115 @ 25	60,300	DST-2 Rec 420 bbls water

Table-5. Upper EVCM water analysis results

The high salinity of this water sample has a profound effect on the measured formation water resistivity and ultimately on the calculated water saturation. Although this water sample has a quality ranking of one, the salinity of the fluid is approaching twice that of seawater, so the source of these additional cations and anions must be explained. In addition to sodium (Na^+) and Chlorine (Cl^-), there are significant volumes of Calcium (Ca^{2+}), Magnesium (Mg^{2+}), and Sulphate ($SO4^{2-}$) ions present. A Tertiary volcano is located 3.3km NNE of the Yolla-1 location, and it is assumed that this could be source for these ions.

Another concern would be that the immovable formation water trapped in the pore throats within the hydrocarbon column might not be represented by this post-volcanic water chemistry. It is likely that oil and gas migration and emplacement was occurring at the same time as the volcanic episodes, and may be continuing today. This indicates that the water trapped within the hydrocarbon column should be equivalent to the free water present in the underlying water-bearing reservoirs, and that the application of this water resistivity in the log analysis is valid.

It has been suggested that waters with high Mg^{2+} and $SO4^{2-}$ contents may be highly aggressive to cement, which may explain the poor quality of the original cement job, and the requirement for several squeeze jobs to rectify the situation.

Water Saturation

An Indonesian saturation equation was applied to derive hydrocarbon saturations in this study. All input values into the Indonesian Equation are summarised in Appendix 1. The tortuosity factor (a) was kept constant at 1.0, the saturation exponent (n) remained constant at 2.0, and the cementation exponent (m) was set as 1.8 in all sandstone intervals, 2.0 in all siltstone intervals, and 2.2 in all claystone intervals. The clay resistivity (RCl) was determined from claystones located directly above the hydrocarbon-bearing reservoirs (Figure-8).

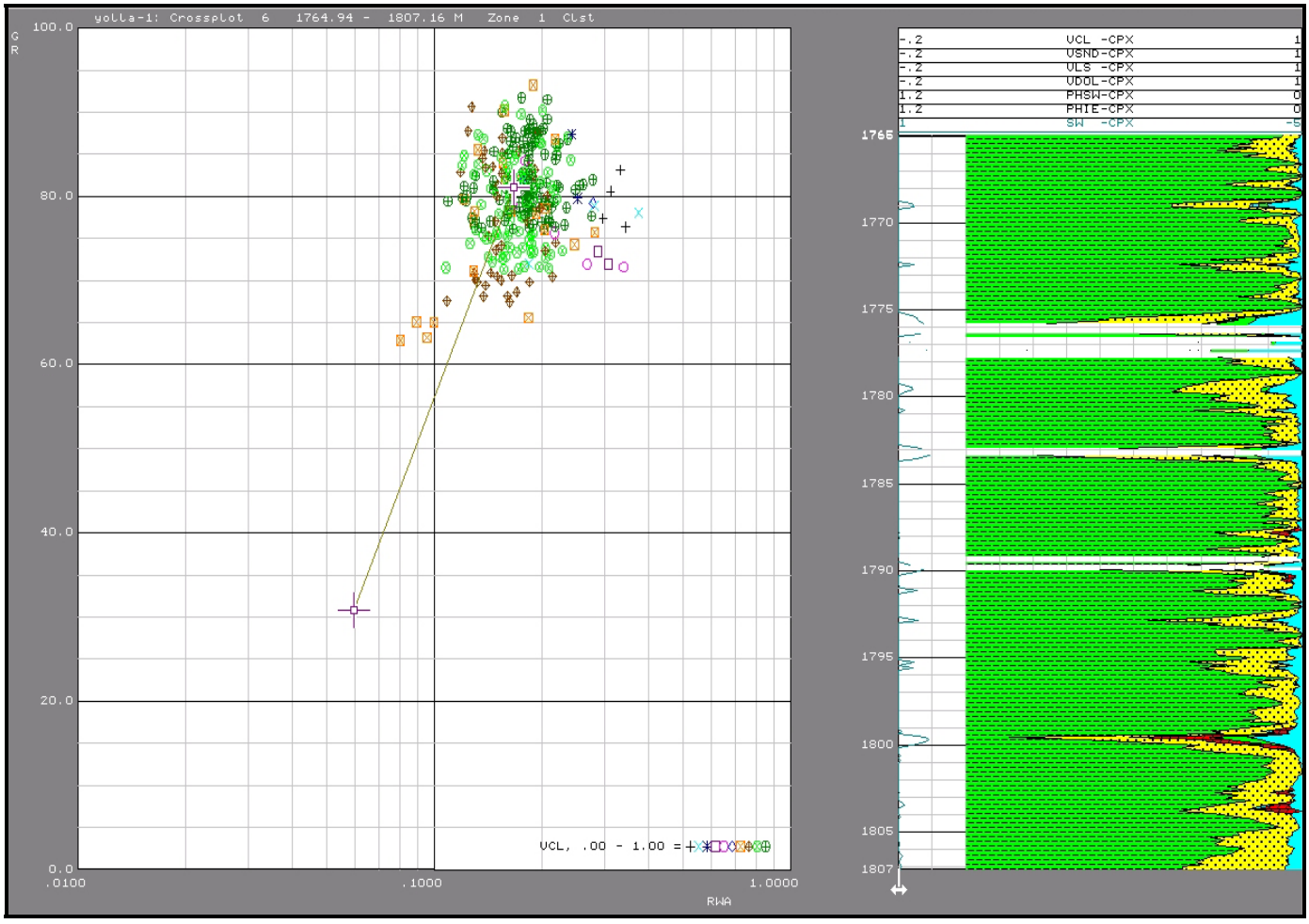

Figure-8. Clay resistivity determination, upper EVCM, 1765.0 – 1807.2 mMDRT

Cut off Parameters

The cut-off limits for petrophysical parameters are detailed in Table-6. The porosity cut-off applied in the gas-bearing zones is 8.0%, and is based upon a permeability cut-off of 0.1mD (see Discussion Chapter and Figure-10). For the fluid-bearing (oil/water) horizons a porosity cut-off of 13.5%, which correlates to a permeability cut-off of 0.5mD, has been applied. The petrophysical results are summarised in Table-7.

Reservoir	VCl < (%)	Φ > (%)	K > (mD)	S_w < (%)
Upper EVCM (Gas)	40	8	0.1	55
Upper EVCM (Oil / Water)	40	13.5	0.5	55

Table-6. Cut Off Parameters

Zonation					Gross Rock	Net Reservoir						Net Pay		
Name	Top		Base		Thickness	Thickness	Av. Clay Volume	Av. Eff. Porosity	Av. Permeability	Ave. kH	Net Res/Gross	Thickness	Av. Water Sat.	Net Pay/Gross
	mKB	mSS	mKB	mSS	metres	metres	%	%	mD	mD.ft	%	metres	%	%
TEV0	1765	1753.9	1800	1788.9	35.0	1.2	30.2	21.4	29.66	118.7	3.5	0		0.0
TEV1	1800.0	1788.9	1807.0	1795.9	7.0	0.0	----	----	----	----	0.0	0.0		0.0
TEV1A	1807.0	1795.9	1817.5	1806.4	10.5	2.7	33.2	11.7	0.81	7.3	26.1	0.0		0.0
TEV2	1817.5	1806.4	1823.1	1812.0	5.6	5.3	28.6	14.0	1.71	29.9	95.2	0.0		0.0
TEV3	1823.1	1812.0	1829.5	1818.4	6.4	5.8	23.2	16.8	3.46	65.7	90.5	0.0		0.0
TEV4	1829.5	1818.4	1839.6	1828.5	10.1	10.1	17.7	25.0	53.59	1775.8	100.0	6.7	46.6	66.4
TEV5	1839.6	1828.5	1843.0	1831.9	3.4	2.4	33.2	20.4	38.50	308.2	71.8	0.0		0.0
TEV6	1843.0	1831.9	1857.8	1846.7	14.8	13.9	21.6	24.2	57.84	2632.0	93.7	0.0		0.0
TEV7	1857.8	1846.7	1866.5	1855.4	8.7	0.2	36.8	14.1	0.61	0.3	1.7	0.0		0.0
TEV8	1866.5	1855.4	1871.4	1860.3	4.9	5.0	5.1	25.0	13.47	222.3	102.7	0.0		0.0
TEV9	1871.4	1860.3	1911.4	1900.3	40.0	9.5	26.9	17.2	2.73	84.6	23.6	0.0		0.0
TEV10	1911.4	1900.3	1929.0	1917.9	17.6	15.5	13.9	21.6	9.53	485.9	88.3	0.0		0.0
Total	1800.0	1788.9	1880.0	1869.6	164.0	71.7	19.6	21.6			43.7	6.7	46.6	4.1
DST-2A	1833.2	1822.1	1833.8	1822.7	0.6	0.6	20.9	24.4	112.26	221.0	100.0	0.6	47.2	100.0
DST-3	1822.0	1810.9	1842.0	1830.9	20.0	17.1	20.4	22.1	17.12	958.6	85.4	6.7	46.6	33.6
Best Sand	1830.3	1819.2	1833.3	1822.2	3.0	3.0	9.6	27.7	74.26	730.9	100.0	3.0	41.4	100.0

Table-7. Reservoir Summary

DISCUSSION

Reservoir quality in the uppermost portion (TEV1A and TEV3) of the upper EVCM above 1830 m is considered poor to moderate. Although a few, thin sandstones exist, this section is dominated by argillaceous sandstones and siltstones that do not contribute to net reservoir. Given the high clay content in the reservoirs that are present (average 34 percent), the average porosity of 19 percent is higher than expected. As previously discussed, this is interpreted to be due to the presence of significant volumes of secondary, microporous kaolinite. While this secondary porosity does contribute to log derived porosity, it will have minimal correlation with permeability. This is confirmed by the routine core analysis measurements, which return high porosity and low permeability results. Minimal net pay is calculated for this section, which is confirmed by the hydrocarbon show evaluation, which yield only a trace of hydrocarbon.

The central hydrocarbon-bearing section (TEV4) between 1830 and 1842.1 mMDRT has moderate reservoir quality. Although these sandstones are cleaner than those described above, the presence of almost 30% average Clay volume, restricts the producibility. The 4.0 metres of

net pay identified yields an average water saturation of 43%. Good quality shows were identified within this interval, yielding a show grading of movable hydrocarbons. Calculated permeability within this reservoir has increased markedly in comparison to those reservoirs described above and approaches 10 mD.

The basal section between 1842.1 and 1858.0m contains good reservoir development, with average porosities of 24 percent and permeabilities of 22 mD. Average clay content has decreased in the sandstones to 25 percent. Unfortunately these sandstones are water bearing, as confirmed by be residual hydrocarbon show evaluation.

The most likely depth of the oil water contact (OWC) is interpreted from the logs at 1842.3 mMDRT (Figure-9). A section dominated by arenaceous claystone exists between 1839.6 and 1842.3 mMDRT, so it is difficult to definite about the location of the OWC. Assuming that the mineralogy, and therefore the resistivity, of this claystone bed is similar to underlying claystone beds, and the presence of small amounts of hydrocarbon saturation in the claystone, suggests that this claystone is within the hydrocarbon-bearing section. A transition zone is interpreted between 1840.7 and 1842.3 mMDRT, with the top of the transition zone located at a depth where hydrocarbon saturation begins to decrease for a constant effective porosity.

Due predominantly to the high clay content in these reservoirs, the thin-bedded nature of high permeability stringers, and the lack of high-resolution wireline logs, a gas oil contact (GOC) is difficult to identify. The results of DST-2A, which initially flowed oil (fluid density = 0.78 g/cc), and later flowed some gas (fluid density = 0.47 g/cc) from a 0.6 metre interval between 1833.2 and 1833.8 mMDRT, suggests that the GOC is a small distance above 1833.2 mMDRT. The section between 1831.2 and 1832.1 mMDRT displays a larger density-neutron separation than lower zones with similar reservoir quality, which is suggestive of gas being present. Given that the GR suggests that these reservoirs are similar in clay content, the most likely depth of the GOC is 1832.1 mMDRT, but it could be as low as 1833.2 mMDRT.

Average permeabilities calculated as part of this study have been derived from only four valid routine core analysis plugs (Table-8). Almost half of the routine core analysis results obtained from the Yolla-1 core were deemed invalid and not used in the derivation of porosity-permeability transform, due to poor core acquisition and handling, inadequate core plug length, and plug

fracturing. Figure-10 displays the derived porosity-permeability transform for the valid plugs. Further work is required to evaluate the effect of clay volume on the permeability, and more cores are required in order to improve this correlation.

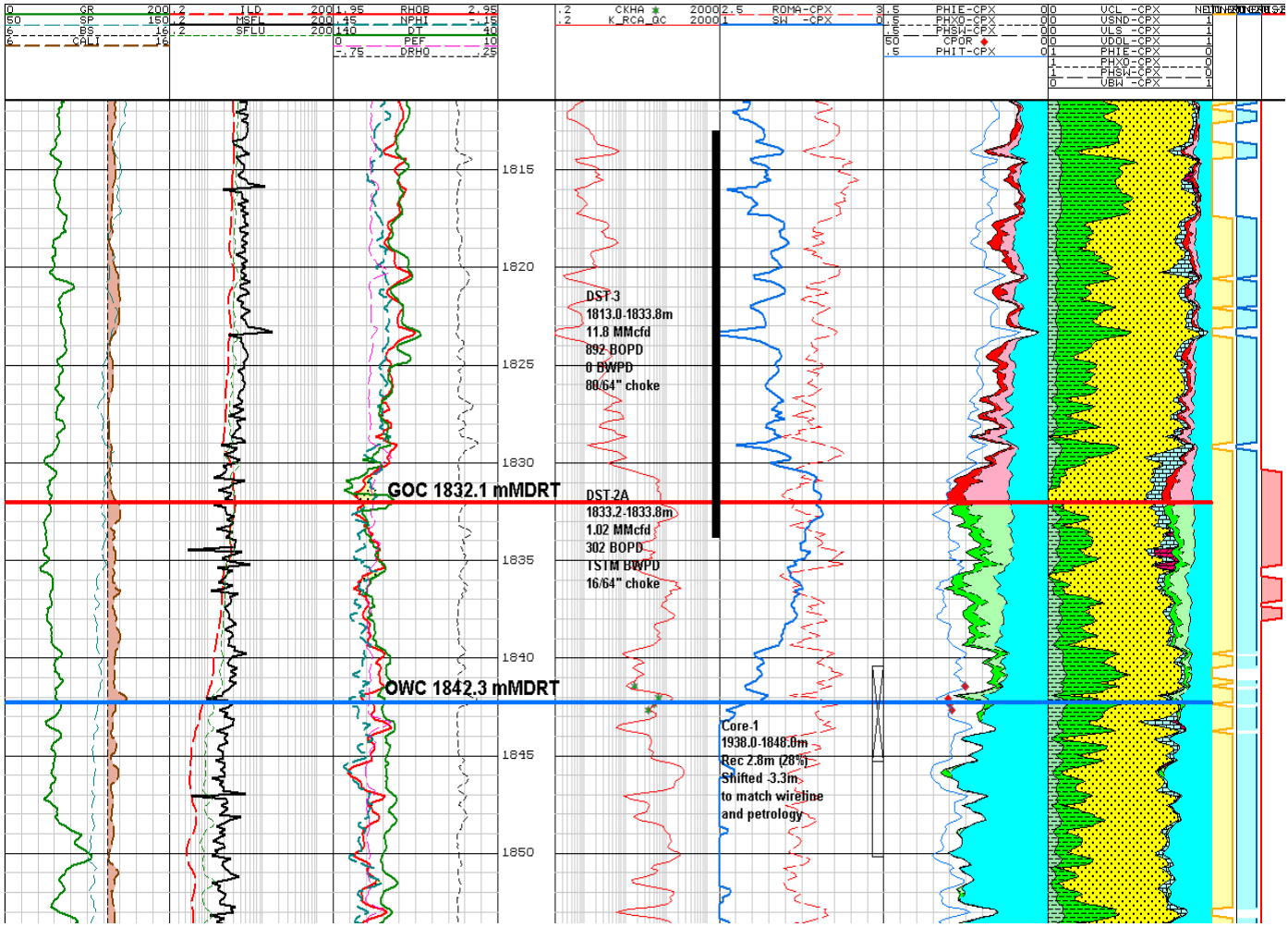

Figure-9. Petrophysical Summary Plot, upper EVCM.

Depth (m)	Porosity Ambient (%)	Hor. Permeability Ambient (mD)	Hor. Permeability Klinkenburg (mD)	Comments
1846.94	25.2	17	13.5	Valid plug
1847.55	30.4	65	54.9	Valid plug
1847.85	30.0	51	42.6	Valid plug
1848.15	29.2	37	30.5	Valid plug
1847.24	25.8	11	8.6	Invalid, short plug
1846.63	29.6	75	63.8	Invalid, short plug
1848.46	30.0	42	63.8	Invalid, short plug
1848.76	30.9	204	181.2	Invalid, short plug

Table-8. Routine Core Analysis Results

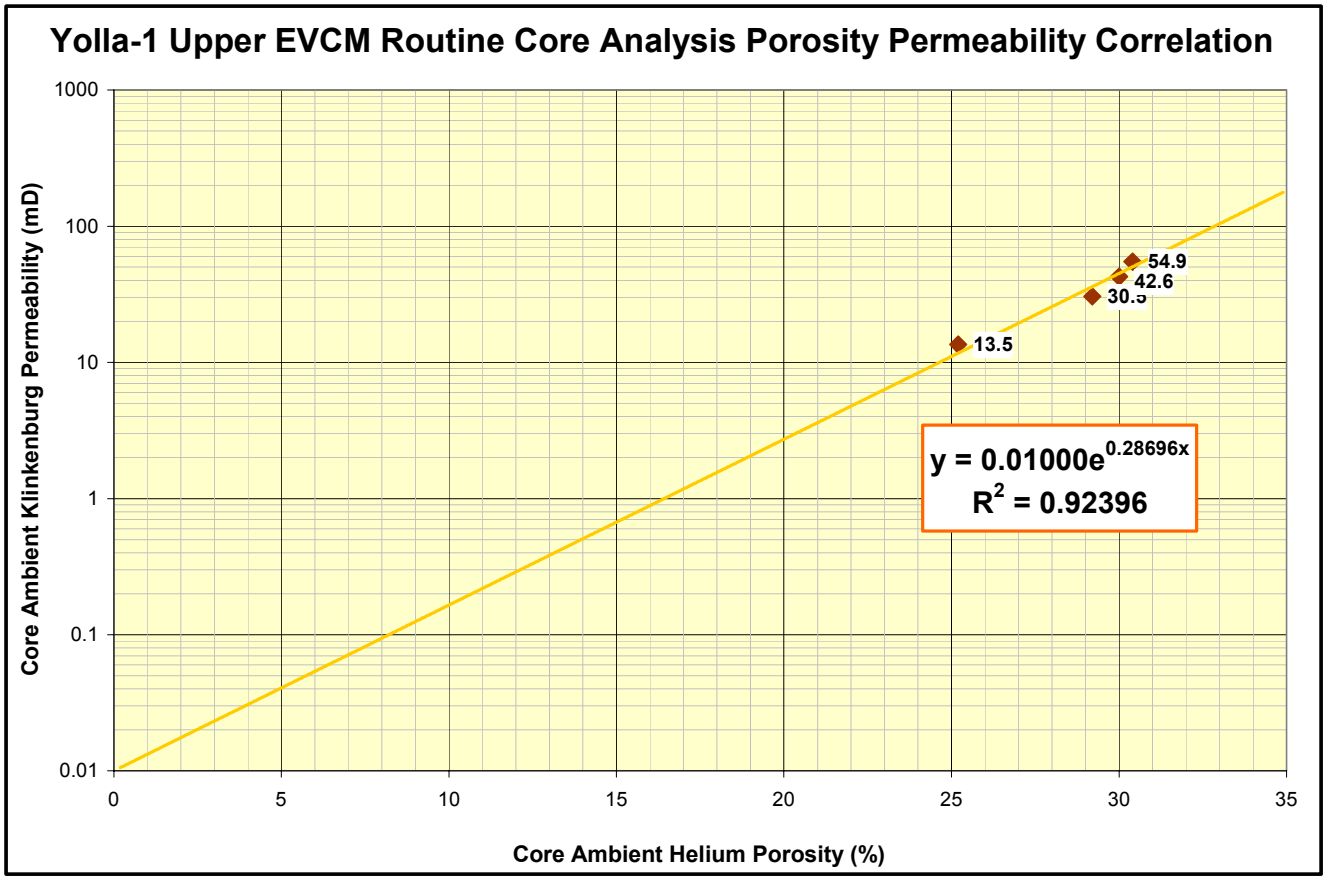

Figure-10. Core-derived porosity-permeability relationship, upper EVCM.

The average permeability-height (kH) functions from the petrophysical analysis are approximately twice that calculated during reservoir simulation for the DST-2A and DST-3 intervals. Drill-stem tests report effective permeability, whereas the core data is reporting total permeability. Core measurements, although corrected for Klinkenburg gas-slippage effects, are not available at overburden conditions. Correcting core analysis permeabilities for overburden effects can result in significant decreases in permeability, particularly in the sub 10mD range. The permeabilities calculated from the petrophysical evaluation are an over-estimation of the true effective permeability, and permeability algorhythms should be re-calculated following the acquisition of further core analysis data in future wells.

Due to the presence of a nearby volcanic intrusion, formation waters in this upper EVCM unit contain significant volumes of calcium, magnesium, sodium, chloride, and sulphate ions. This results in the presence of a highly conductive formation water (60,300 ppm NaCl equivalent), which has significant effects on the calculated water saturations from logs. Formation waters

with high sulphate concentrations can be aggressive to cement (German Building and Engineering Standards Committee, 1991), which may have contributed to the difficulty in obtaining case hole DSTs, and may require special contingencies for cementing programmes for future your wells. Given the high salinity formation water present in these reservoirs, a freshwater gel mud should be utilised to optimise the acquisition of induction logs. Laterolog-type devices should not be applied for this reservoir. If the chemistry of the mud can remain fresh, and rig noise reduced to a minimum during log acquisition, a good quality SP log should be attainable.

A good correlation between mineralogy defined by petrological and petrophysical analysis has been achieved. The complex lithology model applied in this interpretation utilises the RHOB, NPHI, and PEF to derive volumes of quartz+feldspar+lithics, carbonate, clay, and porosity. Petrological analysis identifies the visible macroporosity, where the log analysis calculates a total porosity (PHIT) and, by multiplying PHIT by 1-VCl, arrives at an effective porosity (PHIE). The macroporosity is not the same as PHIE, because PHIE includes microporosity present within the rock matrix. Therefore for the purposes of comparison, both sets of data have been normalised for only quartz+feldspar+lithics, carbonate, and clay (Figure-11).

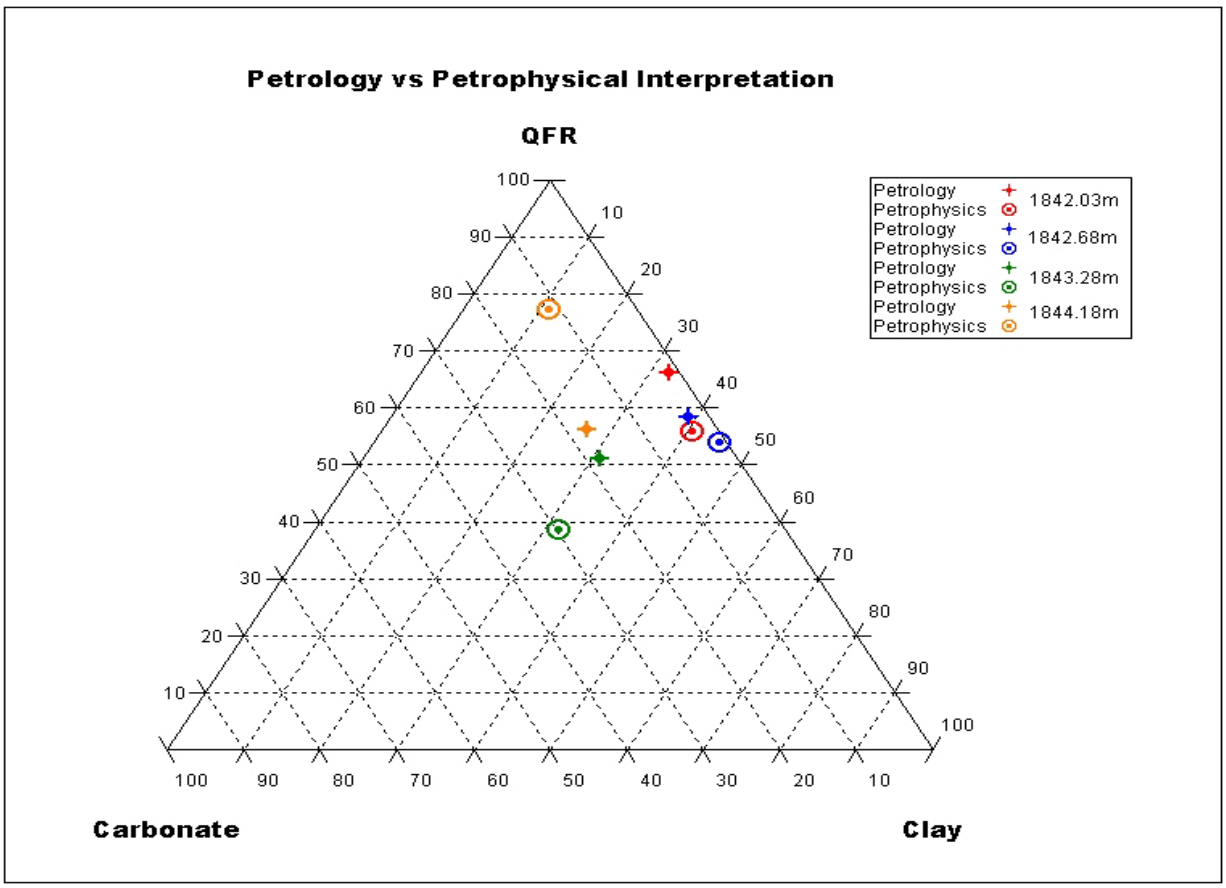

Figure-11. Mineralogical comparison of petrological and petrophysical results.

An increased volume of carbonate was calculated from the petrophysical analysis in the hydrocarbon-bearing zone, which may indicate a change in diagenesis within the hydrocarbon column. This volume of carbonate decreases with depth through the hydrocarbon-bearing zone. It is not uncommon for the emplacement of hydrocarbon to halt diagenesis, which would indicate that carbonate cement predated the hydrocarbon emplacement. The siderite cement described in some of the samples from the petrological study (Baker, 2002) could not form if the formation waters present in the reservoirs had been high in sulphate ions. As the carbonate cement concentration is higher in the hydrocarbon-bearing zone, this suggests that both the carbonate cementation and the emplacement of hydrocarbon pre-date the Tertiary volcanism.

If the emplacement of hydrocarbons pre-dates the Tertiary volcanism, then the immovable water trapped within the hydrocarbon zone may be different to the movable, highly saline water that is present in the water-bearing reservoirs. If this is true, then it is invalid to apply the measured Rw from the produced formation water to the hydrocarbon zone. The formation of siderite most commonly occurs at shallow depths and shortly after burial in a brackish water setting (Baker, pers comm.), which would suggest that the immovable water trapped in the hydrocarbon zone may be substantially fresher than that applied in this interpretation. The effect of decreasing the formation water salinity applied in the petrophysical analysis will result in significant decreases in the hydrocarbon saturation calculated, which would conflict with the DST results. It is therefore assumed that both the emplacement of hydrocarbon and the Tertiary volcanism were occurring simultaneously, but after the development of the siderite cement.

The current geological model for the upper EVCM unit contains a porosity grid. Hydrocarbon saturation is imposed upon this porosity grid by means of a porosity to hydrocarbon saturation correlation (Figure-12). All effective porosity (corrected for hydrocarbon density and shale content) and water saturation data are cross-plotted between the top of the hydrocarbon-bearing reservoirs (1830.3m) and the top of the interpreted transition zone (1840.7m). A correlation coefficient of 61% is adequate to allow the porosity grid to be filled with hydrocarbon saturation.

There exists the potential for fracturing within claystone beds above 1810 mMDRT, however insufficient information was available to identify the cause of these fractures. It is recommended that a resistivity image device is acquired over these claystones in the next development well to identify if these fractures natural or drilling-induced.

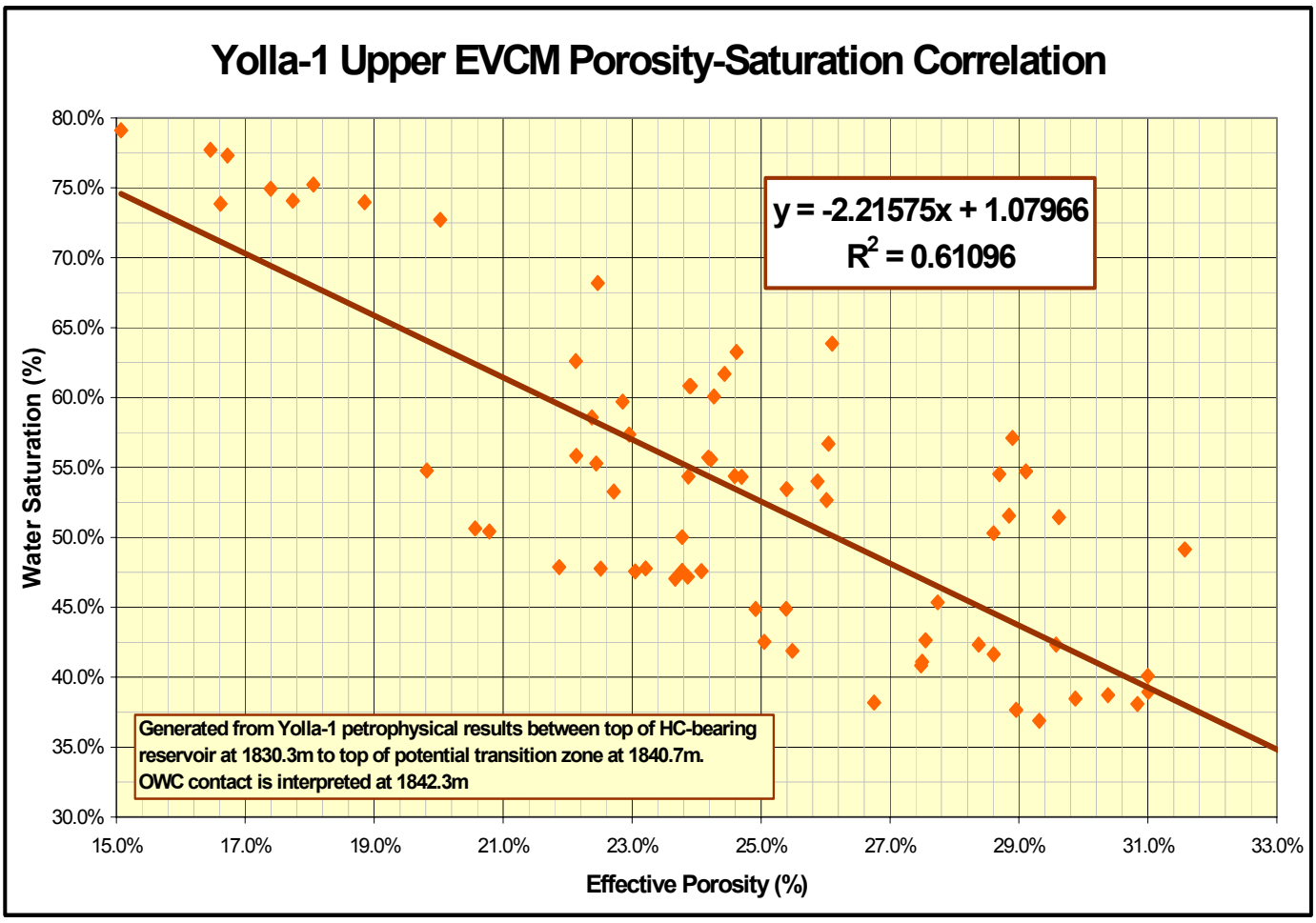

Figure-12. Correlation of effective porosity and water saturation.

Given the thinly interbedded nature of this reservoir it is important that high-resolution logs are acquired to evaluate it. Identification of net pay intervals could be enhanced with the acquisition of resistivity imaging tools over the reservoir sections. One 9 metre core should be planned for the upper EVCM reservoir in the next development well, to allow calibration of the resistivity image. A carefully planned programme of routine and special core analysis, and petrology on plugs from the same depth should greatly improve the porosity-permeability transform. The acquisition of a spectral Gamma Ray should enable log calibration with the core data, and continuation of the porosity-permeability transform outside of the cored interval. Given the high salinity formation water present in these reservoirs, a freshwater gel mud should be utilised to optimise the acquisition of induction logs. Laterolog-type devices should not be applied for this reservoir. If the chemistry of the mud can remain fresh, and rig noise reduced to a minimum during log acquisition, a good quality SP log should be attainable.

CONCLUSIONS / RECOMMENDATIONS

- The upper portion of the upper EVCM unit, above 1829.5 mMDRT, is unlikely to be capable of producing hydrocarbons at economic rates.
- Eight and a half metres of net pay has been identified between 1829.5 and 1839.6 mMDRT in argillaceous sandstones that should have moderate producibility.
- An OWC is identified at 1842.3 mMDRT.
- A GOC is identified between 1832.1 and 1833.2 mMDRT, with the most likely location at 1832.1 mMDRT.
- Hydrocarbon emplacement was occurring at the same time as the Tertiary volcanism to the north of Yolla-1, and both post-date sideritic carbonate cementation.
- In order to optimise the quality of the resistivity wireline log data and to accentuate the contrast with the highly saline formation water, it is recommended that the drilling mud salinity is minimised, and induction, rather than Laterolog, logs are acquired.
- Contingency in the casing plans for any future wells needs to allow for the aggressive nature of the high calcium and magnesium formation waters present.
- A nine metre core should be cut in this upper EVCM reservoir. This would allow evaluation of the thinly-bedded nature of the reservoir, calibration of resistivity image data, measurement of routine and special core analysis characteristics of this lithology, identify the mineralogical components present, and provide improve the porosity and permeability relationships for the reservoir.
- A resistivity image log should be acquired over the upper EVCM reservoir to evaluate the thin-bedded nature of the reservoir, and the claystone-dominated section above 1810 mMDRT to evaluate the nature and origin of fractures noted in Yolla-1.
- High resolution logging passes should be made over the upper EVCM reservoir to optimise evaluation of the thinly bedded nature of the reservoir.
- Spectral Gamma Ray wireline log data should be acquired over the upper EVCM reservoir to enable calibration of porosity-permeability relationships above and below the cored interval.

REFERENCES

Baker, J.C; 2002. Petrology, diagenesis, and reservoir quality of core samples from Yolla-1. Reservoir Solutions Pty Ltd. (unpubl.)

German Building and Engineering Standards Committee, 1991. Assessment of water, soil, and gases for their aggressiveness to concrete. German Standards, DIN 4030 Part II (unpubl.)

Wheeler, B.F; & Kjellgren, G.G; 1986. Yolla-1 final well report. Amoco Australia Petroleum Company. (unpubl.)

Appendix-1
Yolla-1: Petrophysical Parameter Listing

```
LOG ANALYSIS REPORT BY PETROLOG REVISION  8.00
File name: yolla-1.pro    22/01/2002  16:56:38
Software by Crocker Data Processing Pty Ltd

Hole depth M     Temperature C     Gradient Deg C / 100 M
   1982.0           72.00          2.8254

Caliper recorded in : Inches
Mud weight units    : g/cc
Density log units   : g/cc
DRHO    log units   : g/cc
Sonic   log units   : Us/ft
Neutron log units   : LS POR
Density tool type   : LDT
RHO (H,MA,f)  units : g/cc
Dens. X-plots units : g/cc

Log scaling data
----------------
Log         Scaling     Coeff.      Coeff.
Mnemonic    Option        A           B
 NPHI       1         -.03000     1.00000
 RHOB       1          .06000     1.00000
 PEF        1         -.30000     1.00000
```

COMPLEX LITHOLOGY RESULTS

Mineral table

Zone no.		1	2	3	4	5	6	7	8	9
Formation Name		Clst	Slst	GasSst	OilSst	Clst	H2OSst	Slst	H2OSst	Junk
Top depth		1764.944	1807.312	1817.370	1832.153	1856.689	1866.595	1871.320	1919.783	1929.232
Bottom depth		1807.159	1817.218	1832.000	1856.537	1866.443	1871.167	1919.630	1929.079	1981.962
Coal	RHOB min	-INF	-INF	-INF	-INF	-INF	-INF	-INF	-INF	-INF
Coal	RHOB max	2.220	2.030	2.030	2.030	2.220	2.220	2.220	2.220	2.220
Coal	PHIN min	-INF	-INF	-INF	-INF	-INF	-INF	-INF	-INF	-INF
Coal	PHIN max	+INF	+INF	+INF	+INF	+INF	+INF	+INF	+INF	+INF
Coal	GR min	-INF	-INF	-INF	-INF	-INF	-INF	-INF	-INF	-INF
Coal	GR max	+INF	+INF	+INF	+INF	+INF	+INF	+INF	+INF	+INF
Coal	t min	-INF	-INF	-INF	-INF	-INF	-INF	-INF	-INF	-INF
Coal	t max	+INF	+INF	+INF	+INF	+INF	+INF	+INF	+INF	+INF
Coal	RT min	-INF	-INF	-INF	-INF	-INF	-INF	-INF	-INF	-INF
Coal	RT max	+INF	+INF	+INF	+INF	+INF	+INF	+INF	+INF	+INF

```
CPX flag values
 1.  VCL greater than 0.95
 2.  VN  greater than 0.75
 3.  VS  greater than 0.75
 4.  Bad hole condition
 5.  Matrix density greater than Lithological model
 6.  Matrix density less than Lithological model
 7.  Porosity derived from Sonic Log
 8.  Porosity derived from or limited by PHIMAX
 9.  Porosity derived from Density Log
 $.  Pay zone

Water saturation equations
 1.  Indonesia

VGRTYPE :Vclay from GR Equations used
1.  Linear

Cementation factor m
1.  Linear

Logging Company   Mud type     Neutron           RT Determination
0. Schlumberger   0. NaCl      log type          Flags by priority
Formation Water   1. KCl %     0. CNL CORR       23. ERT (external RT)
0=NaCl            2. Oil-base  1. TNPH            1. Dual Laterolog - RXO
1=NaHCO3          3. Barite    2. SNP            20. PHASOR-SFL
```

Zone no.	1	2	3	4	5	6	7	8	9
Formation Name	Clst	Slst	GasSst	OilSst	Clst	H2OSst	Slst	H2OSst	Junk
Top depth	1764.944	1807.312	1817.370	1832.153	1856.689	1866.595	1871.320	1919.783	1929.232
Bottom depth	1807.159	1817.218	1832.000	1856.537	1866.443	1871.167	1919.630	1929.079	1981.962
Logging Comp	0	0	0	0	0	0	0	0	0
Mud type	0	0	0	0	0	0	0	0	0
Fm Water Type	0	0	0	0	0	0	0	0	0

Neutron Log Type	0	0	0	0	0	0	0	0	0
Zone no.	1	2	3	4	5	6	7	8	9
Formation	Clst	Slst	GasSst	OilSst	Clst	H2OSst	Slst	H2OSst	Junk
Top depth	1764.944	1807.312	1817.370	1832.153	1856.689	1866.595	1871.320	1919.783	1929.232
Bottom depth	1807.159	1817.218	1832.000	1856.537	1866.443	1871.167	1919.630	1929.079	1981.962
RM	.682	.682	.682	.682	.682	.682	.682	.682	.682
Temp. RM	20.000	20.000	20.000	20.000	20.000	20.000	20.000	20.000	20.000
RMF	.627	.627	.627	.627	.627	.627	.627	.627	.627
Temp. RMF	17.000	17.000	17.000	17.000	17.000	17.000	17.000	17.000	17.000
RMC	.980	.980	.980	.980	.980	.980	.980	.980	.980
Temp. RMC	16.000	16.000	16.000	16.000	16.000	16.000	16.000	16.000	16.000
Bit size	12.250	12.250	12.250	12.250	12.250	12.250	12.250	12.250	12.250
Mud wt	1.066	1.066	1.066	1.066	1.066	1.066	1.066	1.066	1.066
SSP	-40.000	-40.000	-40.000	-40.000	-40.000	-40.000	-40.000	-40.000	-40.000
RW (SP)	.0750381	.0745961	.0743891	.0740647	.0737836	.0736651	.0732385	.0727815	.0722983
Temperature	66.464	67.204	67.555	68.111	68.597	68.804	69.555	70.373	71.254
RW @ FT	.0593644	.0588687	.0586368	.0582735	.0579589	.0578263	.0573493	.0568389	.0562995
RW@75F(23.9C	.115	.115	.115	.115	.115	.115	.115	.115	.115
RW salinity	60296.020	60296.380	60296.370	60296.400	60296.360	60296.370	60296.390	60296.390	60296.360
RMF @ FT	.275	.272	.271	.270	.268	.267	.265	.263	.260
KPPM (RMF)	.0109957	.0109957	.0109957	.0109957	.0109957	.0109957	.0109957	.0109957	.0109957
RM @ FT	.322	.319	.318	.316	.314	.314	.311	.308	.305
RHO H	.500	.500	.500	.700	.700	.800	.800	.800	.800
RHO F	1.001	1.001	1.001	1.001	1.001	1.101	1.000	1.000	1.000
t F	188.997	188.997	188.997	188.997	188.997	188.997	188.997	188.997	188.997
RHOMA	2.680	2.680	2.680	2.680	2.680	2.680	2.680	2.680	2.680
PHIN min	-.0350000	-.0350000	-.0350000	-.0350000	-.0350000	-.0408974	-.0350000	-.0350000	-.0350000
t MA	55.500	55.500	55.500	55.500	55.500	55.500	55.500	55.500	55.500
t MA min	48.000	48.000	48.000	48.000	48.000	48.000	48.000	48.000	48.000
Sonic option	.000	.000	.000	.000	.000	.000	.000	.000	.000
Compact/Ovrt	1.000	1.000	1.000	1.000	1.000	1.000	1.000	1.000	1.000
CAL cut off	14.000	14.000	14.000	14.000	14.000	14.000	14.000	14.000	14.000
RUGO.cut off	1.000	1.000	1.000	1.000	1.000	1.000	1.000	1.000	1.000
DRHO cut off	.150	.150	.150	.150	.150	.150	.150	.150	.150
Bad Hole	1.000	1.000	1.000	1.000	1.000	1.000	1.000	1.000	1.000
No clay	SP	SP	SP	SP	SP	SP	SP	SP	SP
	RT	RT	RT	RT	RT	RT	RT	RT	RT
	N	N	N	N	N	N	N	N	N
	MN	MN	MN	MN	MN	MN	MN	MN	MN
	SN	SN	SN	SN	SN	SN	SN	SN	SN
Vclay Flag	.000	.000	.000	.000	.000	.000	.000	.000	.000
Vclay type	1.000	1.000	1.000	1.000	1.000	1.000	1.000	1.000	1.000
VclayGR type	1.000	1.000	1.000	1.000	1.000	1.000	1.000	1.000	1.000
GR clean	33.522	33.522	33.522	33.522	33.522	33.522	33.522	33.522	33.522
GR clay	98.904	98.904	98.904	98.904	98.904	98.904	98.904	98.904	98.904
R clay	2.502	2.502	2.502	2.502	2.502	2.502	2.502	2.502	2.502
R limit	1000.000	1000.000	1000.000	1000.000	1000.000	1000.000	1000.000	1000.000	1000.000
Rclay1 flag	.000	.000	.000	.000	.000	.000	.000	.000	.000
Rclay1	1.000	1.000	1.000	1.000	1.000	1.000	1.000	1.000	1.000
Vcl @ Rclay1	.150	.150	.150	.150	.150	.150	.150	.150	.150
RHOB clay	2.449	2.449	2.449	2.449	2.449	2.449	2.449	2.449	2.449
RHO Dry Clay	2.700	2.700	2.700	2.700	2.700	2.700	2.700	2.700	2.700
RHOB silt	2.680	2.680	2.680	2.680	2.680	2.680	2.680	2.680	2.680
PHIN clay	.391	.391	.391	.391	.391	.391	.391	.391	.391
t clay	113.001	113.001	113.001	113.001	113.001	113.001	113.001	113.001	113.001
PHIN 2.2	.265	.265	.265	.265	.265	.265	.265	.276	.265
t 2.2	93.885	93.885	93.885	93.885	93.885	93.885	93.885	93.885	93.885
a	1.000	1.000	1.000	1.000	1.000	1.000	1.000	1.000	1.000
m	2.200	2.000	1.800	1.800	2.200	1.800	2.000	1.800	2.000
m Function	1.000	1.000	1.000	1.000	1.000	1.000	1.000	1.000	1.000
n	2.000	2.000	2.000	2.000	2.000	2.000	2.000	2.000	2.000
Lithomod	1.000	1.000	1.000	1.000	1.000	1.000	1.000	1.000	1.000
SXO limit	.200	.200	.200	.200	.200	.200	.200	.200	.200
PHI max	.320	.248	.310	.356	.263	.280	.292	.299	.310
PHI min c.o.	.0010000	.0010000	.0010000	.0010000	.0010000	.0010000	.0010000	.0010000	.0010000
EXPX	1.500	1.500	1.500	1.500	1.500	1.500	1.500	1.500	1.500
Clay cut off	.400	.400	.400	.400	.400	.400	.400	.400	.400
Por. cut off	.0800000	.0800000	.0800000	.135	.135	.135	.135	.135	.135
SW cut off	.550	.550	.550	.550	.550	.550	.550	.550	.550
RWF	.0593644	.0588687	.0586368	.0582735	.0579589	.0578263	.0573493	.0568389	.0562995
RMFF	.275	.272	.271	.270	.268	.267	.265	.263	.260
PHI Sand	.300	.300	.300	.299	.300	.300	.300	.300	.300
Sw Eq. CPX	1.000	1.000	1.000	1.000	1.000	1.000	1.000	1.000	1.000
RHOMA 1	2.690	2.690	2.690	2.690	2.690	2.690	2.690	2.690	2.690
RHOMA 2	2.776	2.776	2.776	2.776	2.776	2.776	2.776	2.776	2.776
RHOMA 3	3.000	3.000	3.000	3.000	3.000	3.000	3.000	3.000	3.000
UMA 1	4.800	4.800	4.800	4.800	4.800	4.800	4.800	4.800	4.800
UMA 2	17.631	17.631	17.631	17.631	17.631	17.631	17.631	17.631	17.631
UMA 3	11.005	11.005	11.005	11.005	11.005	11.005	11.005	11.005	11.005

Origin energy

YOLLA 1

PETROPHYSICAL SUMMARY

Company	Amoco Australia
Well Name	YOLLA 1
Field	Yolla
Country	Australia
Nation	Australia
State	Tasmania
County or Rig name	Glomar Robert F. Bauer
Latitude	039 50' 18.890" S DMS
Longitude	145 48' 20.550" E DMS
Permanent Datum	MSL
Elevation of KB	11.10 M
Elevation Ground lv	79.00 M
Elevation Log Zero	11.10 M
Log measured from	KB
Drill measured from	KB
Service company	Schlumberger
Basin	Bass
Tenement/Concession	TRL/1
Log date	9-JUL-1985 22-AUG-1985
Date computed	29-01-02
Date plotted	29-01-2002
Time plotted	10:28:27

PETROLOG SOFTWARE Revision 8.00

CROCKER
DATA PROCESSING

Run number	1	2	3
Log date	9-JUL-1985	19-JUL-1985	22-AUG-1985
Day	9	19	22
Month	7	7	8
Year	1985	1985	1985
Depth-Driller		1982.50 M	
Depth-Logger		1986.00 M	
Bottom log interval	1758.00 M	1982.00 M	3347.00 M
Top log interval	399.00 M	1752.00 M	1752.00 M
Casing-Driller	399.00 M	1752.00 M	3340.00 M
Casing Diameter	20.0000 inch	13.3750 inch	9.6250 inch
Bit Size	17.5000 inch	12.2500 inch	8.5000 inch
Hole Fluid type		F/water Gel	
Fluid Density		1.0665 gm/cc	
Fluid Viscosity		49.0000 s	
Fluid PH		11.00	
Fluid Loss		6.0000 C3	
RM @ Surface		.6820 Ohmm	
Mud temp Surface		20.00 degC	
RMF @ Surface		.6270 Ohmm	
MF temp Surface		17.00 degC	
RMC @ Surface		.9800 Ohmm	
MC Temp Surface		16.00 degC	
Surface hole temp		16.00 degC	
Bottom hole temp		72.00 degC	
Max recorded temp		72.00 degC	
Max recorded temp 1		79.00 degC	
Logging Company ID		SLB	
Recorded by		O.Boube	
Witness		B.Wheeler	

COMPUTATION PARAMETERS

DEPTH INTERVAL	RW PPM	RW OHMM	TEMP C	GR MIN	GR MAX	R CLAY	RHOB CLAY	PHIN CLAY	t CLAY	RHOH	a	m
1764.9 - 1807.2	60296	.059	66.5	34	99	2.5	2.45	.391	113	.50	1.00	2.20
1807.3 - 1817.2	60296	.059	67.2	34	99	2.5	2.45	.391	113	.50	1.00	2.00
1817.4 - 1832.0	60296	.059	67.6	34	99	2.5	2.45	.391	113	.50	1.00	1.80
1832.2 - 1856.5	60296	.058	68.1	34	99	2.5	2.45	.391	113	.70	1.00	1.80
1856.7 - 1866.4	60296	.058	68.6	34	99	2.5	2.45	.391	113	.70	1.00	2.20
1866.6 - 1871.2	60296	.058	68.8	34	99	2.5	2.45	.391	113	.80	1.00	1.80
1871.3 - 1919.6	60296	.057	69.6	34	99	2.5	2.45	.391	113	.80	1.00	2.00
1919.8 - 1929.1	60296	.057	70.4	34	99	2.5	2.45	.391	113	.80	1.00	1.80
1929.2 - 1982.0	60296	.056	71.3	34	99	2.5	2.45	.391	113	.80	1.00	2.00

LITHOLOGIES

Bound Water · Cristobilite · Limestone · Bound Water · OIL · GAS · MOVED OIL

MOVED GAS · Water · Sandstone

LEGEND

Oil/Gas · Partial recovery

LOG DESCRIPTION

ROMA-CPX	Apparent Matrix Density (Complex Litho Model)
SW -CPX	Formation Water Saturation <=1.0 (Complex Litho Model)
PHIE-CPX	Effective Porosity (Complex Litho Model)
PHXO-CPX	Product (PHIE * SXO) (Complex Litho Model)
PHSW-CPX	Product (PHIE * SW) (Complex Litho Model)
MINERAL	Special Mineral Table output flag (Salt,Trona,Anhydrite,Gypsum,Coal)
VCL -CPX	Volume of clay (Complex Litho Model)
VSND-CPX	Volume of Sand (Complex Litho Model)
VLS -CPX	Volume of Limestone (Complex Litho Model)
VDOL-CPX	Volume of Dolomite (Complex Litho Model)
PHIE-CPX	Effective Porosity (Complex Litho Model)
PHXO-CPX	Product (PHIE * SXO) (Complex Litho Model)
PHSW-CPX	Product (PHIE * SW) (Complex Litho Model)
VBW -CPX	Volume of bound water (Complex Litho Model)
GR	Gamma Ray
SP	Spontaneous Potential
BS	Bit Size
CALI	Caliper
ILD	Induction Deep Resistivity
MSFL	Micro-spherically-focused Resistivity
SFLU	SFL Resistivity Unaveraged
RHOB	Bulk Density
NPHI	Thermal Neutron Porosity (original Ratio Method) in Selected Lithology
DT	Delta-T (also called Slowness or Interval Transit Time)
PEF	Photoelectric Factor
DRHO	Bulk Density Correction
CPOR	Ambient Core Helium Porosity
CKHA	Ambient Core Air Permeability
PHIT-CPX	Total porosity from CPX model after hydrocarbon correction (Complex Litho Model)
K_RCA_QC	Permeability derived from quality Yolla-1 RCA Data
NET -ROC	
NET -RES	
NET -PAY	

GAMMA RAY 0.0 (API) 200.0
SP 50.0 (MV) 150.0
BS 6.0 (INCH) 16.0
CALIPER 6.0 (INCH) 16.0
DEEP INDUCTION 0.2 (OHMM) 200.0
MICRO SFL 0.2 (OHMM) 200.0
SPHERICAL LOG 0.2 (OHMM) 200.0
DENSITY 1.95 (G/CC) 2.95
COMP. NEUTRON 0.45 (PU) -0.15
COMP. SONIC 140.0 (US/F) 40.0
P.E. ABSORPTION 0.0 ( ) 10.0
DRHO -0.75 (G/CC) 0.25
DEPTH M 1:200
Core Permeability 0.2 (MD) 2000.0
Calc. Permeability 0.2 (MD) 2000.0
RHOMA 2.5 (G/CC) 3.0
SW 1.0 (PU) 0.0
PHIE 0.5 (PU) 0.0
PHIE*SXO 0.5 ( ) 0.0
PHIE*SW 0.5 ( ) 0.0
Core Porosity 50.0 (%) 0.0
Total Porosity 0.5 (PU) 0.0
MINERAL 0.0 ( ) 1.0
CLAY 0.0 (PU) 1.0
SANDSTONE 0.0 (PU) 1.0
LIMESTONE 0.0 (PU) 1.0
DOLOMITE 0.0 (PU) 1.0
PHIE 1.0 (PU) 0.0
PHIE*SXO 1.0 ( ) 0.0
PHIE*SW 1.0 ( ) 0.0
Bound Water Vol 0.0 (V/V) 1.0
Rock
Res
Pay
1775
1800
1825
1850
1875
1900
1925
1950
DST-3
1813.0-1833.8m
11.8 MMcfd
892 BOPD
0 BWPD
80/64" choke
GOC 1832.1 mMDRT
DST-2A
1833.2-1833.8m
1.02 MMcfd
302 BOPD
TSTM BWPD
16/64" choke
OWC 1842.3 mMDRT
Core-1
1938.0-1848.0m
Rec 2.8m (28%)
Shifted -3.3m
to match wireline
and petrology
TEV2 1817.5-1823.1mMDRT
Gross Interval = 5.6m
Net Res Interval = 5.3m
PHIE_average = 14.0%
VCl_average = 28.6%
K_average (Geomet) = 1.71mD
VCl cut-off < 40%
PHIE cut-off > 8%
Net Pay Interval = 0.0m
Net Pay / Gross = 0.0%
Sw Cut-off < 60%
TEV3 1823.1-1829.5mMDRT
Gross Interval = 6.4m
Net Res Interval = 5.8m
PHIE_average = 16.8%
VCl_average = 23.2%
K_average (Geomet) = 3.46mD
VCl cut-off < 40%
PHIE cut-off > 8%
Net Pay Interval = 0.0m
Net Pay / Gross = 0.0%
Sw Cut-off < 60%
TEV4 1829.5-1839.6mMDRT
Gross Interval = 10.1m
Net Res Interval = 10.1m
PHIE_average = 25.0%
VCl_average = 17.7%
K_average (Geomet) = 53.6mD
VCl cut-off < 40%
PHIE cut-off > 8%
Net Pay Interval = 6.7m
Sw_average = 46.6%
Net Pay / Gross = 66.4%
Sw Cut-off < 60%
TEV5 1839.6-1843..0mDRT
Gross Interval = 3.4m
Net Res Interval = 2.4m
PHIE_average = 20.4%
VCl_average = 33.2%
K_average (Geom) = 38.5mD
VCl cut-off < 40%
PHIE cut-off > 13.5%
Net Pay Interval = 0.0m
Net Pay / Gross = 0.0%
Sw Cut-off < 60%
TEV6 1843.0-1857.80mDRT
Gross Interval = 14.8m
Net Res Interval = 13.9m
PHIE_average = 24.1%
VCl_average = 21.6%
K_average (Geom) = 57.8mD
VCl cut-off < 40%
PHIE cut-off > 13.5%
Net Pay Interval = 0.0m
Net Pay / Gross = 0.0%
Sw Cut-off < 60%
TEV8 1866.5-1871.40mDRT
Gross Interval = 4.9m
Net Res Interval = 4.9m
PHIE_average = 25.0%
VCl_average = 5.1%
K_average (Geom) = 13.5mD
VCl cut-off < 40%
PHIE cut-off > 13.5%
Net Pay Interval = 0.0m
Net Pay / Gross = 0.0%
Sw Cut-off < 60%

SPECIAL MINERALS

Coal

APPENDIX 3

YOLLA 1 DST 2A ANALYSIS

Analyst name	C. Chen
Company	Origin Energy
Well	Yolla-1
Field	Yolla
Date	2 October, 1985
Rig Name/Number	
Test	DST #2A
Depth Reference - MSL	RT
Gauge Type	EMR
Gauge Number	
Gauge Depth - Measured	
Gauge Depth - Vertical	
Producing Formation Top	
Producing Formation Bottom	
Perforated interval Top	5948
Perforated interval Bottom	6014

Remarks:

k = 101.4 md
h = 5 ft
s = 18.2
kh = 507 md-ft
Pi = 2697.3 psia

Reservoir Description

Fluid type : Single-phase Oil
Well orientation : Vertical
Number of wells : 1
Number of layers : 1

Layer Parameters Data

	Layer 1
Formation thickness	5.00 ft
Average formation porosity	0.25
Water saturation	0.30
Gas saturation	0.00
Formation compressibility	3.3243e-6 psi-1
Total system compressibility	7.8472e-5 psi-1
Layer pressure	2671.8301 psia
Temperature	212.0000 deg F

Well Parameters Data

	Well 1
Well radius	0.401 ft
Distance from observation to active well	0.0000 ft
Wellbore storage coefficient	8.8407e-3 bbl/psi
Storage Amplitude	0.0000 psi
Storage Time Constant	0.0000 hr
Second Wellbore Storage	0.0000 bbl/psi
Time Change for Second Storage	0.0000 hr
Well offset - x direction	0.00 ft
Well offset - y direction	0.00 ft

Fluid Parameters Data

	Layer 1
Oil gravity	45.5000 API
Gas gravity	0.8700 sp grav
Gas-oil ratio (produced)	3376.0000 scf/STB
Water cut	0.0000
Water salinity	3000.0000 ppm
Check Pressure	2585.0000 psia
Check Temperature	212.0000 deg F
Gas-oil ratio (solution)	820.0810 scf/STB
Bubble-point pressure	7105.2598 psia
Oil density	39.797 lb/ft3
Oil viscosity	0.25128 cp
Oil formation volume factor	1.49674 RB/STB
Gas density	11.4582 lb/ft3
Gas viscosity	0.0203984 cp
Gas formation volume factor	5.7980e-3 ft3/scf
Water density	60.163 lb/ft3
Water viscosity	0.2534 cp
Water formation volume factor	1.03876 RB/STB
Oil compressibility	1.0600e-4 psi-1
Initial Gas compressibility	3.5738e-4 psi-1
Water compressibility	3.1533e-6 psi-1

Layer 1 Correlations
Pb, Rs, Bo Correlation : Glaso
Uo Correlation : Beal et al
Ug Correlation : Carr et al

Layer Boundaries Data
Layer 1 Boundary Type : Infinitely acting

	Layer 1
L1	0.0000 ft
L2	0.0000 ft
L3	0.0000 ft
L4	0.0000 ft
Drainage area	0.0000 acres
Dietz shape factor	0.0000

Layer 1 Model Data
Layer 1 Model Type : Radial homogeneous

	Layer 1
Permeability	101.349 md
Skin factor (Well 1)	18.2082

Rate Change Data

Time Hours	Pressure psia	Rate STB/day
42.86600	3164.8701	0.0000
56.16089	1902.3340	302.0000
62.61000	2679.5901	0.0000

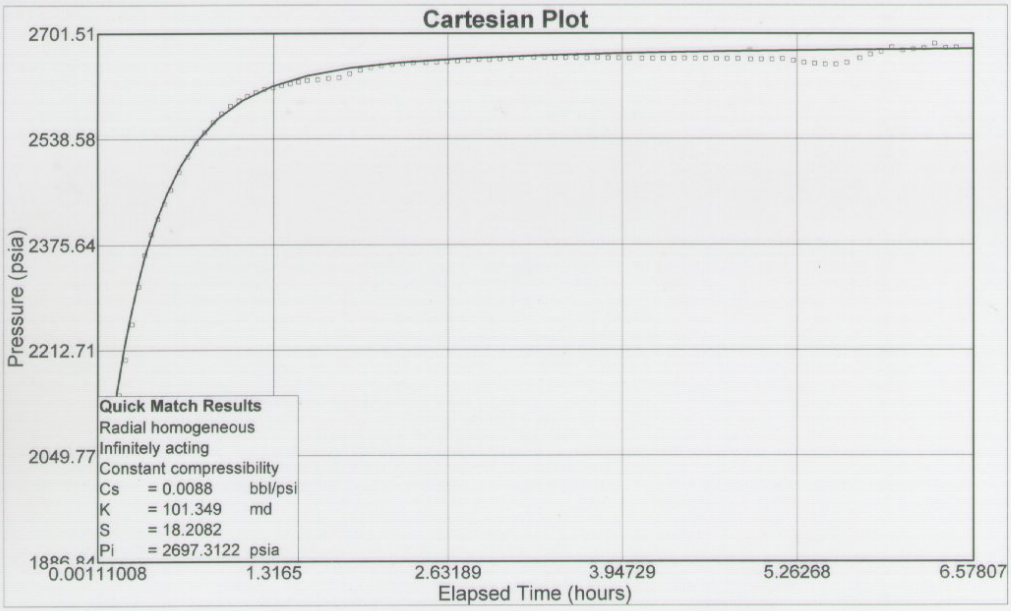

Radial Flow Plot

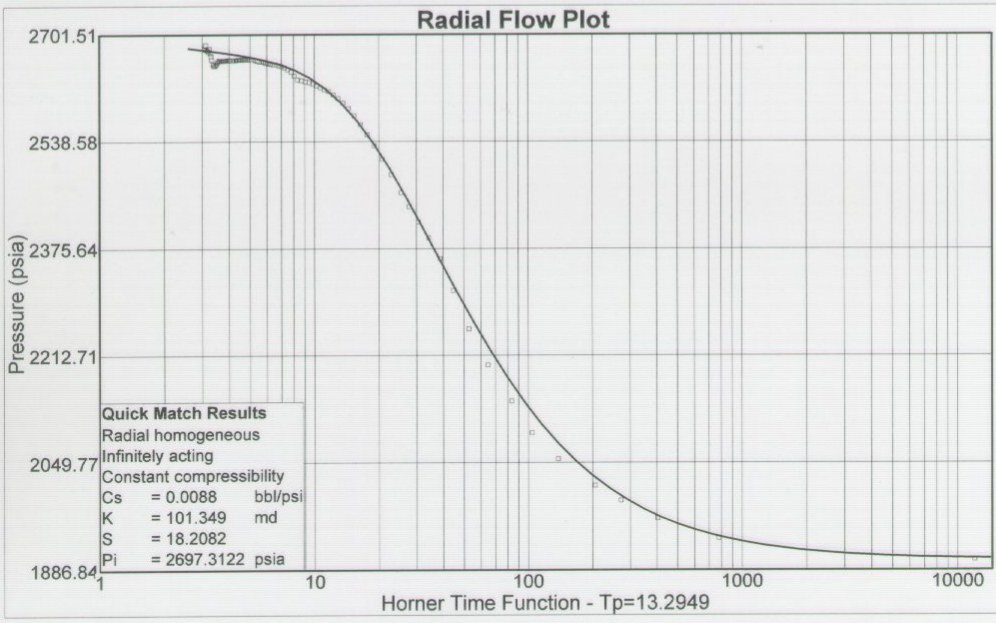

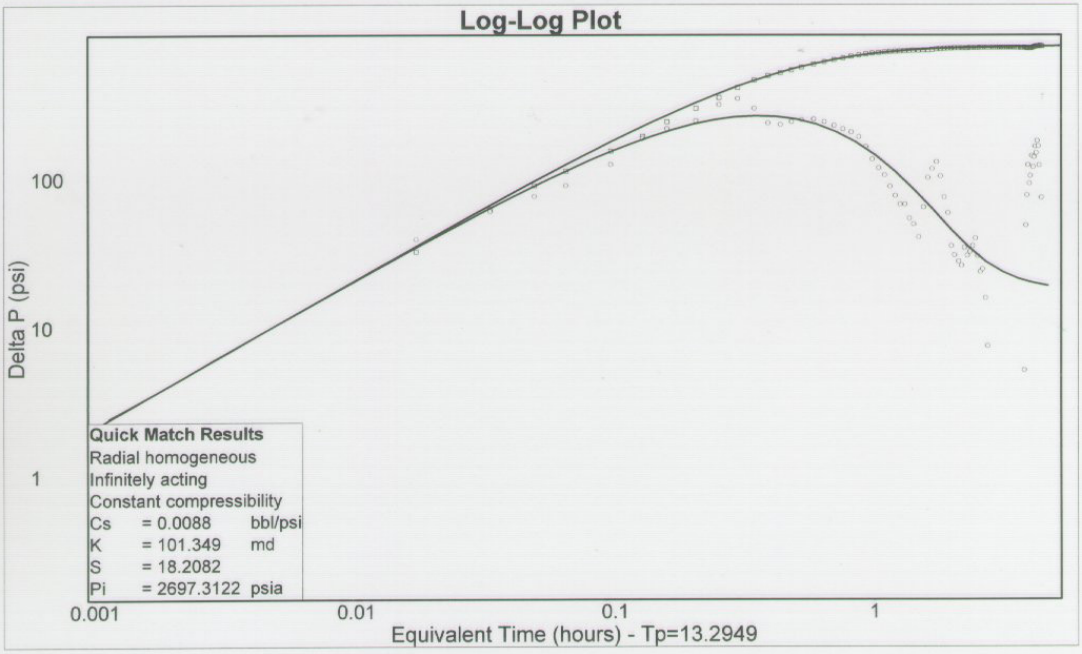
Log-Log Plot
Delta P (psi)
100
10
1
0.001
0.01
0.1
1
Equivalent Time (hours) - Tp=13.2949
Quick Match Results
Radial homogeneous
Infinitely acting
Constant compressibility
Cs = 0.0088 bbl/psi
K = 101.349 md
S = 18.2082
Pi = 2697.3122 psia

APPENDIX 4

YOLLA 1 DST 3 ANALYSIS

(Using oil Properties)

Analyst name	C Chen
Company	Origin
Well	Yolla 1
Field	Yolla
Date	5 October, 1985
Rig Name/Number	
Test	DST #3
Depth Reference - MSL	
Gauge Type	Amerada
Gauge Number	1114
Gauge Depth - Measured	5770.2 ft
Gauge Depth - Vertical	
Producing Formation Top	
Producing Formation Bottom	
Perforated interval Top	5948.2
Perforated interval Bottom	6016.8

Remarks:

oil

Reservoir Description

Fluid type : Single-phase Oil
Well orientation : Vertical
Number of wells : 1
Number of layers : 1

Layer Parameters Data

	Layer 1
Formation thickness	20.00 ft
Average formation porosity	0.20
Water saturation	0.25
Gas saturation	0.00
Formation compressibility	3.6468e-6 psi-1
Total system compressibility	1.0289e-4 psi-1
Layer pressure	2622.4485 psia
Temperature	212.0000 deg F

Well Parameters Data

	Well 1
Well radius	0.401 ft
Distance from observation to active well	0.0000 ft
Wellbore storage coefficient	3.1110e-3 bbl/psi
Storage Amplitude	0.0000 psi
Storage Time Constant	0.0000 hr
Second Wellbore Storage	0.0000 bbl/psi
Time Change for Second Storage	0.0000 hr
Well offset - x direction	0.00 ft
Well offset - y direction	0.00 ft

Fluid Parameters Data

	Layer 1
Oil gravity	50.6000 API
Gas gravity	0.7900 sp grav
Gas-oil ratio (produced)	1.3851e4 scf/STB
Water cut	0.0000
Water salinity	3000.0000 ppm
Check Pressure	2625.1001 psia
Check Temperature	212.0000 deg F
Gas-oil ratio (solution)	841.1480 scf/STB
Bubble-point pressure	1.3592e4 psia
Oil density	38.5516 lb/ft3
Oil viscosity	0.21413 cp
Oil formation volume factor	1.49159 RB/STB
Gas density	9.8306 lb/ft3
Gas viscosity	0.0189504 cp
Gas formation volume factor	6.1366e-3 ft3/scf
Water density	60.1617 lb/ft3
Water viscosity	0.2534 cp
Water formation volume factor	1.03878 RB/STB
Oil compressibility	1.3127e-4 psi-1
Initial Gas compressibility	3.7112e-4 psi-1
Water compressibility	3.1543e-6 psi-1

Layer 1 Correlations
Pb, Rs, Bo Correlation : Glaso
Uo Correlation : Beal et al
Ug Correlation : Carr et al

Layer Boundaries Data
Layer 1 Boundary Type : Infinitely acting

	Layer 1
L1	0.0000 ft
L2	0.0000 ft
L3	0.0000 ft
L4	0.0000 ft
Drainage area	0.0000 acres
Dietz shape factor	0.0000

Layer 1 Model Data
Layer 1 Model Type : Radial homogeneous

	Layer 1
Permeability	13.5851 md
Skin factor (Well 1)	2.9051

Rate Change Data

Time Hours	Pressure psia	Rate STB/day
6.16670	2561.8000	0.0000
12.76670	1345.4000	892.0000
21.13330	2569.2000	0.0000

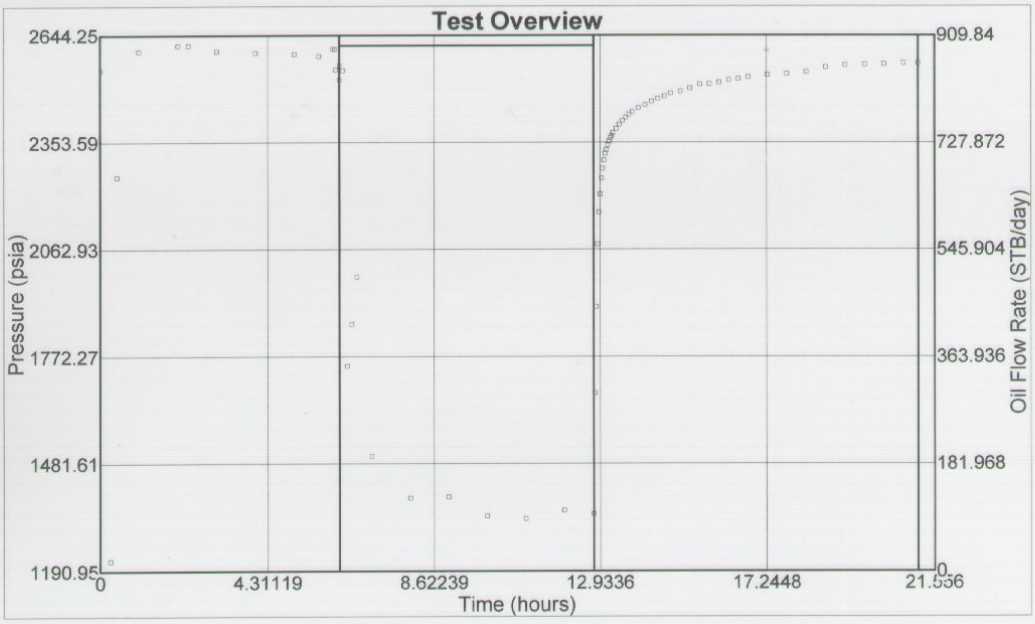

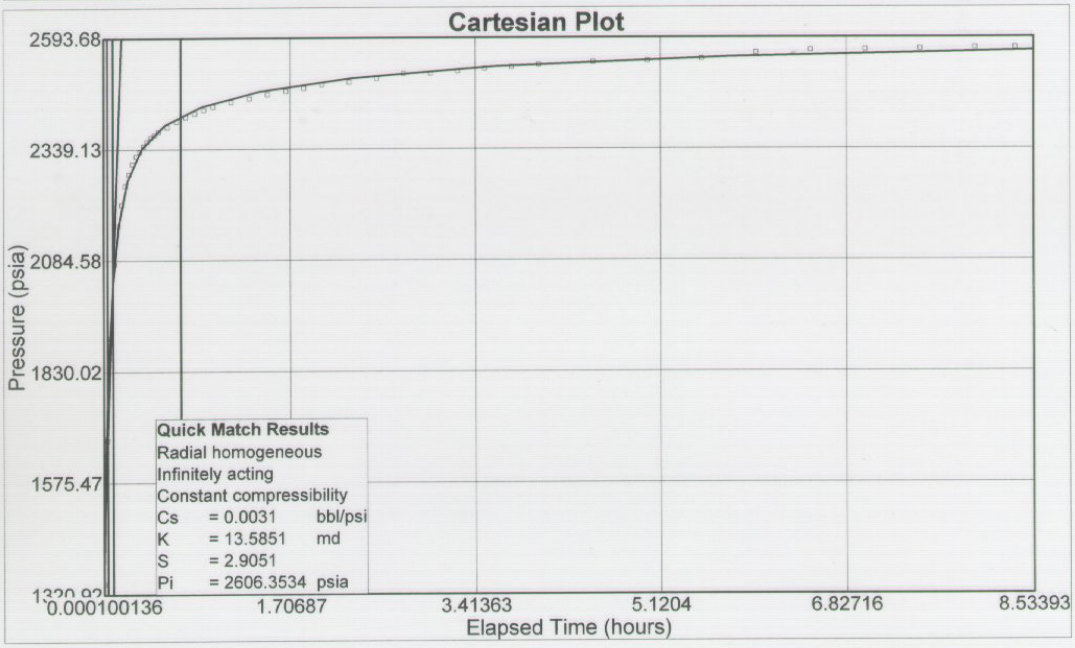

Cartesian Plot Model Results
Radial homogeneous - Infinitely acting

Classic Wellbore Storage

	Value
Wellbore storage coefficient	7.8924e-3 bbl/psi
Dimensionless wellbore storage	106.6168

Cartesian Plot Line Details
Line type : Wellbore storage
Slope : 7024.14
Intercept : 1438.99
Coefficient of Determination : 1

Number of Intersections = 0

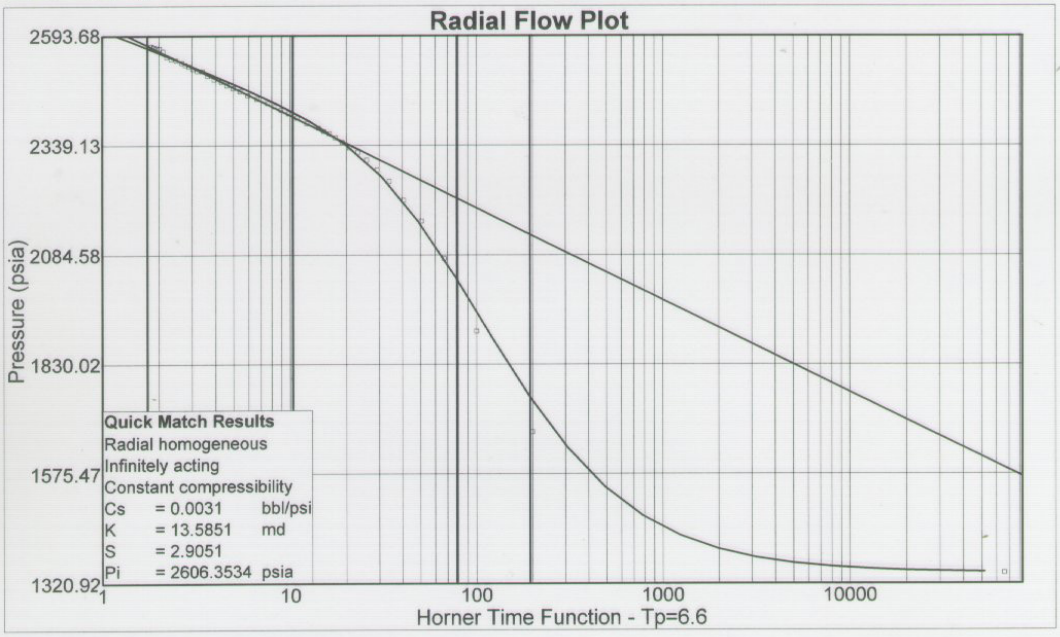

Radial Flow Plot Model Results
Radial homogeneous - Infinitely acting

Classic Wellbore Storage

	Value
Permeability	10.8102 md
Permeability-thickness	216.2043 md.ft
Radius of investigation	131.3870 ft
Flow efficiency	0.8010
dP skin (constant rate)	254.0935 psi
Skin factor	1.3656
Extrapolated pressure	2622.4485 psia

Radial Flow Plot Line Details
Line type : Radial flow
Slope : -214.211
Intercept : 2622.45
Coefficient of Determination : 0.996608

	Radial flow
Extrapolated pressure	2622.4485 psia
Pressure at dt = 1 hour	2433.7686 psia

Number of Intersections = 0

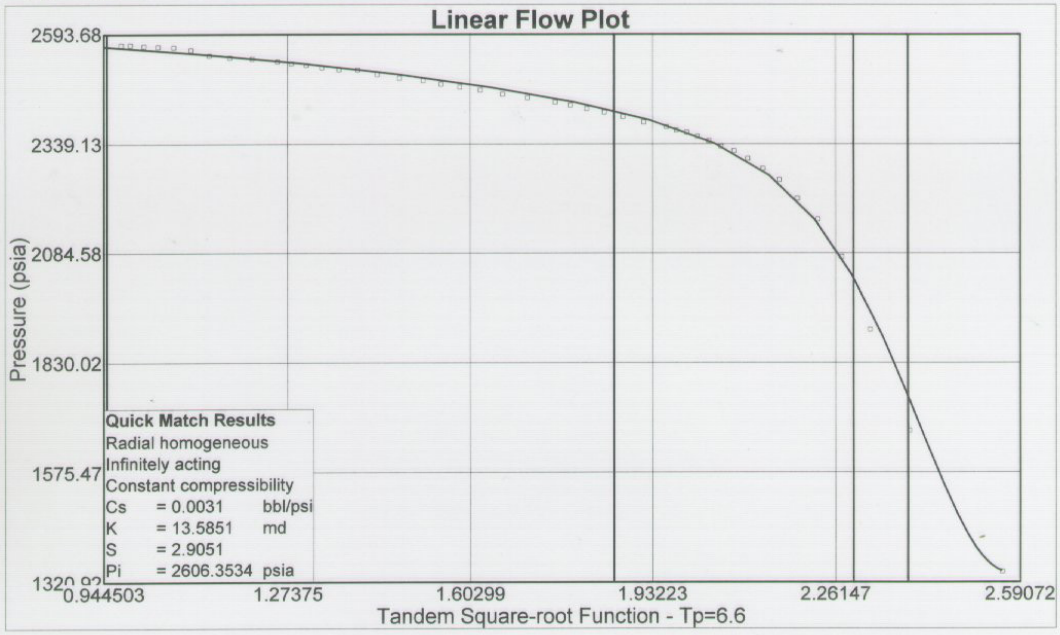

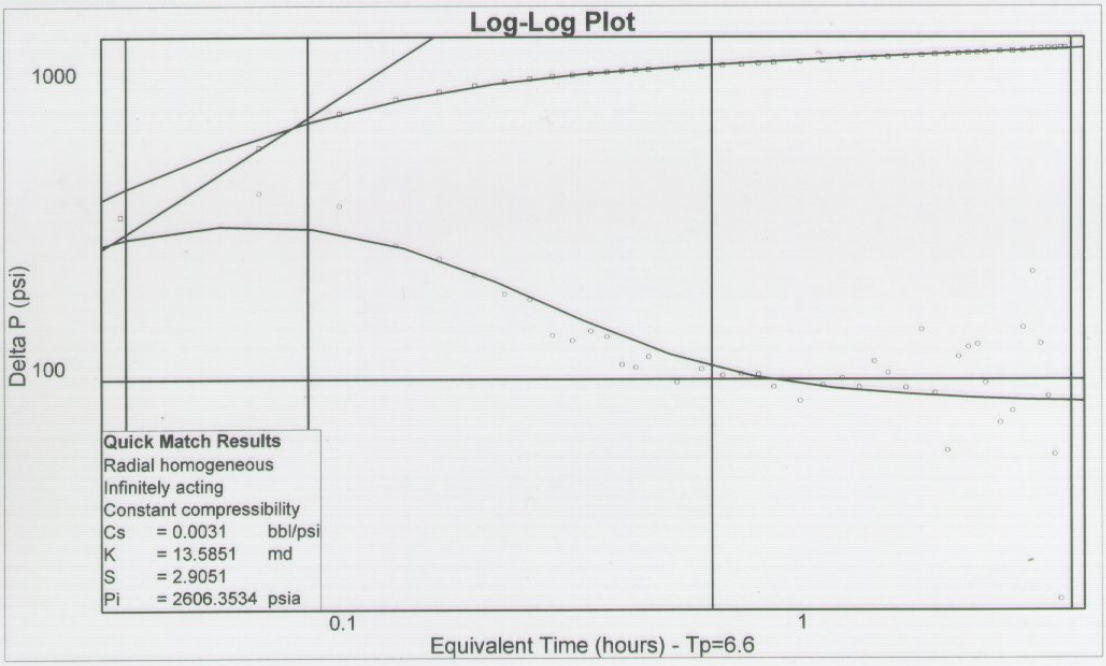

Log-Log Plot Model Results
Radial homogeneous - Infinitely acting

Classic Wellbore Storage

	Value
Wellbore storage coefficient	6.5847e-3 bbl/psi
Dimensionless wellbore storage	88.9507
Permeability	11.0653 md
Permeability-thickness	221.3059 md.ft

Log-Log Plot Line Details
Line type : Wellbore storage
Slope : 1
Intercept : 8419.17
Coefficient of Determination : Not Used

Line type : Radial flow
Slope : 0
Intercept : 90.8861
Coefficient of Determination : Not Used

Number of Intersections = 0

APPENDIX 5

YOLLA 1 DST 3 ANALYSIS

(Using gas Properties)

Analyst name	C Chen
Company	Origin
Well	Yolla 1
Field	Yolla
Date	5 October, 1985
Rig Name/Number	
Test	DST #3
Depth Reference - MSL	
Gauge Type	Amerada
Gauge Number	1114
Gauge Depth - Measured	5770.2 ft
Gauge Depth - Vertical	
Producing Formation Top	
Producing Formation Bottom	
Perforated interval Top	5948.2
Perforated interval Bottom	6016.8

Remarks:

gas

Reservoir Description
Fluid type : Condensate
Well orientation : Vertical
Number of wells : 1
Number of layers : 1

Layer Parameters Data

	Layer 1
Formation thickness	20.00 ft
Average formation porosity	0.20
Water saturation	0.25
Gas saturation	0.75
Formation compressibility	3.6468e-6 psi-1
Total system compressibility	2.5402e-4 psi-1
Layer pressure	2625.1001 psia
Temperature	212.0000 deg F

Well Parameters Data

	Well 1
Well radius	0.401 ft
Distance from observation to active well	0.0000 ft
Wellbore storage coefficient	0.2004 bbl/psi
Storage Amplitude	0.0000 psi
Storage Time Constant	0.0000 hr
Second Wellbore Storage	0.0000 bbl/psi
Time Change for Second Storage	0.0000 hr
Well offset - x direction	0.00 ft
Well offset - y direction	0.00 ft

Fluid Parameters Data

	Layer 1
Gas gravity	0.6500 sp grav
Condensate gravity	45.3750 API
Condensate/Gas ratio	99.9999 STB/MMscf
Water-Gas ratio	0.0000 STB/MMscf
Water salinity	0.0000 ppm
Check Pressure	2570.0000 psia
Check Temperature	212.0000 deg F
Gas density	7.76491 lb/ft3
Initial gas viscosity	0.018803 cp
Gas formation volume factor	6.6377e-3 ft3/scf
Water density	60.0414 lb/ft3
Water viscosity	0.27052 cp
Water formation volume factor	1.03872 RB/STB
Initial Z-factor	0.89744
Initial Gas compressibility	3.6818e-4 psi-1
Water compressibility	3.2030e-6 psi-1
Separator Pressure	1440.0000 psia
Separator Temperature	60.0000 deg F
Vapourising volume ratio	1374.2700 scf/STB
Wet stream gravity	0.9059 sp grav
Wet stream rate multiplier	1.13743

Layer 1 Correlations
Ug Correlation : Carr et al
Vap Vol Correlation : Leshikar

Layer Boundaries Data
Layer 1 Boundary Type : Infinitely acting

	Layer 1
L1	0.0000 ft
L2	0.0000 ft
L3	0.0000 ft
L4	0.0000 ft
Drainage area	0.0000 acres
Dietz shape factor	0.0000

Layer 1 Model Data
Layer 1 Model Type : Radial homogeneous

	Layer 1
Permeability	9.018 md
Skin factor (Well 1)	-3.5995
Rate dependent skin coefficient (D)	1.9189e-4 1/(Mscf/day)

Layer 1 m(p) Table

P_lay psia	m(p) psi2/cp (*1E-06)
14.6500	0.0000
66.8000	0.4801
118.9500	1.4856
171.1000	2.9477
223.2500	4.8121
275.4000	7.0344
327.5500	9.5774
379.7000	12.4100
431.8500	15.5055
484.0000	18.8411
536.1500	22.3968
588.3000	26.1555
640.4500	30.1018
692.6000	34.2224
744.7500	38.5054
796.9000	42.9403
849.0500	47.5174
901.2000	52.2286
953.3500	57.0656
1005.5000	62.0225
1057.6500	67.0922
1109.8000	72.2697
1161.9500	77.5493
1214.1000	82.9270
1266.2500	88.3982
1318.4000	93.9589
1370.5500	99.6060

Layer 1 m(p) Table (cont)

P_lay psia	m(p) psi2/cp (*1E-06)
1422.7000	105.3361
1474.8500	111.1343
1527.0000	116.9963
1579.1500	122.9311
1631.3000	128.9363
1683.4500	135.0101
1735.6000	141.1504
1787.7500	147.3555
1839.9000	153.6237
1892.0500	159.9534
1944.2000	166.3434
1996.3500	172.7925
2048.5000	179.2995
2100.6499	185.8638
2152.8000	192.4839
2204.9500	199.1591
2257.1001	205.8890
2309.2500	212.6730
2361.3999	219.5100
2413.5500	226.4002
2465.7000	233.3429
2517.8501	240.3374
2570.0000	247.3835

Rate Change Data

Time Hours	Pressure psia	Rate MMscf/day
6.16670	2561.8000	0.0000
12.76670	1345.4000	11.8000
21.13330	2569.2000	0.0000

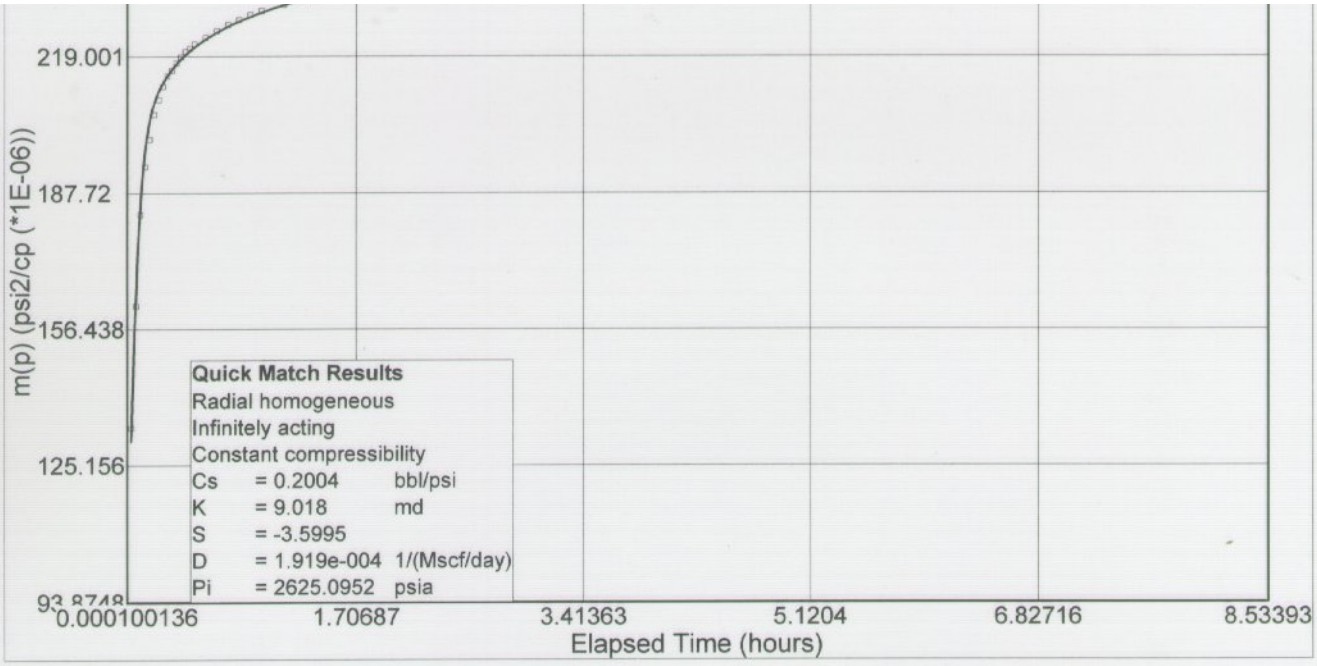
219.001
187.72
156.438
125.156
93.8748
m(p) (psi2/cp (*1E-06))
Quick Match Results
Radial homogeneous
Infinitely acting
Constant compressibility
Cs = 0.2004 bbl/psi
K = 9.018 md
S = -3.5995
D = 1.919e-004 1/(Mscf/day)
Pi = 2625.0952 psia
0.000100136
1.70687
3.41363
5.1204
6.82716
8.53393
Elapsed Time (hours)

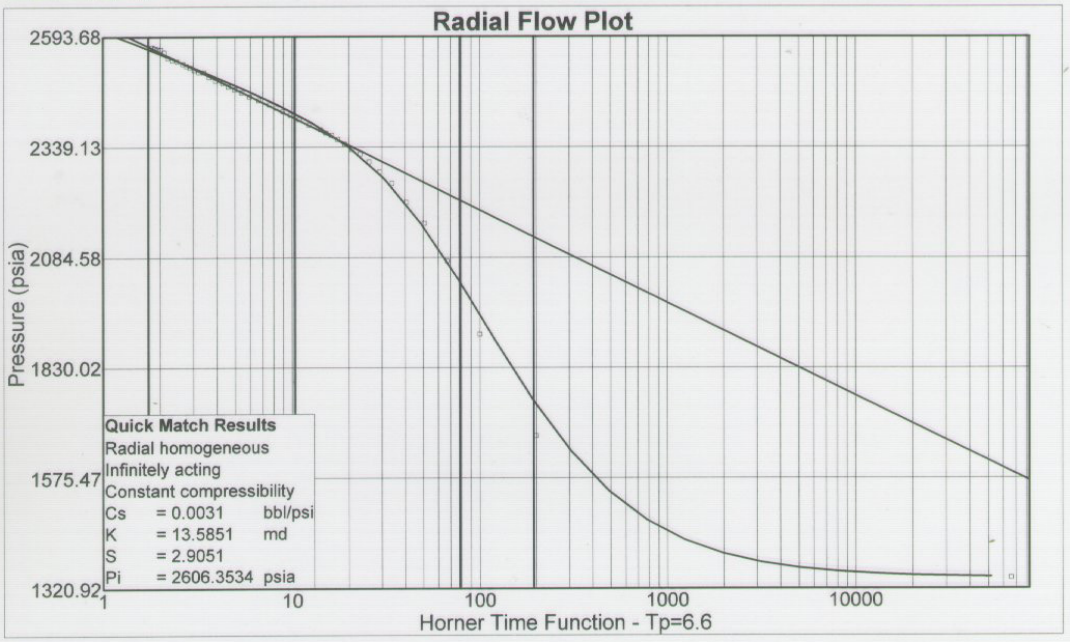

Radial Flow Plot Model Results
Radial homogeneous - Infinitely acting

Classic Wellbore Storage

	Value
Permeability	10.8102 md
Permeability-thickness	216.2043 md.ft
Radius of investigation	131.3870 ft
Flow efficiency	0.8010
dP skin (constant rate)	254.0935 psi
Skin factor	1.3656
Extrapolated pressure	2622.4485 psia

Radial Flow Plot Line Details
Line type : Radial flow
Slope : -214.211
Intercept : 2622.45
Coefficient of Determination : 0.996608

	Radial flow
Extrapolated pressure	2622.4485 psia
Pressure at dt = 1 hour	2433.7686 psia

Number of Intersections = 0

Linear Flow Plot

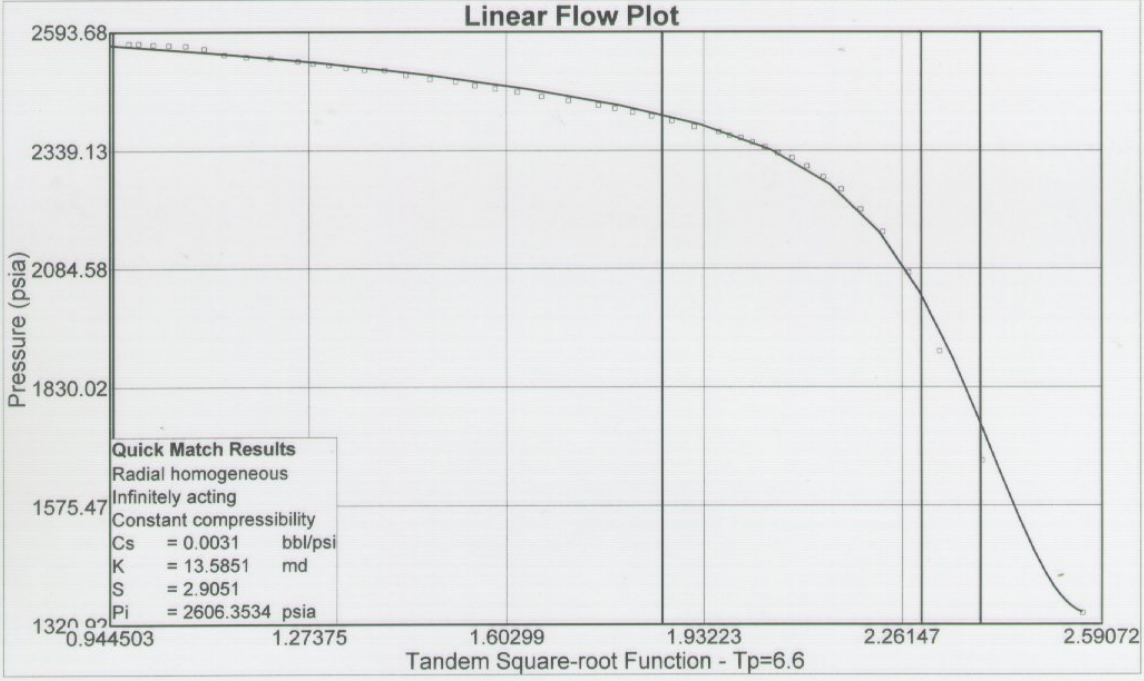

Log-Log Plot

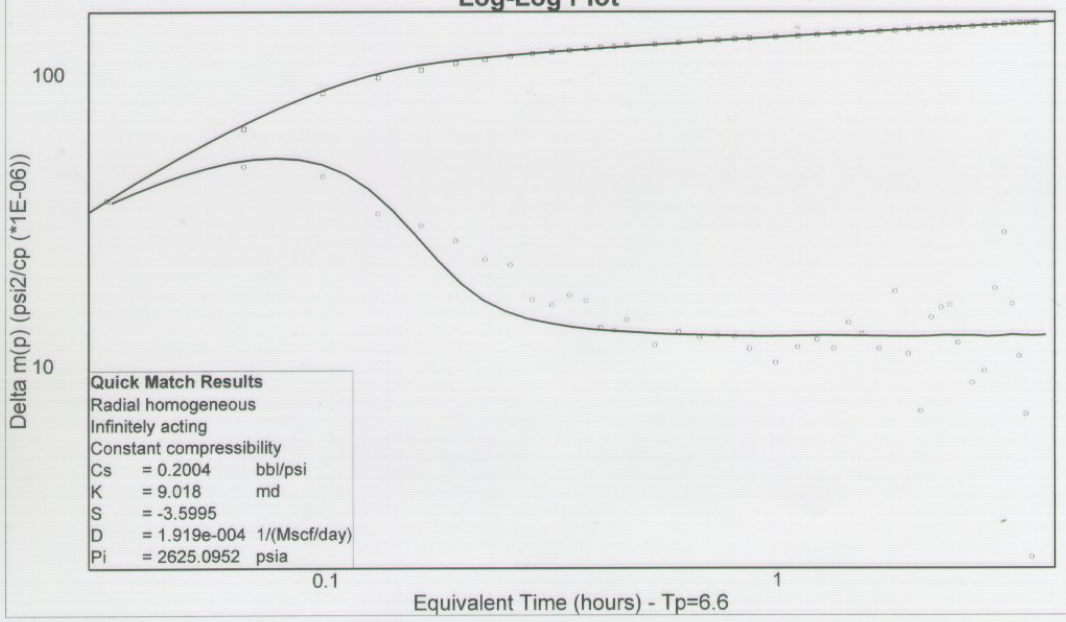

APPENDIX 6:

YOLLA 1830M SAND RADIAL MODEL DATASET

```
--   Origin Energy
--   Yolla 1830m Oil Sand -- Single Well Radial Model
--
RUNSPEC
TITLE
Yolla 1830m Radial Model -- DST 3 Matching (with Gas Cap & 0 skin)

RADIAL

DIMENS
--R  THETA  Z
--************************
  40   1    40  /

FIELD
OIL
WATER
GAS
DISGAS

TABDIMS
--NTSFUN  NTPVT  NSSFUN  NPPVT  NTFIP
     2      1      50      20    15  /

EQLDIMS
-- NTEQUL   NDPRVD  NDRXVD  NTTRVD  NSTRVD
     1   /

WELLDIMS
--NWMAXZ  NCWMAX  NGMAXZ  NWGMAX
    25       25      1     25    /

REGDIMS
  10  10   0   0   0   0  /

--VFPPDIMS
--   6   7   5   4   1   2   /

--AQUDIMS
--MXNAQN MXNAQC NIFTBL NRIFTB NANAQU NCAMAX
--     0      0      0      0      5     80  /

SATOPTS
  'HYSTER'   /

START
 31 'DEC' 2003  /

-- NOSIM

UNIFIN
UNIFOUT

NSTACK
  300  /

NOECHO

------------------------------------------------------------------------
GRID
GRIDFILE
  1 /
INIT

OLDTRAN

-- SPECIFY INNER AND OUTER RADIUS
INRAD
```

```
 0.40  /  -- 9.625 IN HOLE
OUTRAD
 2591.422  /  -- 789.9m, INCREMENTAL RATIO 1.252
-- SPECIFY ROCK AND FORMATION PROPERTIES
EQUALS
 'DTHETA'   360  /
--
 'TOPS'  5994.09   1  40  1   1   1   1  /  -- 1827m
--
 'DZ'     3.2808   1  40  1   1   1   6  /  -- 1.0m thickness, 1827   - 1833m
 'DZ'     0.6562   1  40  1   1   7   7  /  -- 0.1m thickness, 1833   - 1833.2m
 'DZ'     0.4921   1  40  1   1   8  11  /  -- 0.4m thickness, 1833.2 - 1833.8m
 'DZ'     0.6562   1  40  1   1  12  12  /  -- 0.3m thickness, 1833.8 - 1834.0m
 'DZ'     1.6404   1  40  1   1  13  40  /  -- 0.5m thickness, 1834   - 1848.0m
/

--
EQUALS
  PORO     0.250       1  40  1  1  1  40  /
--
  PERMR        11.5       1  40  1  1  1  6  / gas zone
  PERMR        18.7       1  40  1  1  7 40  / oil + water zone
--
/

COPY
  PERMR    PERMTHT      1  40  1  1  1  40  /
  PERMR    PERMZ        1  40  1  1  1  40  /
/

EQUALS
  NTG      1.0        1  40  1  1  1  40  /
--
  MULTZ    0.25           1  40  1  1  1  40  /
/

-----------------------------------------------------------------------
PROPS

EHYSTR
0.05  4  2.0  6.0  'BOTH'  /

HYSTCHCK
 /

GRAVITY
-- Oil   wtr   Gas
   45.5  1.01   0.867 /

ROCK
--  P       Compress
   4500       3.E-06 /

PVTW
--  P     Bw     Cw   Visc    v/v/psi
  4500   1.0   3.E-6   0.40      0     /

PVDG
-- P       Bg       Vg
  315    10.380   0.0123
  615     5.169   0.0130
  915     3.386   0.0137
 1215     2.492   0.0145
 1515     1.957   0.0154
 1815     1.603   0.0163
 2115     1.355   0.0172
 2415     1.179   0.0182
 2725     1.041   0.0192
 3500     0.796   0.0220
 4500     0.608   0.0261
/
```

```
PVTO
-- Rs      P       Bo     Vo
 0.154    315    1.181   0.284  /
 0.253    615    1.234   0.264  /
 0.344    915    1.278   0.252  /
 0.437   1215    1.322   0.240  /
 0.528   1515    1.366   0.228  /
 0.634   1815    1.415   0.214  /
 0.747   2115    1.468   0.201  /
 0.872   2415    1.530   0.187  /
 0.998   2725    1.601   0.175
         3500    1.582   0.187
         4500    1.557   0.203  /
/

--2nd set of SWFN are used to specify for IMB curves for each cell
SWFN
--Sw          Krw      Pcow, psi
0.2500      0.0000     6.0000
0.3000      0.0000     3.0000
0.3500      0.0000     1.4000
0.4000      0.0003     0.6100
0.4500      0.0013     0.2880
0.5000      0.0041     0.1480
0.5500      0.0102     0.0805
0.6000      0.0221     0.0463
0.6500      0.0432     0.0278
0.7000      0.0778     0.0174
0.7500      0.1317     0.0112
0.8000      0.2121     0.0074
0.8500      0.3277     0.0050
0.9000      0.4889     0.0035
0.9500      0.7082     0.0020
1.0000      1.0000     0.0000
/
0.25        0.0000     6.0000
0.30        0.0003     2.0000
0.35        0.0024     0.7000
0.40        0.0081     0.3000
0.45        0.0192     0.1000
0.50        0.0376     0.0500
0.55        0.0649     0.0000
0.60        0.1031    -0.0500
0.65        0.1539    -0.100
0.70        0.2191    -0.300
0.75        0.3005    -0.600
0.80        0.4000    -4.000
/

SGFN
0.0000      0.0000     0.0
0.0500      0.0000     0.0
0.1000      0.0000     0.0
0.1500      0.0000     0.0
0.2000      0.0000     0.0
0.2500      0.0000     0.0
0.3000      0.0028     0.0
0.3500      0.0161     0.0
0.4000      0.0444     0.0
0.4500      0.0911     0.0
0.5000      0.1591     0.0
0.5500      0.2510     0.0
0.6000      0.3690     0.0
0.6500      0.5152     0.0
0.7000      0.6916     0.0
0.7500      0.9000     0.0
/
0.0000      0.0000     0.0
0.0500      0.0000     0.0
0.1000      0.0000     0.0
```

```
0.1500     0.0000     0.0
0.2000     0.0000     0.0
0.2500     0.0000     0.0
0.3000     0.0000     0.0
0.3500     0.0000     0.0
0.4000     0.0000     0.0
0.4500     0.0000     0.0
0.5000     0.0102     0.0
0.5500     0.0577     0.0
0.6000     0.1591     0.0
0.6500     0.3266     0.0
0.7000     0.5705     0.0
0.7500     0.9000     0.0
/

SOF3
--So       Krow       Krog
0.010      0.000      0.000
0.050      0.1969     0.000
0.100      0.2985     0.000
0.150      0.3807     0.000
0.200      0.4525     0.0000
0.250      0.5173     0.0083
0.300      0.5771     0.0331
0.350      0.6330     0.0744
0.400      0.6858     0.1322
0.450      0.7360     0.2066
0.500      0.7841     0.2975
0.550      0.8302     0.4050
0.600      0.8747     0.5289
0.650      0.9177     0.6694
0.700      0.9594     0.8264
0.750      1.0000     1.0000
/
0.200      0.0000     0.0000
0.250      0.0008     0.0204
0.300      0.0060     0.0816
0.350      0.0203     0.1837
0.400      0.0481     0.3265
0.450      0.0939     0.5102
0.500      0.1623     0.7347
0.550      0.2577     0.7878
0.600      0.3847     0.8408
0.650      0.5477     0.8939
0.700      0.7513     0.9469
0.750      1.0000     1.0000
/


------------------------------------------------------------------------
REGIONS

SATNUM
 1600*1 /

IMBNUM
 1600*2 /Tab No: 2 are used for IMB


------------------------------------------------------------------------
SOLUTION
RPTSOL
  'RESTART=2'  'FIP=2' 'SOIL'  'SGAS' /

EQUIL
-- Datum   P@datum   WOC   Pc@WOC   GOC     Pc@GOC

  6013.78  2615.0   6044.95  0.0    6013.78   0  / -- GOC 1833m, OWC 1842.5m


------------------------------------------------------------------------
```

```
SUMMARY

BPR
 1 1 11  /
/

WBHP
/

WOPR
/

WOPT
/

WGPR
/

WGPT
/

RUNSUM
SEPARATE
DATE
EXCEL

-----------------------------------------------------------------------

MESSAGES
  8* 10000 10000 /

SCHEDULE

RPTSCHED
 'RESTART=2'  'FIP=2'  'WELLS=2'  'SUMMARY=2'  'WELSPECS'/

TUNING
 0.001   0.01    0.0001  /  -- 5 minutes 0.000694 days
/
 12  1  200  1 /

WELSPECS
  'Y1'  'G'  1  1  1*  'OIL'  /
/

COMPDAT
--                                  ID      KH   Skin  D
  'Y1'  1   1   1  17  'OPEN'  2*  0.80    1*   0.0  0.0000/ -- Hole size 9.625", 1827 to
1836.5 m
  'Y1'  1   1  23  25  'OPEN'  2*  0.80    1*   0.0  0.0000/ -- Hole size 9.625", 1839 to
1840.5 m
/

TUNING
 0.0001   0.01    0.0001  /  -- 5 minutes 0.000694 days
/
 12  1  200  1 /

WCONHIST
 'Y1'  'OPEN'  'ORAT'  892.0  0.0  11800.0  3*  1300  /
/

TSTEP
 0.2715 /  -- DD Period

WCONPROD
-- name  flag   mode    Qo  Qw    Qg    Ql&Rl   BHP   THP  VFP
  'Y1'  'STOP'  'ORAT'  0    1*   1*     2*     100   2*  /
/

TSTEP
```

```
 0.3486 /  -- SI Period

END
```